AD_____

Award Number: DAMD17-99-1-9272

TITLE: Resources for Precision Analysis of Human Breast Cancer

PRINCIPAL INVESTIGATOR: Peter Watson, M.B.

CONTRACTING ORGANIZATION: University of Manitoba
Winnipeg, Manitoba, R3E OW3 Canada

REPORT DATE: August 2000

TYPE OF REPORT: Annual

PREPARED FOR: U.S. Army Medical Research and Materiel Command
Fort Detrick, Maryland 21702-5012

NOTICE

USING GOVERNMENT DRAWINGS, SPECIFICATIONS, OR OTHER DATA INCLUDED IN THIS DOCUMENT FOR ANY PURPOSE OTHER THAN GOVERNMENT PROCUREMENT DOES NOT IN ANY WAY OBLIGATE THE U.S. GOVERNMENT. THE FACT THAT THE GOVERNMENT FORMULATED OR SUPPLIED THE DRAWINGS, SPECIFICATIONS, OR OTHER DATA DOES NOT LICENSE THE HOLDER OR ANY OTHER PERSON OR CORPORATION; OR CONVEY ANY RIGHTS OR PERMISSION TO MANUFACTURE, USE, OR SELL ANY PATENTED INVENTION THAT MAY RELATE TO THEM.

LIMITED RIGHTS LEGEND

Award Number: DAMD17-99-1-9272
Organization: University of Manitoba

Those portions of the technical data contained in this report marked as limited rights data shall not, without the written permission of the above contractor, be (a) released or disclosed outside the government, (b) used by the Government for manufacture or, in the case of computer software documentation, for preparing the same or similar computer software, or (c) used by a party other than the Government, except that the Government may release or disclose technical data to persons outside the Government, or permit the use of technical data by such persons, if (i) such release, disclosure, or use is necessary for emergency repair or overhaul or (ii) is a release or disclosure of technical data (other than detailed manufacturing or process data) to, or use of such data by, a foreign government that is in the interest of the Government and is required for evaluational or informational purposes, provided in either case that such release, disclosure or use is made subject to a prohibition that the person to whom the data is released or disclosed may not further use, release or disclose such data, and the contractor or subcontractor or subcontractor asserting the restriction is notified of such release, disclosure or use. This legend, together with the indications of the portions of this data which are subject to such limitations, shall be included on any reproduction hereof which includes any part of the portions subject to such limitations.

THIS TECHNICAL REPORT HAS BEEN REVIEWED AND IS APPROVED FOR PUBLICATION.

Carole B. Christian _____

8/3/01 _____

REPORT DOCUMENTATION PAGE

Form Approved
OMB No. 074-0188

1. AGENCY USE ONLY (Leave blank)	2. REPORT DATE	3. REPORT TYPE AND DATES COVERED
	August 2000	Annual (15 Jul 99 - 15 Jul 00)

4. TITLE AND SUBTITLE
Resources for Precision Analysis of Human Breast Cancer

5. FUNDING NUMBERS
DAMD17-99-1-9272

6. AUTHOR(S)
Peter Watson, M.B.

7. PERFORMING ORGANIZATION NAME(S) AND ADDRESS(ES)
University of Manitoba
Winnipeg, Manitoba, R3E OW3 Canada

E-MAIL:
pwatson@cc.umanitoba.ca

8. PERFORMING ORGANIZATION REPORT NUMBER

9. SPONSORING / MONITORING AGENCY NAME(S) AND ADDRESS(ES)
U.S. Army Medical Research and Materiel Command
Fort Detrick, Maryland 21702-5012

10. SPONSORING / MONITORING AGENCY REPORT NUMBER

11. SUPPLEMENTARY NOTES

12a. DISTRIBUTION / AVAILABILITY STATEMENT
Distribution authorized to U.S. Government agencies only (proprietary information, Aug 00). Other requests for this document shall be referred to U.S. Army Medical Research and Materiel Command, 504 Scott Street, Fort Detrick, Maryland 21702-5012.

12b. DISTRIBUTION CODE

13. ABSTRACT ***(Maximum 200 Words)***

This USArmy academic award guarantees ongoing protection and a balance of 75/25% of my time for research/clinical activities. This ensures my continued active contribution to breast cancer research through specific projects underway in my laboratory as well as through efforts to maintain and improve on resources that offer appropriately processed, relevant and pathologically defined tissue samples to other investigators. This award has allowed the PI to 1) continue to advance research projects that are currently ongoing in the laboratory focusing on the role of the psoriasin and lumican genes, the identification of additional novel genes associated with progression of preinvasive DCIS to invasive disease, and alteration of ER and associated proteins that may affect response to endocrine therapies, and 2) continue to direct the NCIC-Manitoba Breast Tumor Bank and offer clinical pathology expertise and advice to many investigators who seek access to appropriate tissues to test their ideas in conjunction with tissues associated with NCIC-clinical trial datasets, and tissues comprising pre-neoplastic and pre-invasive lesions.

14. SUBJECT TERMS
Breast Cancer, Ductal carcinoma in-situ, Tumor Bank

15. NUMBER OF PAGES
78

16. PRICE CODE

17. SECURITY CLASSIFICATION OF REPORT	18. SECURITY CLASSIFICATION OF THIS PAGE	19. SECURITY CLASSIFICATION OF ABSTRACT	20. LIMITATION OF ABSTRACT
Unclassified	Unclassified	Unclassified	Unlimited

TABLE OF CONTENTS

"RESOURCES FOR PRECISION ANALYSIS OF HUMAN BREAST CANCER"

Dr Peter H. Watson

INTRODUCTION.

The past decade has seen dramatic progress in our understanding of the basic cell and molecular biology of breast cancer. However, the translation of this basic science knowledge and ideas has been impeded by the limited numbers of clinician-scientists with skills to effectively collaborate with basic scientists and to accurately interpret tissue pathology, quality and the cellular composition of heterogeneous tissue samples subjected to molecular study. Beyond this there is the problem of access to appropriate human tissue samples. The PI's overall goal is the improvement in our current ability to predict individual risk of development of invasive disease and to predict further progression of invasive disease in terms of resistance to therapies. The specific aims of the PI are 1) continue to advance the two general avenues of research that are currently ongoing in the laboratory and which have direct relevance to important clinical problems in the management of early pre-invasive and the therapy of later advanced disease, 2) continue to direct the NCIC-Manitoba Breast Tumor Bank and offer clinical pathology expertise and advice to many investigators who seek access to appropriate tissues to test their ideas, and 3) to work with others to develop and analyze new tissue resources such as those based on collection of pre-invasive lesions and tissue samples and collection of tumor samples associated with clinical trials.

BODY OF REPORT

The accomplishments over the first year of this award are detailed below in four sections with reference to the tasks defined in the statement of work.

Task 1. To develop the National Clinical Trial Tumor Bank Module

- Complete supervision of collection of material from recently completed NCIC-CTG Trials and conduct histological analysis of all samples (months 0-12)
- Continue and refine prospective collection mechanism from collaborating centers (months 0-24)
- Travel to new centers in Canada to discuss protocols and enrol in the network (months 0-24)

The PI has continued to work closely with Dr K. Pritchard (breast site group chair for the NCIC-clinical trials group, NCIC-CTG) and other colleagues across Canada, to develop a clinical trial breast tumor bank (funded by an NCIC grant to Dr K Pritchard and coordinated by the NCIC-CTG central office). The intention has been a) to obtain paraffin tissue blocks from two recently completed trials (MA5 and MA12) and to transport and store these at the CTG site in Kingston, Ontario, b) to collect all frozen tissues from MA5 and MA12 that still might be stored in ER/PR laboratories across the country and to transport these to the NCIC-Manitoba Breast Tumor Bank for processing and storage in our facility, and c) to establish a mechanism for prospective collection of paraffin and if possible frozen tissues with new trials. The specific role for the PI has been to undertake aim b) and assist with aims a) and c) above. For the first aim a) we have currently collected (as of spring 2000) over 80% of the paraffin specimens for the MA5 study (80% x 753 patients = 600) and over 80% of the specimens from the currently randomized patients on MA12 (80% x 700 = 560) for a total of 1160 paraffin specimens. For the second aim b) we have accrued frozen tissues from 11 MA5, 54 MA12 (completed trials) and 25 MA14 (currently ongoing trial) cases. The low yield for MA5 was not unexpected but we had anticipated more cases from the more recently completed MA12 trial. The gap between our expectation and the actual yield reflects an uphill battle that we have faced with the rapid discontinuation of the frozen tissue estrogen receptor (ER) and progesterone receptor (PR) labs across the country, as ER and PR began to be measured by immunohistochemical techniques. Nevertheless we are continuing to collect frozen tissues from the MA12 trial. For aim c) the PI is currently working with other groups within the CTG to develop tissue resources specifically

associated with all clinical trials in Canada, including those on breast cancer. Since the submission and just prior to the start of this US Army award, the PI served as Chair of the NCIC-CTG biological studies section and assisted in writing and defending (at a site visit, Kingston Dec'98) the relevant components of the renewal of the NCIC-CTG major program grant application to the NCIC. This successfully secured some additional funding for the CTG to support administrative functions associated with Tissue Banking. More recently the PI has continued to work with and contribute to an application from the CTG to the Canada Foundation for Innovation (submitted Jan 1999), to seek more substantial funds for Tumor Banking within the CTG. However this application was recently judged to be unsuccessful and we plan to resubmit a revised proposal later this year.

Task 2. To develop the Pre-neoplastic Tissue Tumor Bank Module

- Continue supervision of database of Manitoba Breast Surgical Events and collection of representative paraffin blocks from collaborating pathology centers (months 0-36)
- Continue to direct accrual of tissue samples and data from collaborating center in Warsaw and conduct histological analysis of all samples (months 0-36)
- Travel to Warsaw to discuss protocols and collection system (months 0-12 and 24-36)

The first objective in this task is to continue to expand on the Manitoba Breast Surgical Events Database (MBED) in order to create a virtual database of patients with breast lesions including preneoplastic and preinvasive lesions within paraffin blocks stored in clinical pathology departments. Initiated in 1996, it now comprises a virtual database linked to specific paraffin blocks in the archives of 8 pathology departments linked by a common laboratory program. As of July 2000 this database contained 12,081 events on 8,800 patients. This represents a steady rate of case accrual since our last audit in summer 1999 of approximately 2,200 patients and 3,727 events. These events include a spectrum of pathological changes limited to only normal tissue, fibrocystic changes, papilloma, fibroadenoma, ductal hyperplasia, atypical ductal hyperplasia, LCIS (44 cases), DCIS (543 cases), and also cases with invasive carcinoma (2244 cases) and combinations of pre-invasive lesions. In time we will create a large dataset of pre-neoplastic lesions in paraffin blocks and a small but invaluable 'longitudinal' dataset comprised of lesions in breast biopsies associated with later higher grade lesions or invasive tumors in the same patients 'captured' in the Tumor Bank. Based on data from Health Canada and published retrospective studies we

estimate that over 100 invasive tumors will occur within this total biopsy cohort within 5 years and will these samples will be captured in the Manitoba Breast Cancer Database.

A second objective is to further augment the ability of the tumor bank to support research into preneoplastic and preinvasive disease by accruing frozen tissues containing these lesions (in addition to paraffin block tissues encompassed by the MBED). Given the very focal and sporadic nature of such lesions in biopsies, our strategy has been to accrue tissues from areas adjacent to breast tumors where such lesions are most common and can often be identified within normal structures. This simple strategy, though once feasible, is now hard to apply in North America where changes in surgical and pathology practice dictate that limited tissue is resected and the peripheral tissue surrounding the tumor is usually mostly required for clinical assessment of margin status. Therefore we have tried to forge collaborations with pathology departments in countries where clinical practice still allows extensive sampling from larger specimens. After a pilot shipment of 40 cases in 1998 to test tissue quality, we have since accrued and processed 104 additional specimens from the department of pathology at the Warsaw Cancer Center. Over 50% of these cases include multiple tissue blocks and analysis of the pathology contained is in process. However, communication with this center has recently become intermittent, indicating to us that collaboration with additional centers may become necessary to achieve our goal. In view of this the PI visited the 2nd affiliated hospital, Wuhan, Hubei Province, China in 1999 and discussed plans to collaborate with the director of this center and the head of dept of Pathology. However, due to the scarcity of electrical power and cold storage, we have been unable to proceed with this collaboration until we had worked to raise funds locally to purchase a suitable cryocontainer that can be loaded with sufficient liquid nitrogen in Manitoba, shipped to Wuhan, loaded over several days with material, and then returned with frozen specimens. We are now trying to set up a first test shipment.

Task 3. To direct the NCIC-Manitoba Breast Tumor Bank

- Continue to direct accrual of primary tumor tissue samples and data and conduct histological analysis of all samples (months 0-36)
- Continue to provide advice to external applicants to the Bank (months 0-36)
- Continue to supervise the review of applications, and undertake review and selection of appropriate cases for each study (months 0-36)

The Manitoba Breast Cancer Database (MBCD) section of the Bank contains over 3000 fully processed cases (566 A category cases, 1337 B category cases, 1705 C category cases, 90 D category cases) and many further samples collected and partially processed in reserve to maintain the 'stocks'. All cases are associated with a database comprising pathological data derived from uniform assessment of the tissue blocks and clinical staging. A subset (1337 cases) is also associated with complete clinical follow-up. By August 2000 the Bank has provided support to over 46 researchers for projects conducted in research laboratories across North America, has 2 new applications currently under review and 3 enquiries that are likely to lead to applications in the near future. These include laboratories from within Manitoba (13) and elsewhere in Canada (24), the USA (7), and Europe (2). The total aggregate of sections released in support of these projects (including 10 new projects since June 1999) is 61,966 frozen tumor sections (14,963 since June 1999), 10,652 frozen normal tissue sections (4327 since June 1999), 10,332 paraffin tumor sections (525 since June 1999), 1177 paraffin normal tissue sections (20 since June 1999).

In addition to continued direction of the NCIC-Manitoba Breast Tumor Bank, the PI has also become actively engaged in committee based discussions with the NCIC concerning the future and funding mechanisms for Tumor Banks in Canada. The NCIC 'tumor bank' program has successfully attracted many applications and has funded 4 Banks since 1993 (Breast, Lung, Brain, Sarcoma), all through regular operating grants. However NCIC has recently become uncomfortable with the funding commitment to Banks and has engaged the current Tumor Bank groups in discussions since spring 1999 to identify a way to alter NCIC's commitment to these currently established Banks. These discussions have revolved around the premise that NCIC would like to partner with other agencies to support the future costs of Banks (such as the newly created Cancer Institute within the Canadian Institutes of Health) and advocates the 'networking' of current Banks to create a larger self-sustaining enterprise that could for example attract outside funding from industry and also develop a user fee schedule. The PI has acted as Chair of the 'Tumor bank working group' committee, appointed by NCIC, to explore these issues.

Task 4. To direct the research program in our laboratory

- Continue to direct laboratory studies to understand and identify markers of resistance to endocrine therapy and examine the role of estrogen receptor variants and their influence on determination of ER/PR status and response to therapy. (months 0-36)
- Continue to direct laboratory studies to understand and identify markers of risk of progression from pre-invasive to invasive disease and examine the role of the psoriasin gene in conferring this risk (months 0-36)

ER related projects.

Basic research into the mechanisms which underlie the clinical evolution of breast cancer from hormone dependent to hormone independent growth has identified alterations in specific components of the mechanism of estrogen action which may shortcircuit the requirement for estrogen and so contribute to 'hormonal progression'. Our aim is to determine the in-vivo existence and the clinical relevance of these potential mechanisms, focusing on alterations at the level of the estrogen receptor (ER). Over the past year (1999-2000) we have made the following progress, much of it in close collaboration with Dr L C. Murphy's laboratory in our research group;

1. We have now shown that discrepancies in ER status determined by immunohistochemical assay (ER-IHA) can occur between different ER antibodies and that this may be attributable to the expression of truncated ERα variant proteins (1).
2. To assess alternative indirect methods to assess ER status (from ligand binding and immunohistochemical assay) we have examined the application of Infrared (IR) spectroscopy applied to tissue sections to provide a molecular fingerprint of the tissue. In a cohort of 77 breast tumors and using a multivariate pattern recognition strategy to analyze IR spectra we have shown IR patterns relate to different biological characteristics of tumors and can predict both grade and ER status (2).
3. To assess whether ERα variant expression measured in the primary tumor will reflect that seen in the metastasis we have examined synchronous primary and metastatic tumors (n=15) and found similar patterns and levels of truncated and deleted ERα mRNA variant expression, suggesting that altered expression of ERα is an event that occurs early in tumorigenesis (3).
4. To assess the level of estrogen receptor (ER)-beta mRNA in tumors, we have examined the level of ER-β mRNA and found that this can be significantly lower in PR+ tumors compared with PR- tumors

(p=0.036) but that no association with ER status (determined by ligand binding assay) is seen, suggesting the possibility that expression of ER-β in human breast tumors may be an additional marker of endocrine therapy responsiveness. Finally we have found that changes in the relative expression of ER-beta1, -beta2, and -beta5 variant mRNAs also occur (study cohort n=53) during breast tumorigenesis and tumor progression (4,5)

5. We have also begun to assess the expression several steroid receptor associated molecules, including the RNA activator (SRA). In a cohort of 27 breast tumors, we found that SRA expression was similar in ER+/PR+ and in ER-/PR- tumors, but was significantly ($p < 0.05$) lower than in ER+/PR- and ER-/PR+ tumors. A variant form of SRA was also found and correlated with grade in breast tumor tissues ($r = 0.53$, $n = 27$, $p= 0.004$). The expression of a specific repressor of estrogen receptor activity (REA) was also investigated in 40 human breast tumor biopsy samples and was found to be positively correlated with estrogen receptor (ER) levels ($r = 0.3231$; $P = 0.042$) and also significantly higher in ER+ compared with ER- tumors ($p = 0.04$), with no significant differences associated with PR status. REA was also inversely correlated with tumor grade ($r = -0.4375$; $P = 0.005$). These observations implicate changes in the expression of SRA-related and REA molecules as an additional factor in breast tumor progression and possibly alteration in response to endocrine therapy (6,7)

Ductal Carcinoma in-situ (DCIS) related projects.

To address the critical issue of the biology of early breast tumor progression and improved determination of risk of progression in pre-invasive lesions, we have applied a novel microdissection approach in combination with our uniquely designed tissue resource and molecular methodologies, in order to directly identify alterations that mark and may contribute to the development pre-invasive lesions and the subsequent development of the invasive phenotype in-vivo. Over the past year;

- We have microdissected and screened 8 invasive tumors using Research Genetics Array filters, combined with Pathways computer analysis software and identified a number of cDNA's that are differentially expressed between adjacent in-situ and invasive elements within the same tumor (Tumour #1: 120 cDNA's, Tumour #2: 119, Tumour #3: 36, Tumour #4: 71; Tumour #5: 79. Tumour #6: 42, Tumour #7: 68, Tumour #8: 58. Further assessment to identify highly and/or consistently differentially expressed cDNA's in more than one in-situ/invasive tumor pair and confirmation of differential expression (by other techniques including in-situ hybrization and RT-PCR) is now in progress.

- We have also microdissected and screened 8 in-situ tumors (4 high grade and 4 low grade DCIS) using Research Genetics Array filters and identified a number of cDNA's (12 cDNA's) that are consistently differentially expressed between high and low grade cases of DCIS. To pursue the significance of these cDNA's the PI has visited the University of Oxford, UK to develop a collaboration with Prof Adrian Harris's group, University of Oxford who are leaders in the field of tumor hypoxia and angiogenesis. We are currently examining together which of these differentially expressed genes is also induced in breast cell lines exposed to hypoxic growth conditions. We anticipate that such cDNA's will be of considerable interest, as they may be related to the process of necrosis. Necrosis is thought to be indicative of severe hypoxia in-vivo and also a marker of high risk of progression of DCIS to recurrence and invasive disease.
- We have continued to study the psoriasin (S100A7) gene that we have previously identified as differentially expressed between in-situ (DCIS) and invasive carcinoma. We have developed an anti-psoriasin polyclonal antibody and we have investigated the role of persistent expression in invasive disease. Antibody specificity was confirmed by analysis of transfected cell lines and the strong correlation between RT-PCR / in-situ hybridization detected levels of mRNA and western blot / immunohistochemistry detected protein. Persistence of psoriasin expression in invasive tumors was significantly associated with poor prognostic markers including ER and PR negative ($p<0.0001$, $p=0.0003$) and lymph node positive status ($p=0.035$). Psoriasin protein expression is also associated with inflammatory infiltrates (all tumors excluding medullary where inflammation is a diagnostic criteria, $p=0.0022$). These results suggest that psoriasin may be a marker of aggressive behaviour in invasive tumors and are also consistent with a function as a chemotactic factor (8)
- We have also found that psoriasin protein, studied by immunohistochemistry in skin and breast tumors, is localized predominantly (but not exclusively) to epithelial cells, and we were intrigued to find that it appears to localize to both cytoplasm and nuclei (the latter most prominent in breast tumor cells). Therefore, we became interested to pursue the possible intracellular role and interactions of psoriasin. To identify interacting proteins we used the yeast 2-hybrid assay to screen a normal breast cell library. From the first screen we have identified 4 positive clones. The first two genes are both recently identified components of the centrosome, RanBPM and spindle pole body protein hGCP3, while the other two cDNAs are a transcription factor binding protein and a gene of unknown function (CXX-1). RT-PCR experiments have confirmed that RanBPM mRNA is expressed in both fibroblast and

epithelial breast cell lines, but suggest that RanBPM is higher in tumor cells relative to normal cells. This is consistent with the result of a CGAP cDNA profiler search which found RanBPM expressed in a library of pooled invasive breast tumors but not in pooled normal tissue.This data and the co-incidental finding of 2 centrosome related proteins encourages us to pursue the role of association of psoriasin, RanBPM and hGCP3 in early progression towards the invasive phenotype (manuscript in preparation).

- We have examined the effect of psoriasin on invasive breast tumor cells. On the basis of our preliminary hypothesis in which we took the view that loss of psoriasin might facilitate invasiveness in the neoplastic breast cell, we transfected a CMV-psoriasin construct into the psoriasin negative but invasive MDA-MB-231 breast cell line. We isolated 2 MDA-231^{psoriasin} clones that demonstrate high and low mRNA and protein expression and have completed assessment of these cells by both in-vitro growth and Boyden chamber invasion assays as well as in-vivo assay in nude mice. We have found that psoriasin overexpression has no significant effect on the growth or invasiveness of this already invasive breast tumor cell line. This data, together with our recent in-vivo tumor data described above, has persuaded us to reconsider the alternative hypothesis that overexpression of psoriasin in DCIS associated with invasive tumor contributes to the malignant phenotype in this setting as does persistence of psoriasin in invasive tumors. Therefore we propose now to assess the effect of overexpression of psoriasin on the pre-invasive phenotype in specific cell models of preneoplasia (MCF10 series and HMT-3522 series).
- Using our microdissection approach we have also previously identified lumican mRNA as differentially expressed between the stroma adjacent to pre-invasive and central invasive components of early breast tumors. Further study of lumican and other members of the small leucine-rich proteoglycan (SLRP) gene family in breast tissues has now been completed (in collaboration with Dr Peter Roughley, Montreal) to explore their role in breast tumor progression. Lumican and decorin are expressed by similar fibroblast-like cells and are relatively abundant, while biglycan and fibromodulin are only detected occasionally and at low levels in breast tissues. However, while lumican mRNA expression was significantly increased in tumors ($n=34$, $p<0.0001$), decorin mRNA was decreased ($p=0.0002$) in neoplastic relative to adjacent normal stroma. This was accompanied by similar changes in both lumican ($p=0.0122$) and decorin (similar trend but p=ns) proteins. Alteration of lumican expression in breast tumor stroma may also be manifested by discordance between mRNA and protein

localization in some tumors, where some areas (mostly central regions) can demonstrate mRNA expression by in-situ hybridization but no detectable protein in parallel sections assessed both by immunohistochemistry and microdissection + western blot (9)

Collaborations

Access to our nationally funded Tumor Bank resource and our tissue expertise is in no way dependent on establishing direct collaborations with the PI. Nevertheless some investigators have sought formal collaborations and assistance in detailed study design and analysis, and the PI also collaborates with colleagues within the University of Manitoba Breast Cancer Research Group on other projects. In the past year this has resulted in the following additional publications;

- T. Toyama, H. Iwase, P. Watson, H. Muzik, E. Saettler, A. Magliocco, L. DiFrancesco, P. Forsyth, I. Garkavtsev, S. Kobayashi, and K. Riabowol. Suppression of ING1 expression in sporadic breast cancer. *Oncogene* 18 (37):5187-5193, 1999.
- W. R. Zeng, P. Watson, J. Lin, S. Jothy, R. Lidereau, M. Park, and A. Nepveu. Refined mapping of the region of loss of heterozygosity on the long arm of chromosome 7 in human breast cancer defines the location of a second tumor suppressor gene at 7q22 in the region of the CUTL1 gene. *Oncogene* 18 (11):2015-2021, 1999.
- H. Dotzlaw, E. Leygue, P. Watson, and L. C. Murphy. The human orphan receptor PXR messenger RNA is expressed in both normal and neoplastic breast tissue. *Clin.Cancer Res.* 5 (8):2103-2107, 1999.
- E. Leygue, H. Dotzlaw, P. H. Watson, and L. C. Murphy. Altered expression of exon 6 deleted progesterone receptor variant mRNA between normal human breast and breast tumour tissues. *Br.J.Cancer* 80 (3-4):379-382, 1999.
- B. Lu, H. Dotzlaw, E. Leygue, L. J. Murphy, P. H. Watson, and L. C. Murphy. Estrogen receptor-alpha mRNA variants in murine and human tissues. *Mol.Cell Endocrinol.* 158 (1-2):153-161, 1999.
- J. W. Clark, L. Snell, R. P. Shiu, F. W. Orr, N. Maitre, C. P. Vary, D. J. Cole, and P. H. Watson. The potential role for prolactin-inducible protein (PIP) as a marker of human breast cancer micrometastasis. *Br.J.Cancer* 81 (6):1002-1008, 1999.

KEY RESEARCH ACCOMPLISHMENTS

1. Continued operation and development of the NCIC-Manitoba Breast Tumor Bank and support for 10 new projects
2. Observation that discrepancies in ER status determined by immunohistochemical assay and ligand binding assay may be attributable to the expression of truncated ERα variant proteins
3. Demonstration that altered expression of ER-beta and steroid receptor cofactor molecules can occur in breast tumors and therefore should be considered as factors that may influence response to therapies.
4. Establishing the potential importance of psoriasin expression in invasive tumors, through its association with poor prognostic markers and potential to influence invasiveness through interactions with intracellular proteins
5. Identification of lumican and decorin as the most important among the small leucine rich proteoglycan genes in breast tissues and showing that these extracellular proteins show reciprocal alterations that may influence breast tumorigenesis

REPORTABLE OUTCOMES

1. Papers,
   - Huang, E. Leygue, H. Dotzlaw, L. C. Murphy, and P. H. Watson. Influence of estrogen receptor variants on the determination of ER status in human breast cancer. *Breast Cancer Res.Treat.* 58 (3):219-225, 1999.
   - E. Leygue, R. E. Hall, H. Dotzlaw, P. H. Watson, and L. C. Murphy. Oestrogen receptor-alpha variant mRNA expression in primary human breast tumours and matched lymph node metastases. *Br.J.Cancer* 79 (5-6):978-983, 1999.
   - M. Jackson, J. R. Mansfield, B. Dolenko, R. L. Somorjai, H. H. Mantsch, and P. H. Watson. Classification of breast tumors by grade and steroid receptor status using pattern recognition analysis of infrared spectra. *Cancer Detect.Prev.* 23 (3):245-253, 1999.
   - H. Dotzlaw, E. Leygue, P. H. Watson, and L. C. Murphy. Estrogen receptor-beta messenger RNA expression in human breast tumor biopsies: relationship to steroid receptor status and regulation by progestins. *Cancer Res.* 59 (3):529-532, 1999.
   - E. Leygue, H. Dotzlaw, P. H. Watson, and L. C. Murphy. Expression of estrogen receptor beta1, beta2, and beta5 messenger RNAs in human breast tissue. *Cancer Res.* 59 (6):1175-1179, 1999.
   - E. Leygue, H. Dotzlaw, P. H. Watson, and L. C. Murphy. Expression of the steroid receptor RNA activator in human breast tumors. *Cancer Res.* 59 (17):4190-4193, 1999.
   - S. L. Simon, A. Parkes, E. Leygue, H. Dotzlaw, L. Snell, S. Troup, A. Adeyinka, P. H. Watson, and L. C. Murphy. Expression of a repressor of estrogen receptor activity in human breast tumors: relationship to some known prognostic markers. *Cancer Res.* 60 (11):2796-2799, 2000.
   - S. Al Haddad, Z. Zhang, E. Leygue, L. Snell, A. Huang, Y. Niu, T. Hiller-Hitchcock, K. Hole, L. C. Murphy, and P. H. Watson. Psoriasin (S100A7) expression and invasive breast cancer. *Am.J.Pathol.* 155 (6):2057-2066, 1999.
   - Leygue E, Snell L, Dotzlaw H, Hole K, Hiller-Hitchcock T, Murphy LC, Roughley PJ, Watson P,. "Lumican and decorin are differentially expressed in human breast carcinoma" in press, J Pathology

2. Databases.
   - NCIC-Manitoba Breast Tumor Bank – continued operation and development of a unique tissue resource and provision of cases to external investigators across North America

3. Funding

   Operating Grants awarded;
   - NCIC/CBCRI, "The role of Psoriasin in progression of early breast cancer", $109,000 pa, 2000-2003 (renewal)
   - MRC, "The role of the small leucine rich proteoglycan in human breast cancer", $120,000pa, 2000-2003 (renewal)
   - NCIC/CBCRI Streams of Excellence, group grant, "The role of extracellular matrix in mediating risk of breast cancer", $60,000 pa, 2000-2003
   - MRC group grant, "Markers of Breast cancer progression", core grant, 2000.

   Travel Grants awarded:
   - Detweiler Travel Fellowship, Royal College of Physicians & Surgeons of Canada
   - Burroughs Welcome Fund, Travel Fellowship

CONCLUSIONS

Importance & Implications: It is anticipated that the many studies that will be conducted by the users of the Tumor Bank, will be facilitated and enhanced by access to histologically defined tissues containing invasive and pre-invasive breast lesions. This will lead to the identification of biological markers and cellular alterations that are directly relevant to the prediction of the natural history of onset and the later response to treatment of breast cancer. This knowledge will in turn ultimately contribute to strategies to predict and reduce risk of breast cancer or to circumvent resistance and improve on current treatments for invasive and metastatic disease. Our own research studies described above will hopefully contribute to this knowledge.

Future strategy: In the next year, the PI will continue to pursue the strategies, as outlined in the original Statement of Work. We recognize that successful completion of Task 1 and parts of Task 2 remains a different type of challenge from Tasks 3 & 4, as they are highly dependent on the continued involvement and motivation of other groups and centers beyond our own. However we will continue to strive to achieve these goals. In addition, direct involvement with the NCIC in discussions over the issue of how to fund and operate Tumor Bank resources in Canada has become an important aspect of pursuing Tasks 1,2, & 3. Task 4 revolves around the PI's own research program, and successful renewal of operating grant funding from MRC and CBCRI promises continued discovery of differentially expressed genes associated with the early stages of breast tumor progression and improved understanding of the biological role and importance of psoriasin and lumican genes in this process.

REFERENCES

1. Huang, E. Leygue, H. Dotzlaw, L. C. Murphy, and P. H. Watson. Influence of estrogen receptor variants on the determination of ER status in human breast cancer. *Breast Cancer Res.Treat.* 58 (3):219-225, 1999.

2. M. Jackson, J. R. Mansfield, B. Dolenko, R. L. Somorjai, H. H. Mantsch, and P. H. Watson. Classification of breast tumors by grade and steroid receptor status using pattern recognition analysis of infrared spectra. *Cancer Detect.Prev.* 23 (3):245-253, 1999.

3. E. Leygue, R. E. Hall, H. Dotzlaw, P. H. Watson, and L. C. Murphy. Oestrogen receptor-alpha variant mRNA expression in primary human breast tumours and matched lymph node metastases. *Br.J.Cancer* 79 (5-6):978-983, 1999.

4. H. Dotzlaw, E. Leygue, P. H. Watson, and L. C. Murphy. Estrogen receptor-beta messenger RNA expression in human breast tumor biopsies: relationship to steroid receptor status and regulation by progestins. *Cancer Res.* 59 (3):529-532, 1999.

5. E. Leygue, H. Dotzlaw, P. H. Watson, and L. C. Murphy. Expression of estrogen receptor beta1, beta2, and beta5 messenger RNAs in human breast tissue. *Cancer Res.* 59 (6):1175-1179, 1999.

6. E. Leygue, H. Dotzlaw, P. H. Watson, and L. C. Murphy. Expression of the steroid receptor RNA activator in human breast tumors. *Cancer Res.* 59 (17):4190-4193, 1999.

7. S. L. Simon, A. Parkes, E. Leygue, H. Dotzlaw, L. Snell, S. Troup, A. Adeyinka, P. H. Watson, and L. C. Murphy. Expression of a repressor of estrogen receptor activity in human breast tumors: relationship to some known prognostic markers. *Cancer Res.* 60 (11):2796-2799, 2000.

8. S. Al Haddad, Z. Zhang, E. Leygue, L. Snell, A. Huang, Y. Niu, T. Hiller-Hitchcock, K. Hole, L. C. Murphy, and P. H. Watson. Psoriasin (S100A7) expression and invasive breast cancer. *Am.J.Pathol.* 155 (6):2057-2066, 1999.

9. Leygue E, Snell L, Dotzlaw H, Hole K, Hiller-Hitchcock T, Murphy LC, Roughley PJ, Watson P. "Lumican and decorin are differentially expressed in human breast carcinoma" in press, J Pathology

APPENDICES

Manuscripts

A. Huang, et al, Influence of estrogen receptor variants on the determination of ER status in human breast cancer. *Breast Cancer Res.Treat.* 58 (3):219-225, 1999. (7 pages)

M. Jackson, et al. Classification of breast tumors by grade and steroid receptor status using pattern recognition analysis of infrared spectra. *Cancer Detect.Prev.* 23 (3):245-253, 1999. (9 pages)

E. Leygue,et al. Oestrogen receptor-alpha variant mRNA expression in primary human breast tumours and matched lymph node metastases. *Br.J.Cancer* 79 (5-6):978-983, 1999. (6 pages)

H. Dotzlaw,et al. Estrogen receptor-beta messenger RNA expression in human breast tumor biopsies: relationship to steroid receptor status and regulation by progestins. *Cancer Res.* 59 (3):529-532, 1999. (4 pages)

E. Leygue, et al. Expression of estrogen receptor beta1, beta2, and beta5 messenger RNAs in human breast tissue. *Cancer Res.* 59 (6):1175-1179, 1999. (5 pages)

E. Leygue, et al. Expression of the steroid receptor RNA activator in human breast tumors. *Cancer Res.* 59 (17):4190-4193, 1999. (4 pages)

S. L. Simon, et al Expression of a repressor of estrogen receptor activity in human breast tumors: relationship to some known prognostic markers. *Cancer Res.* 60 (11):2796-2799, 2000. (4 pages)

S. Al Haddad, et al. Psoriasin (S100A7) expression and invasive breast cancer. *Am.J.Pathol.* 155 (6):2057-2066, 1999. (10 pages)

Leygue E et al "Lumican and decorin are differentially expressed in human breast carcinoma" in press, J Pathology. (9 pages)

Breast Cancer Research and Treatment **58:** 219–225, 1999.

Report

Influence of estrogen receptor variants on the determination of ER status in human breast cancer

Aihua Huang[1], Etienne Leygue[2], Helmut Dotzlaw[2], Leigh C. Murphy[2], and Peter H. Watson[1]
[1]*Department of Pathology,* [2]*Department of Biochemistry and Molecular Biology, University of Manitoba, Winnipeg, Manitoba, Canada*

Key words: estrogen receptor variant mRNAs, estrogen receptor status, immunohistochemistry, breast cancer

Summary

Determination of estrogen receptor alpha (ER) status in breast cancer is an important predictive factor for clinical response to endocrine therapy. We have recently shown that discrepancies in ER status determined by immunohistochemical assay (ER-IHA) can occur between amino-terminal (1D5) and carboxyl-terminal (AER-311) targeted ER antibodies and that those tumors which demonstrate discordance are associated with increased expression of truncated ER variant mRNAs. In this study, we have explored this observation to examine if ER variant expression can exert a direct effect on ER-IHA or whether this association is attributable to the characteristics of the antibodies. ER negative cos-1 cells were transfected with expression vectors containing wild type ER (wt-ER) and/or a frequently expressed truncated variant, ER-clone-4 variant. We found that ER-IHA performed with the same *N*- and *C*-terminal targeting ER antibodies on cos-1 cells expressing wt-ER alone demonstrated no difference in signals by western blot ($P > 0.1$). However, co-expression of wt-ER and the truncated ER-clone-4 variant, resulted in discordant IHA results with relatively higher ER-IHA H-scores from *N*-terminal antibodies ($P < 0.03$). Furthermore, re-examination of a subset of breast tumors previously studied by ER-IHA showed persistent concordance in 4/5 cases and persistent differences in 3/5 cases with a different pair of ER antibodies. We conclude that the presence of truncated ER variant proteins can interfere with the interpretation of ER status determined by IHA and that this may account for some of the inconsistencies between ER status and response to endocrine therapy.

Introduction

The measurement of estrogen receptor alpha (ER) status in breast tumors is widely used as a clinical index of potential therapeutic response to endocrine therapy. However, while up to 2/3 of breast tumors are ER positive, only 2/3 of this subset of patients will respond well to endocrine therapy [1]. Several factors have been considered in the past to account for this discrepancy, including tissue-related factors such as sampling, cellularity, and heterogeneity and biological factors such as functional status of the ER protein detected and the integrity of the downstream components of the ER signalling pathway.

More recently other potentially important biological factors that have emerged are the complexity of ER alpha gene expression as well as the recent discovery of the closely related ER beta gene that is also expressed in breast cancer tissues [2]. ER alpha gene expression is now known to be often associated with a range of ER variant mRNAs in breast tumors [3]. These ER mRNA variants include exon-deleted, exon-duplicated, or truncated ER mRNA transcripts that may encode a variety of incomplete ER-like proteins [3, 4]. Individual ER variant proteins have been demonstrated [5, 6], but in most instances may well be expressed at low levels in most tumors compared to wt-ER [4]. Nevertheless ER variant expression may be important to consider with the adoption of the IHA

as an alternative to the classical ligand binding dextran coated charcoal (DCC) assay to determine ER status [7–9]. The IHA affords the opportunity to determine ER status in paraffin tumor sections and so allows the parallel assessment of tissue factors. However, this has also meant that ER is now defined on the basis of structural epitopes as opposed to functional ligand binding. Expression of most ER variants would not be detected by the DCC assay because in many cases the predicted variant proteins have loss or disruption of the *C*-terminus and ligand binding domain (E/F region) of the protein [10]. However, the total accumulation of multiple ER-like proteins might well be expected to interfere with IHA determination of ER status, depending on the target specificity of the antibody employed. Thus, although in practice a good overall correlation between IHA and DCC exists, discrepant results occur in a proportion of tumors [8, 9, 11–13]. These discrepancies are not only between IHA and DCC assays [8, 9], but also between IHA performed with different antibodies on the same tumors [11–13]. While tissue related factors can be invoked to account for some of the former discrepancies, differences between comparable IHAs scored on the same areas within serial sections [11] are more difficult to explain.

In order to understand such discrepancies we have recently examined ER mRNA variant expression and shown that those variants that specifically encode putative truncated ER-like proteins, are preferentially expressed in these 'IHA-discordant' cases [14]. This suggests that ER variant proteins encoded by ER variant mRNAs may contribute to discrepancies in ER status determined by IHA using different antibodies. In this study, we have now compared the signal intensities of different ER targeted antibodies and used these to examine experimentally the direct effect of truncated ER variant expression on the determination of wild type ER (wt-ER) status by IHA.

Materials and methods

ER expression vectors and transfection assays

Wt-ER (HEGO, kindly provided by Dr P. Chambon) was cloned into the vector pSG5 and expression was driven by an SV40 promotor. Truncated ER-clone-4 was cloned into the pcDNA3.1 vector (Invitrogen) and expression was driven by a CMV promotor. ER-negative cos-1 cells were grown in DMEM supplemented with 5% (v/v) fetal bovine serum. The cells were transiently transfected with either pHEGO, pER-clone-4, or both expression plasmids in varying proportions (5 μg total plasmid, as described in Figure 2). After 48 h, transfected cells were harvested for immunoblotting or fixed for immunohistochemical assay. All transfections were done in 60-mm dishes (for western blot samples) or in chamber slides (for immunohistochemistry samples) in parallel and using the superfect transfection system (Qiagen, CA) as described by the manufacturer. Plasmid pCH110 (encoding β-galactosidase protein, Pharmacia) was co-transfected and galactosidase activity was determined by standard methods to control for and confirm transfection efficiency (25–35% cells positive).

Western blot analysis

Whole cell extracts were prepared from cells transfected with wt-ER, ER-clone-4, or both plasmids. Cells were washed with chilled phosphate-buffered saline (PBS), scraped, collected in PBS, and centrifuged at 1000 g for 5 min at 4°C, and cell pellets were re-suspended in 200 μl of 50 mM Tris–HCl, 20 mM EDTA, 5% sodium dodecyl sulphate (SDS), 1 mM phenylmethylsulphonyl fluoride (PMSF), 5 mM β-glycerophosphate, and 1 mM aprotinin. Protein concentration was determined by the Bio-Rad (Hercules, CA) protein assay kit as described by the manufacturer. Twenty-five micrograms of protein was separated on a 10% SDS-polyacrylamide gel and transferred to nitrocellulose. Western blot analysis to detect ER present in different transfected cells was carried out with ER-specific mouse monoclonal antibodies 1D5 (DAKO, Canada) or AER314 raised against *N*-terminal epitopes and AER311 or AER320 (Neomarkers, CA) raised against *C*-terminal epitopes (at 1/1000 dilution for all antibodies) of the wild type protein (Figure 1D). The second antibody used was a horseradish peroxidase (HRP)-conjugated goat anti-mouse antibody (Hyclone Laboratories, Logan, UT, USA). Visualization was accomplished using the Supersignal detection system (Pierce, USA) according to the manufacturer's instructions. Densitometry on western blot signals was performed using a video-computer image analysis system (M4, Imaging Research, St Catherines, Ontario). Western blot experiments were performed at least in triplicate on independent cell transfections. Statistical comparisons were assessed by the student *t*-test.

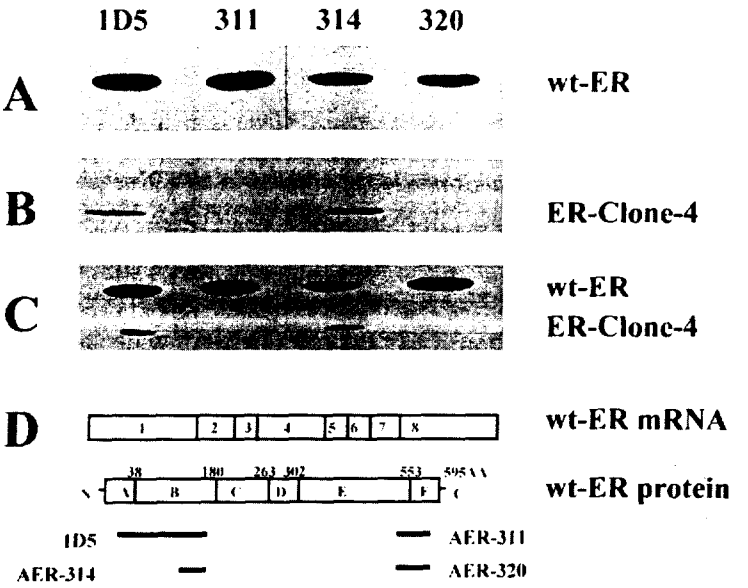

Figure 1. Western blot analysis of estrogen receptor expression detected with different antibodies in cos-1 cells following transient transfection with ER and/or ER-clone-4 variant. Twenty five micrograms of whole cell extract protein prepared from transfected cos-1 cells were loaded in each lane and separated by 0.1% SDS-10% PAGE. (A) Cos-1 cells transfected with 5 μg wt-ER plasmid. (B) Cos-1 cells transfected with 5 μg ER-clone-4, (C) cos-1 cells transfected with both wt-ER and ER-clone-4 (0.5 and 4.5 μg). Monoclonal antibodies used to detect ER proteins were 1D5 or AER314, and AER311 or AER320, which target epitopes within the *N*-terminal and *C*-terminal of the ER protein, respectively (D).

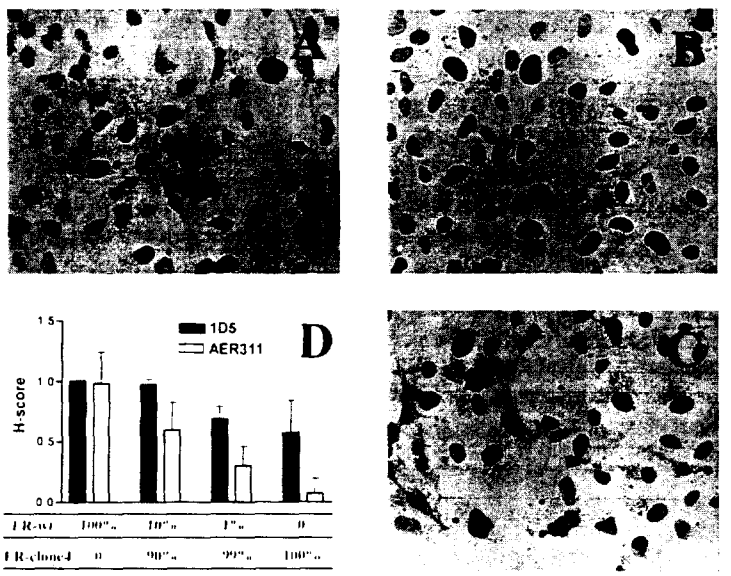

Figure 2. Immunohistochemical detection of estrogen receptor-like protein in transfected cos-1 cells. IHA-1D5 assay (A, B) and IHA-AER311 assay (C) were conducted on cells transfected with either ER-wt alone (A), or co-transfected with ER-wt and ER-clone-4 (ratio 1%:99%, B&C). The graph (D) summarizes the H-score values obtained by either IHA-1D5 or IHA-AER311 applied to cos-1 cells transfected with ER-wt and ER-clone-4 in different proportions. Each bar represents the mean and standard deviation relative to 1D5 H-score applied to ER-wt transfected cells derived from 7 (ER-wt alone) or 3 (all other) independent transfection experiments.

Immunohistochemistry

In parallel experiments, cos-1 cells were grown in chamber slides (Nalge Nunc, Intl., Il, USA). Transfections were performed as above. Cells were fixed in 2% paraformaldehyde–PBS for 30 min and washed twice with PBS for 2 min. Then IHA was performed as described previously [11]. Briefly, the slides were incubated in 10% goat serum in PBS for 20 min to block non-specific binding. Primary antibody 1D5 or AER311 (at 1/50 dilution for both) was added and incubation carried out overnight at 4°C, followed by two washes in PBS for 5 min. The second antibody (biotinylated goat anti-mouse IgG, Vector Labs, CA) was used at 1:200 dilution in PBS for 45 min at room temperature. After a rinse in PBS, the slides were incubated in AB Complex (Elite kit, Vector Labs) at 1:100 dilution for 45 min. The label was developed using diaminobenzidine/hydrogen peroxide and slides were then lightly counterstained with methyl green, dehydrated, cleared, and mounted.

Human breast tumor specimens (10 cases) were obtained from the NCIC-Manitoba Breast Tumor Bank. Formalin fixed and paraffin embedded tissue blocks were sectioned to provide serial sections from tumors and examined by IHA using the same protocol except that a different pair of ER antibodies (AER314 and AER320, Neomarkers, CA) were used.

Semi-quantitative H-scoring for all IHA experiments was done as previously described [11]. Brown immunoreactivity of cell nuclei was taken as positive and the proportion of negative cells (P_0) and those staining at low (P_1), moderate (P_2), or high (P_3) levels of intensity were scored. The score for each section (H-score = $[(0 \times P_0) + (1 \times P_1) + (2 \times P_2) + (3 \times P_3)] \times 100$) was calculated from the mean of $\times 5$ representative high power fields (Leica DMRB, $\times 40$ objective). For transfection experiments where non-specific background was uniformly higher than in tumor sections, only P_2 and P_3 values entered into the final H-score. Initial IHA experiments were also analyzed with the video-densitometry system as above, to compare with and validate the H-scoring quantification. All IHA slides were coded and assessment was done without knowledge of the antibody, transfection conditions, or tumor identity. As described previously [11], tumors which exhibited an H-score difference of >50 between IHA assays performed with different ER antibodies on serial sections were classified as 'IHA-discordant'.

Results

Comparison of ER antibodies

A panel of ER antibodies directed to different epitopes was tested by IHA and western blot assay in parallel, applied to an ER-negative cos-1 cell line transfected with wt-ER. Cos-1 cells were selected as ER mRNA or protein expression is undetectable in these cells (unpublished data) to avoid the possibility of endogenous ER and ER variant expression present in many breast cell lines. All antibodies detected a 65 kDa protein on western blot (Figure 1A) and comparison using a video-densitometry system showed that there was no significant difference between the signals obtained with 1D5 and AER311 antibodies (optical density units mean^{SD} for 1D5 = $0.79^{0.22}$ vs mean^{SD} AER311 = $0.78^{0.19}$; $n = 4$, $P > 0.1$). IHA was performed in parallel on transfected cells using these antibodies at the same relative concentrations. These were also the concentrations that we had previously used to study breast tumors. Initially IHA was assessed by both video-densitometry and semi-quantitative H-score (applied independently and without knowledge of the antibody) and it was found that these provided comparable results ($n = 10, r = 0.96, p = 0.004$, data not shown). Subsequently all IHA signals were quantitated by H-score. Positive immunoreactivity in approximately 30% of nuclei was seen with IHA-1D5 and IHA-AER311 with no significant difference in ER levels (H-score 1D5 $\text{mean}^{SD} = 63^{8}$; AER311 $\text{mean}^{SD} = 60^{17}$, $n = 7$, $P > 0.1$, Figure 2D).

Effect of modulation of ER variant expression on IHA

The ER-clone-4 variant was used for these experiments as this variant is predicted to encode a *C*-terminally truncated ER-like protein and has previously been shown to be frequently expressed in breast tumors [14–16]. Following transfection of ER-clone-4 alone, a single 24 kDa protein was detected by western blot analysis (Figure 1B) and positive nuclear staining was only seen by IHA using *N*-terminal antibodies (1D5 and AER314). However, *C*-terminal antibodies (AER311 and AER320) failed to detect it on western blot (Figure 1B & C) or IHA (Figure 2D). IHA was then performed using the same protocol as used in our previous study of breast tumors applied to cells following co-transfection with ER-clone-4 variant and wt-ER to obtain different proportions of ER variant expression relative to wt-ER. A consistently lower signal

Table 1. Immunohistochemical determination of ER level in tumors with different ER antibodies

			H-scores					
#	ER	PR	1D5	AER311	1D5 ↔ 311	AER314	AER320	314 ↔ 320
1	69	18	200	100	**100–**	150	80	**70–**
2	7	26	134	14	**120–**	180	90	**90–**
3	33	21	182	88	**94–**	110	60	**50–**
4	140	101	160	66	**94–**	125	100	25–
5	19	10	190	20	**170–**	90	80	10–
6	39	44	132	128	4–	105	140	35+
7	79	22	124	138	14+	150	170	20+
8	85	125	120	150	30+	150	150	0
9	27	10	228	200	28–	165	135	25–
10	24	59	128	104	24–	150	50	**100–**

Columns are as follows; #: case number; ER/PR: estrogen/progesterone receptor levels in fmol/mg protein as determined by DCC assay; 1D5, AER311, AER314, AER320: H-score values for ER levels determined by IHA using the corresponding antibody; 1D5 ↔ 311, 314 ↔ 320: Difference in H-score values with each antibody pair, with higher or lower values with *C*-terminal antibody shown as + or −, respectively, and 'IHA-discordant'; H-Scores (difference ≥50) shown in bold and 'IHA-consistent' H-Scores (<50) shown in regular typeface.

intensity for transfected ER-clone-4 relative to wt-ER was obtained with the *N*-terminal antibodies that was probably attributable to differences in efficiency between the expression plasmids (Figure 1). Nevertheless we observed that while both 1D5 and AER311 antibodies recognized wt-ER on western blot (Figure 1C) and gave similar H-score values with wt-ER alone, a significant and increasing discordance in IHA H-score occurred between *N*-terminal and *C*-terminal antibodies as the relative proportion of ER-clone-4 variant increased ($P < 0.03$, *t*-test, Figure 2D).

ER-IHA on breast tumors

We then investigated the reproducibility of our original observation in breast tumors. A different pair of antibodies was selected for repeat IHA assay (AER314 and AER320 targeting *N*- and *C*-terminal ER epitopes, respectively) as these were found to give similar results in cos-1 cells following wt-ER transfection and western blot analysis (AER314 $\text{mean}^{SD} = 0.67^{0.28}$ vs AER320 $\text{mean}^{SD} = 0.65^{0.22} n = 4$, $P > 0.1$) and IHA (data not shown). The original tissue blocks were available on a subset of 10 cases that were all ER/PR positive by DCC assay (and therefore expressing wild type ER and likely to also express a range of ER variants). All five tumors that had previously been classified as 'IHA-discordant' by our previous definition (H-score difference >50) showed lower H-scores by IHA-AER320 as compared to IHA with the matching AER314 antibody. In 3/5 the lower H-score was sufficient to remain classified as 'IHA-discordant' (Table 1). In contrast, amongst an equal number of cases previously classified as 'IHA-consistent', 4/5 showed equivalent H-scores and remained classified as 'IHA-consistent' with AER320. In 1/5 of the latter cases the IHA was discordant.

Discussion

Multiple ER alpha mRNA variants are expressed in normal breast tissue and in breast tumors [3]. However, in considering the role of ER variants in breast cancer, it has been argued that expression of ER mRNA variants may not be important on the basis that expression may not change during tumorigenesis and that the evidence to date for expression of specific variant proteins that might play a role in hormonal progression is limited [17, 18]. Nevertheless, studies founded on histologically characterized tissue sections have clearly shown that certain mRNA variants are differentially expressed between normal and neoplastic tissues and also between tumors [19, 20]. Differential expression has also been found in association with contrasting responses to estrogen and resistance to tamoxifen in cell lines [21–24] and parameters of hormone response and prognosis *in vivo* [16, 25]. Overexpression of an ER mRNA variant deleted in exon 5 (D5-ER) has also been shown to occur in certain tamoxifen resistant tumors [26] and has been used successfully to predict reponse to hormonal therapy of

hepatocellular carcinoma [27]. It is also conceivable that ER variants might exert indirect functional effects through competition with wt-ER for ER binding proteins [28] or with proteins involved in interactions with antiestrogens [29].

Although expression of specific variant proteins has not yet been proven in breast tumors, partly because it has been difficult to develop antibodies that will distinguish variants, expression of ER-like variant proteins expressed recombinantly can be demonstrated *in vitro* and in breast cell lines [21, 22]. In some cases these variant proteins have been shown to possess either hormone independent and constitutive activity or to exert a dominant negative influence on estrogen regulated target genes in *ex vitro* models. At the same time our own data suggest that previous attempts to demonstrate these proteins *in vivo* may have been hampered by the fact that, although total expression of ER variants of all forms may be significant, many individual variants such as D5-ER may be expressed at only low levels in breast tissues [4]. Furthermore, our recent observation that discordant immunostaining with ER antibodies correlates with the total overall expression of mRNA variants encoding out-of-frame proteins (i.e. predicted to encode *C*-terminally truncated ER-like proteins) also supports the view that ER-like variant proteins are present *in vivo* [11, 14]. In the latter study, we examined ER expression in breast tumors by DCC and IHA using both '*N*-terminal' (1D5) and '*C*-terminal' (AER-311) targeting ER alpha antibodies. The IHA provided similar results to the DCC assay in terms of overall ER status. However, the ER-IHA levels assessed in almost 25% of tumors were discordant (H-score difference of >50) between these different antibodies, even when scored on the same areas within serial sections [11]. Further analysis of these 'IHA-discordant' cases by RT-PCR assays [4, 20] showed that those ER mRNA variants that encode putative truncated ER-like proteins, were preferentially expressed in 'IHA-discordant' cases [14].

However, although the antibodies we used provided similar signal intensities by IHA on strongly ER positive tumors, and in many tumors the IHA signals were concordant [11], it remained possible that the discordant IHA signals might be explained by different antibody affinities. Furthermore, the principle that ER variants may interfere with IHA results had not previously been tested experimentally. Our results here show that the 1D5 and AER-311 antibodies can provide similar signal intensities of wt-ER by both western blot and IHA when used at the same relative concentrations as in our previous study [11]. But the relative IHA signal intensity obtained with these antibodies changes and becomes discordant with increasing expression of a truncated ER variant protein alongside the wt-ER. IHA consistency or inconsistency is also apparently quite reproducible when tumor blocks that have previously been studied by IHA and RT-PCR are re-examined using a different pair of matched ER monoclonal antibodies targeting similar *N*- and *C*-terminal epitopes. The degree of reproducibility between IHA with different pairs of antibodies in the small subset of cases available for reexamination should be considered against the fact that although RT-PCR assays using primers to span regions of deletion [4] can detect most exon-deleted ER mRNA variants, many of which encode putative truncated proteins, the spectrum of truncated ER mRNA variants analogous to the frequently expressed ER clone 4 is more difficult to study and is currently unknown [4, 15]. Therefore, given also that the precise epitopes recognized by the ER antibodies used are unknown, it is possible that additional truncated mRNA variants are expressed in particular cases, similar to ER-clone-4, that would remain undetected by the RT-PCR assays we have previously used [15, 16].

In summary, we have shown that ER status determined by IHA can be directly influenced by expression of a *C*-terminally truncated ER variant and that discordant IHA results in tumors using different ER antibodies are reproducible. We conclude that ER variant mRNA's and their putative variant proteins may interfere with the interpretation of ER status assessed by IHA and that this may underlie some of the inconsistencies in determination of ER status in breast tumors [30]. It should be emphasized that the clinical significance of discordance in IHA, in terms of assignment of IHA status, remains to be tested, but is likely to affect only a small subset of breast tumors. The relationship between ER variant expression, 'IHA-discordant' status, and clinical response to endocrine therapy remains to be determined.

Acknowledgement

This work was supported by grants from the Canadian Breast Cancer Research Initiative (CBCRI) and the U.S. Army Medical Research and Materiel Command (USAMRMC). The Manitoba Breast Tumor Bank is supported by funding from the National Cancer Institute of Canada (NCIC). EL is a USAM-

RMC postdoctoral fellow. LCM is a Medical Research Council of Canada (MRC) Scientist. PHW is an MRC Clinician-Scientist.

References

1. McGuire WL: Hormone receptors: their role in predicting response to endocrine therapy. Semin Oncol 5: 428–433, 1978
2. Dotzlaw H, Leygue E, Watson PH, Murphy LC: Expression of estrogen receptor-beta in human breast tumors. J Clin Endocrinol Metab 82: 2371–2374, 1997
3. Murphy LC, Leygue E, Dotzlaw H, Douglas D, Coutts A, Watson PH: Oestrogen receptor variants and mutations in human breast cancer. Ann Med 29: 221–234, 1997
4. Leygue E, Huang A, Murphy L, Watson P: Prevalence of estrogen receptor variant mRNAs in human breast cancer. Cancer Res 56: 4324–4327, 1996
5. Park W, Choi JJ, Hwang ES, Lee JH: Identification of a variant estrogen receptor lacking exon 4 and its coexpression with wild-type estrogen receptor in ovarian carcinomas. Clin Cancer Res 2: 2029–2035, 1996
6. Desai AJ, Luqmani YA, Walters JE, Coope RC, Dagg B, Gomm JJ, Pace PE, Rees CN, Thirunavukkarasu V, Shousha S, Groome NP, Coombes R, Ali S: Presence of exon 5-deleted oestrogen receptor in human breast cancer: functional analysis and clinical significance. Brit J Cancer 75: 1173–1184, 1997
7. Taylor CR.: Paraffin section immunocytochemistry for estrogen receptor. Editorial Cancer 77: 2419–2422, 1996
8. Allred DC, Bustamante MA, Daniel CO, Gaskill HV, Cruz AJ: Immunocytochemical analysis of estrogen receptor in human breast carcinomas. Evaluation of 130 cases and review of the literature regarding concordance with biochemical assay and clinical relevance. Arch Surg 125: 107–113, 1990
9. Alberts SR, Ingle JN, Roche PR, Cha SS, Wold LE, Farr GH, Krook JE, Wieland HS: Comparison of estrogen receptor determinations by a biochemical ligand assay and immunohistochemical staining with monoclonal antibody ER1D5 in females with lymph node positive breast carcinoma entered on two prospective clinical trials. Cancer 78: 764–772, 1996
10. Dowsett M, Daffada A, Chan CMW, Johnston SRD: Oestrogen receptor mutants and variants in breast cancer. Euro J Cancer 33: 1177–1183, 1997
11. Huang A, Pettigrew N, Watson P: Immunohistochemical assay for estrogen receptors in paraffin wax sections of breast carcinoma using a new monoclonal antibody. J Pathol 180: 223–227, 1996
12. Pertschuk LP, Feldman JG, Kim YD, Braithwaite L, Schneider F, Braverman AS, Axiotis C: Estrogen receptor immunocytochemistry in paraffin embedded tissues with ER1D5 predicts breast cancer endocrine response more accurately than H222Spy in frozen sections or cytosol-based ligand-binding assays. Cancer 77: 2514–2519, 1996
13. Nedergaard L, Christensen L, Rasmussen BB, Jacobsen GK: Comparison of two monoclonal antibodies for the detection of estrogen receptors in primary breast carcinomas. Pathol Res Pract 192: 983–988, 1996
14. Huang A, Leygue E, Snell L, Murphy L, Watson P: Expression of estrogen receptor variant mRNAs and determination of estrogen receptor status in human breast cancer. Am J Pathol 150: 1827–1833, 1997
15. Dotzlaw H, Alkhalaf M, Murphy L: Characterization of estrogen receptor variant mRNAs from breast cancers. Mol Endocrinol 6: 773–785, 1992
16. Murphy LC, Hilsenbeck SG, Dotzlaw H, Fuqua SAW: Relationship of clone 4 estrogen receptor variant messenger RNA expression to some known prognostic variables in human breast cancer. Clin Cancer Res 1: 155–159, 1995
17. Pfeffer U, Fecarotta E, Arena G, Forlani A, Vidali G: Alternate splicing of the estrogen receptor primary transcript normally occurs in estrogen receptor positive tissues and cell lines. J Steroid Biochem 56: 99–105, 1996
18. Gotteland M, Desauty G, Delarue JC, Liu L, May E: Human estrogen receptor messenger RNA variants in both normal and tumor tissues. Mol Cell Endocrinol 112: 1–13, 1995
19. Leygue E, Watson P, Murphy L: Estrogen receptor variants in normal human mammary tissue. J Natl Cancer Inst 88: 284–290, 1996
20. Leygue E, Murphy L, Watson P: Triple primer polymerase chain reaction: a new way to quantify truncated mRNA expression. Am J Pathol 148: 1097–1103, 1996
21. Castles CG, Fuqua SAW, Klotz DM, Hill SM.: Expression of a constitutively active estrogen receptor variant in the estrogen receptor-negative BT-20 human breast cancer cell line. Cancer Res 53: 5934–5939, 1993
22. Pink JJ, Wu SQ, Wolf DM, Bilimoria MM, Jordan VC: A novel 80 kDa human estrogen receptor containing a duplication of exons 6 and 7. Nucleic Acids Res 4: 962–969, 1996
23. Madsen MW, Reiter BE, Lykkesfeldt AE: Differential expression of estrogen receptor mRNA splice variants in the tamoxifen resistant human breast cancer cell line, MCF-7/TAMR-1 compared to the parental MCF-7 cell line. Mol Cell Endocrinol 109: 197–207, 1995
24. Castles CG, Klotz DM, Fuqua SAW, Hill SM: Coexpression of wild type and variant estrogen receptor mRNAs in a panel of human breast cell lines. Br J Cancer 71: 974–980, 1995
25. Fuqua SAW, Chamness GC, McGuire WL: Estrogen receptor mutations in breast cancer. J Cell Biochem 51: 135–139, 1993
26. Daffada AA, Johnston SR, Smith IE, Detre S, King N, Dowsett M: Exon 5 deletion variant estrogen receptor messenger RNA expression in relation to tamoxifen resistance and progesterone receptor/pS2 status in human breast cancer. Cancer Res 55: 288–293, 1995
27. Villa E, Dugani A, Fantoni E, Camellini L, Buttafoco P, Grottola A, Pomper G, Santis MD, Ferrari A, Manenti F: Type of estrogen receptor determines response to antiestrogen therapy. Cancer Res 56: 3883–3885, 1996
28. Halachmi S, Marden E, Martin G, Mackay H, Abbondanza C, Brown M: Estrogen receptor associated proteins: possible mediators of hormone induced transcription. Science 264: 1455–1458, 1994
29. Yang NN, Venugopalan M, Hardikar S, Glasebrook A: Identification of an estrogen response element activated by metabolites of estradiol and raloxifene. Science 273: 1222–1225, 1996
30. Stierer M, Rosen H, Weber R, Hanak H, Auerbach L, Spona J, Tuchler H. Comparison of immunohistochemical and biochemical measurement of steriod receptors in primary breast cancer: Evaluation of discordant findings. Breast Cancer Res Treat 50: 125–134, 1998

Address for offprints and correspondence: Dr. Peter Watson, Department of Pathology, Faculty of Medicine, D212-770 Bannatyne Ave, University of Manitoba, Winnipeg, MB, R3E 0W3, Canada; *Tel:* (204)-789-3435; *Fax:* (204)-789-3931; *E-mail:* pwatson@cc.umanitoba.ca

Cancer Detection and Prevention, 23(3):245–253 (1999)

Classification of Breast Tumors by Grade and Steroid Receptor Status Using Pattern Recognition Analysis of Infrared Spectra

Michael Jackson, Ph.D.,[a] James R. Mansfield, M.Sc.,[a]
Brion Dolenko, M.Sc.,[a] Rajmund L. Somorjai, Ph.D.,[a]
Henry H. Mantsch, Ph.D.,[a] and Peter H. Watson, M.D.[b]

[a]Institute for Biodiagnostics, National Research Council Canada, Winnipeg, Manitoba, Canada; and [b]Department of Pathology, Faculty of Medicine, Health Sciences Center, University of Manitoba, Winnipeg, Manitoba, Canada

Address all correspondence and reprint requests to: Michael Jackson, Ph.D., Institute for Biodiagnostics, National Research Council Canada, 435 Ellice Ave., Winnipeg, Manitoba, Canada, R3B 1Y6.

Accepted for publication January 26, 1999.

ABSTRACT: Infrared (IR) spectroscopy applied to tissue sections yields complex spectra that provide a molecular fingerprint of the tissue. We have studied a cohort of 77 breast tumors by IR spectroscopy to develop an objective method for the assignment of grade of breast tumors. Although the major variations between spectra from different tumors were in absorptions arising from triglycerides (adipose tissue) and collagen, subtle changes in spectra could be detected that were independent of cellularity and tissue composition. Using a specific multivariate pattern recognition strategy to associate these changes in spectra with different tumor grades, we then were able to accurately reclassify tumors by grade (87% accuracy; $\kappa = 0.835$). A similar approach allowed classification of steroid receptor status (93% accuracy; $\kappa = 0.852$). We conclude that IR spectroscopy may have clinical utility in the objective assignment of breast tumor grade.

KEY WORDS: breast cancer grade, classification strategy, diagnosis, estrogen receptors, Fourier transform infrared spectroscopy, multivariate analysis, progesterone receptors.

I. INTRODUCTION

The clinical management of breast cancer patients is guided by several clinical and pathological measures of tumor growth, hormone response, and metastatic potential.[1] These indicators include tumor size, histologic type, grade, stage, and the presence of steroid receptors.[2,3] However, an increasing proportion of cases now present at an earlier stage as axillary node negative or preinvasive *in situ* disease where determination of the likelihood of local or distant recurrence becomes even more dependent on assessment of the inherent biology of the tumor.[2] Improvement in the accuracy of this assessment may in part come from better methods for the determination and integration of known prognostic factors. Amongst these, tumor grade has been shown by some to be an excellent indicator of biological potential.[4] However, reliable assessment of tumor grade has been hindered in the past by difficulties in determining reproducible criteria and the problem of interobserver variability.[5]

In search of improved benchmarks by which to measure characteristics within tumor tissue that would allow accurate assignment into grade categories, we have used Fourier transform infrared (FTIR) spectroscopy to assess frozen breast tumor sections. FTIR spectroscopy is based upon the absorption of infrared (IR) light by covalent bonds as they vibrate. The frequency of light that is absorbed depends upon the nature of the bond between the atoms (e.g., C-C versus C=C), the atoms involved in the bond (e.g., C=C versus C=O), the type of vibration (e.g., bending versus stretching), and factors such as the strength of any hydrogen bonding interactions. Furthermore, as with other forms of optical spectroscopy, the amount of light absorbed by a vibrating bond is linearly related to concentration. The infrared spectrum of a sample is therefore a direct indicator of its chemi-

0361-090X/99/$14.00

cal composition. In biological systems, functional groups that strongly absorb infrared light include C=O, N-H, C-H, and P=O groups. The intensity of the absorption bands in the infrared spectrum of a tissue sample therefore provides information concerning lipid, protein, and nucleic acid content of the sample, whereas the frequency of the absorption provides information relating to structure/conformation and intermolecular interactions. In other words, the infrared spectrum of tissues provides information that reflects the biochemistry of the tissue.

If the infrared spectrum of a tissue sample can provide information with regard to tissue biochemistry, then the changes in tissue biochemistry accompanying a disease process should be reflected in changes in the infrared spectrum of the diseased tissue. We have recently demonstrated that this is indeed so, identifying spectroscopic features characteristic of Alzheimer's disease,[6] chronic lymphocytic leukemia,[7] multiple sclerosis,[8] and scar formation in ventricular tissue following infarction.[9] By extension, it is reasonable to speculate that tumors of differing grades will also show different spectroscopic features, in principle allowing characterization of tumor spectra by grade.

IR spectra are thus characterized by a high information content that can be viewed and analyzed from different perspectives. In this respect IR spectroscopy is not unlike light microscopy, but this information relates directly to tissue biochemistry. We have therefore investigated the possibility of using FTIR spectroscopy to derive parameters from tumor sections analogous to but more objective than light microscopic tumor grade. This was achieved using a novel, multivariate classification (pattern recognition) strategy specifically developed to deal with complex spectra.

II. MATERIALS AND METHODS

A. Sample Preparation and Data Acquisition

A cohort of 77 cases of invasive ductal breast carcinomas for which full historical data (including case records, slides, paraffin blocks, and tumor tissue) was available was selected for study from the Manitoba Breast Tumor Bank. These were chosen primarily on the basis of tumor grade to provide three equivalent groups at each of three grade levels. All tumors were graded uniformly by a single pathologist according to the Nottingham grading system[4] applied to an H&E section from a formalin-fixed and paraffin-embedded tissue block. Additional criteria included good histologic tissue quality and the presence of invasive tumor in >30% of the surface of the block selected for study. In all cases, the percentage of tumor cells, normal ducts/lobules, fibrous stroma, and fat was also estimated and scored as a percentage of the surface area of the tissue section to allow analysis of the effect of cellularity and stromal compostion and interpretation of spectra. The estrogen and progesterone receptor status was assessed by ligand binding assay performed on an adjacent portion of tumor tissue and shown to be positive for 45 and 49 tumors, respectively. Tumors were considered estrogen and/or progesterone receptor positive if the receptor concentration was greater than 3 fg/mg or 15 fg/mg, respectively. Thin frozen sections (10 μm) were then obtained in each case from frozen tissue blocks that corresponded to tissue immediately adjacent and mirror image to the paraffin sections.[10] Frozen sections were transported in dry ice to the laboratory and rapidly removed from their containers using cooled forceps, transferred to a CaF_2 window having a specially machined 10 μm depression, covered with a second CaF_2 window and mounted in a demountable cell holder. The use of a window with a machined depression ensured that when the tissue is lightly compressed during cell assembly, a constant sample thickness is obtained. The cell holder was placed in a Digilab FTS 60 A Fourier transform infrared spectrometer (Digilab Laboratories, Cambridge, MA) equipped with a liquid nitrogen–cooled mercury cadmium telluride detector and continuously purged with dry air. For each sample, 256 interferograms were collected, signal averaged, and Fourier transformed to generate spectra with a nominal resolution of 2 cm^{-1}. Absorptions from the CaF_2 windows and residual water vapour were interactively subtracted from all spectra.

B. Data Processing

Given the complex manner in which biochemical information is encoded in the spectra, in addition to

traditional methods of spectral analysis, we have developed a new and specific strategy to extract the information relevant for classification of tumor spectra. The strategy was implemented in three stages: (i) a preprocessing stage in which the spectral subregions most useful for classification were determined,[11] (ii) regional classification, and (iii) aggregation of classifier outcomes.[12,13] Particular emphasis has been placed on developing robust, reliable classifiers. This was achieved by a specific cross-validation methodology, based on bootstrapping,[14] applied at each of the three stages. For further details, see Appendix 1. To ensure that classification was not based upon variations in sample thickness, spectra were normalized with repect to integrated area prior to analysis.

III. RESULTS

Infrared spectra of sections from three low-grade breast tumors (Nottingham grade score: 3–5) normalized with respect to maximum absorption intensity are shown in Figure 1. The most noticeable feature of each spectrum is the complexity, with prominent absorptions in almost all regions of the spectrum. The region between 2700 and 3100 cm^{-1} is populated by absorptions arising from C-H vibrations of lipids, proteins and DNA.[15–17] Obvious differences exist in both the absolute and relative intensities of these absorptions in the three spectra, which must be related to compositional differences among the three tumors. The absolute intensity of each of the C-H stretching absorptions increases progressively from Figure 1A to Figure 1C, indicating increasing concentrations of fatty acyl chains. In addition, the relative intensity of the absorptions at around 2950 to that at 2920 cm^{-1} changes. In Figure 1A, the relative intensity is highest (similar to that seen for pure phospholipid systems), progressing to the lowest relative intensity in Figure 1(C) (similar to that seen for isolated proteins). These results suggest that the tissue section giving rise to Figure 1C is lipid/acylglyceride rich, the one giving rise to Figure 1A is protein rich, and the one giving rise to Figure 1B contains significant amounts of both lipids and/or acylglyceride and protein.

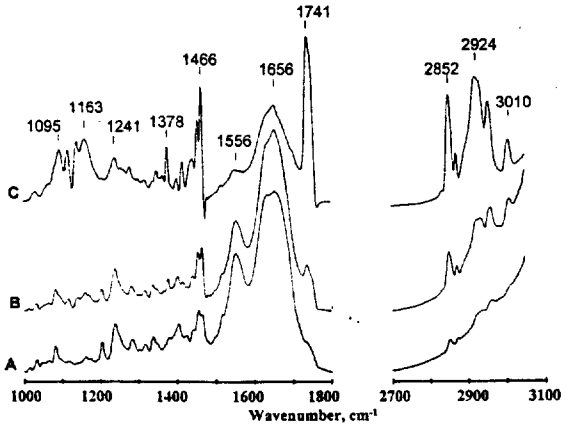

FIGURE 1. Infrared spectra of 10-μm sections of low-grade (Nottingham grade 3–5) breast tumors.

Variations in lipid/acylglyceride and protein content are confirmed by analysis of spectra between 1000 and 1800 cm^{-1}. Absorptions at 1741, 1466, 1378, 1163, and 1095 cm^{-1} in Figure 1C arise from C=O, CH_2, CH_3, and C-O-C vibrations of phospholipids and/or acylglycerides.[15–17] Phospholipids exhibit two intense absorptions at 1240 and 1080 cm^{-1}, arising from PO_2^- vibrations of phosphodiester groups.[15] These characteristic absorptions are absent in Figure 1, suggesting that the material giving rise to the intense C-H, C=O, and C-O-C absorptions is predominantly acylglyceride rather than phospholipid. This observation is supported by the known storage of fatty acids in the breast as acylglycerides. The intensity of the acylglyceride absorptions in Figure 1C is much greater than that seen in Figure 1A, with the intensity in Figure 1B again being intermediate.

The intensity of the strong absorption at 1656 cm^{-1}, termed the amide I absorption and arising from C=O vibrations of the amide groups of polypeptide backbones, also varies between tissue sections. This variation suggests that different tumor sections have different protein content. In addition to changes in intensity, differences in the shape of the amide I are also apparent. A distinct absorption is apparent at around 1634 cm^{-1} in Figure 1A, which is reduced in intensity in Figure 1B and completely absent from Figure 1C. As the position of amide I absorptions is sensitive to protein conformation,[18] this implies conformational changes in tissue proteins or the expression of a new set of proteins. Changes in intensity in the 1634 cm^{-1} region of the spectrum of cancerous tissue have been suggested to arise from an altered proportion of β-sheet secondary structures in such tissue. However, we have shown that such spectral changes in a variety of tissues can be explained based

on an increase in the type I collagen content of tissue—for example, in the rat myocardium following an infarct.[9] In addition, the presence of collagen was accompanied by the appearance of absorptions at 1033, 1082, 1204, 1240, 1280, and 1338 cm^{-1}. Similar absorption bands can easily be identified in Figure 1 A and B, suggesting that the altered shape and increased intensity of the amide I absorptions in Figure 1 A and B is indeed related to the presence of type I collagen in these tumor sections.

Based upon these results, human breast tumors appear to fall into three classes upon visual inspection of their IR spectra: class I, characterized by high acylglyceride content and little collagen; class II, characterized by the presence of appreciable amounts of both acylglyceride and collagen; class III, characterized by large amounts of collagen and little or no acylglyceride. The differences among these three classes do not arise as a result of the disease being at different stages in the different tumors, as the tumors were matched with respect to grade, but result from normal spatial variations in the composition of breast tissue.

IV. DISCUSSION

Given that breast tumors of similar grade show such large spectral variation as a consequence of normal variations in histology, this raises the question, Can one detect the much less pronounced changes in the spectrum expected as a consequence of the progression of the disease? Many spectral changes expected to accompany disease progression may be masked by variations in acylglyceride and/or collagen content. For example, progression to a high-grade tumor is accompanied by the appearance of nuclear abnormalities (e.g., altered chromosomal structure, increased DNA content). The infrared absorption bands most useful in studies of DNA arise from the stretching vibrations of phosphodiester groups seen at 1080 and 1240 cm^{-1}. Since this region of the spectrum is dominated by absorptions from both collagen (see Figure 1A) and acylglycerides (see Figure 1C), the changes in cellular DNA that accompany disease progression may be masked by the large changes in collagen and acylglyceride content which are possible between tumors. Changes in protein expression accompanying the disease process, expected to be manifested in changes in the amide I absorption, may be masked by differences in collagen content. Finally, changes in cell membrane properties that would be manifested as changes in C-H absorptions may be masked by differences in acylglycerides content. These problems are highlighted in a number of studies which have attempted to interpret differences among spectra of normal and neoplastic colon,[19] bladder,[20] skin,[21] and breast tissue[22,23] in terms of such differences in DNA hydrogen bonding interactions and membrane and protein structural properties. However, inspection of the data presented in these studies clearly indicates that the changes the authors describe are in fact related to changes in collagen (colon, bladder, and skin) or adipose tissue content (breast).

An alternative approach to visual discrimination among spectra of tumors of different grade is to use the power of modern classification methods, which can assess variations in many variables simultaneously. In the case of spectra, these variables may include the absolute intensity of one or more absorptions, the position of one or more absorptions, the relative intensities of two absorptions, the width of one or more absorptions, the relative width of two absorptions, and so on. To decode complex information from spectra, typically at least 10 such variables are required to adequately describe differences between groups of measurements. This is a particularly challenging task when the changes under investigation are subtle and masked by other, nonspecific features such as noise and redundant or irrelevant information. However, such subtle changes in spectra can indeed be detected by multivariate pattern recognition methods, including hierarchical clustering, linear discriminant analysis, and artificial neural network analysis.[24,25] Such multivariate methods are powerful tools for identifying patterns that characterize different classes of spectra (hence the term "pattern recognition") based upon the comparison of a large number of variables that describe the spectra (hence the term "multivariate").

Multivariate pattern recognition methods are divided into "unsupervised" and "supervised" categories. The former, such as hierarchical clustering or fuzzy clustering, classify spectra based upon the degree of their overall similarity, and require no training. We have recently successfully applied such techniques to the classification of control and Alzheimer's-diseased central nervous system tissue,[24,25] and

benign and leukemic leukocytes.[7] However, in the present study application of cluster analysis produced two distinct groups of spectra, corresponding to spectra containing either significant contributions from collagen or from adipose tissue (not shown), with no correlation between these two clusters and any clinical criteria (e.g., tumor grade).

The lack of success of such unsupervised methods, which are generally driven by gross differences, is not surprising given the fact that the changes expected as a result of the clinical condition are subtle compared to the large changes resulting from normal histologic variation. Supervised pattern recognition methods make use of the fact that the investigator often has available a substantial amount of biochemical or clinical information concerning the samples from which the spectra were obtained. In short, we have in our possession the "class identities" of the samples with which to train our classifier. This trained classifier is then used to predict the class identity of unknown samples. We have previously applied such methods with great success to the classification of spectra of synovial fluid samples from control and arthritic joints.[26,27] We applied these more discriminatory supervised pattern recognition methods to our data. Unfortunately, even this approach was less than satisfactory, and we had to develop the novel classification strategy described in the Appendix.

Tumors were graded using the Nottingham scale[4] and classified as low grade (score: 3–5), intermediate grade (score: 6–7), or high grade (score 8–9).[8,9] The results of application of our robust classification strategy to spectra based upon tumor grade are presented in Table I. Numbers in rows represent the results of histopathological classification of the tumors, whereas numbers in columns represent the classification predicted by the trained classifier. Numbers on the diagonal (in bold italics) show the number of correctly classified spectra. Thus, for 21 tumors pathologically classified as low grade, 19 (90.5%) gave rise to spectra which could be correctly classified as arising from low-grade tumors. For intermediate-grade tumors, the accuracy of the classification was significantly reduced, only 26 of 34 spectra (76.5%) were correctly classified. In fact, perhaps not surprisingly, the accuracy of the classification of the intermediate-grade tumors was lowest of the three classifications attempted. It is interesting, however, that the classifier always misclassified intermediate-grade tumors as high-grade tumors, and never as low-grade tumors. All 22 high-grade tumors were correctly classified. The overall accuracy of the method was 87%, with 67 of 77 tumors correctly classified. Also included in Table I is κ, a chance-corrected measure of agreement, which indicates the probability that the tumor grade predicted by this method agrees with the clinical diagnosis. If the prediction was generated at random, the agreement measure would be zero, whereas for perfect classification the value would be unity. The agreement measure for this data set is 0.835.

The Nottingham grade is derived from a composite score of several quite different parameters that can be assessed under a light microscope. These include assessment of the arrangement of cells in tubule formations, nuclear morphology, and mitotic activity, and can be time-consuming to assess if done properly by counting mitoses in multiple fields. Nevertheless tumor grade as assessed in this fashion has been shown to be able to classify tumors into categories that show distinct biological potential as indicated by patient survival rates. However, as reviewed by Robbins et al.[5] concordance in grading score between pathologists in published series can range from 54 to 78%. Reproducibility between pathologists at differ-

TABLE I
Results of Classification of Breast Tumor Spectra by Grade

	L	I	H	% accuracy	SP (%)	PPV (%)
L	***19***	1	1	90.5	100	100
I	0	***26***	8	76.5	97.6	94.1
H	0	0	***22***	100	85.9	77.9

Note: Numbers in rows represent the pathological classification of tumors; results in columns are the calculated classifications. L = low grade; I = intermediate grade; H = high grade; SP = specificity; PPV = positive predictive value. Bold italics indicate correct classifications. See text for more details. Overall accuracy = 87%, κ = 0.835.

TABLE II
Results of Classification of Breast Tumor Spectra According to Estrogen Receptor Presence (+ve) or Absence (–ve)

	+ve	–ve	% accuracy	SP (%)	PPV (%)
+ve	***16***	2	88.9	96.3	96.0
–ve	1	***26***	96.3	88.9	89.2

Note: SP = specificity; PPV = positive predictive value. Numbers in rows represent the immunological classification of tumors; results in columns are the calculated classifications. Bold italics indicate correct classifications. See text for more details. Overall accuracy = 93.3%; $\kappa = 0.852$.

TABLE III
Results of Classification of Breast Tumor Spectra According to Progesterone Receptor Presence (+ve) or Absence (–ve)

	+ve	–ve	% accuracy	SP (%)	PPV (%)
+ve	***23***	1	95.8	84.0	85.7
–ve	4	***21***	84.0	95.8	95.3

Note: SP = specificity; PPV = positive predictive value. Numbers in rows represent the immunological classification of tumors; results in columns are the calculated classifications. Bold italics indicate correct classifications. See text for more details. Overall accuracy = 89.8%; $\kappa = 0.798$.

ent centers is of particular concern in the assessment of clinical trial results.[2,5,10] Even though a more standardized approach to grading of breast tumors may now be gaining acceptance, concordance among expert groups of pathologists in grading standard formalin-fixed paraffin-embedded sections remains below 75%, even after training.[5] Therefore, our results, which show a high degree of concordance between a single pathologist and FTIR spectroscopic grade, suggest that this new methodology may provide an alternative approach to microscopic grading and improved standardization of a valuable prognostic parameter. It should be made clear however, that the present study was based on a tumor series that had been selected to provide approximately equivalent representation of low, intermediate and high grade tumors. Previous studies of unselected cases may have included relatively few low-grade tumors for which the degree of concordance between pathologists is higher.[5]

We also examined the relationship between infrared spectra and steroid receptor status. The results of our classification of tumors based upon the ER/PR status is presented in Tables II and III. For estrogen receptors, correct classification as either receptor positive or negative was achieved for 93.3% of tumors ($\kappa = 0.852$), with classification of estrogen negative tumors being superior to classification of receptor positive tumors (88.9 vs. 96.3%). This situation was reversed for progesterone receptors, with 95.8% of receptor-positive tumors being correctly classified compared with 84% of receptor-negative tumors, and the overall accuracy of prediction was slightly reduced (89.8%; $\kappa = 0.798$). It should be stressed that it is unlikely that steroid receptors *per se* are being detected, as the concentration of the receptors (fg/mg tissue) is significantly below the detection limit of infrared spectroscopy. Rather, it is most likely the consequences of the presence or activation of the receptors, such as protein phosphorylation, that are being detected.

The spectral regions selected as the most diagnostic for the prediction of tumor grade and hormone receptor status are shown as the shaded areas superimposed over class average spectra (produced by calculating the arithmetic mean of all spectra in each class) in Figure 2 and Figure 3. For the prediction of tumor grade, diagnostic subregions were only found in the low-frequency (1077–1258 cm^{-1}) region of the

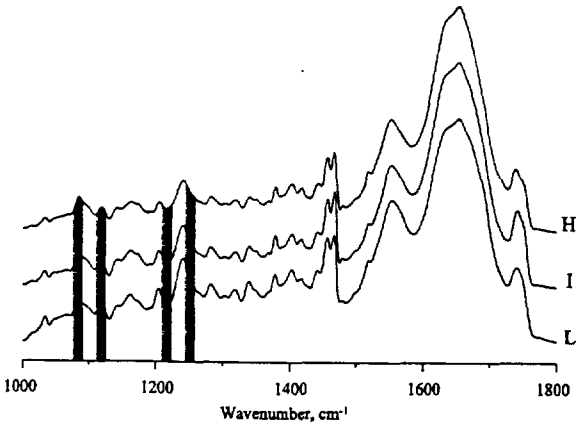

FIGURE 2. Class average infrared spectra of low- (L, Nottingham grade 3–5), intermediate- (I, Nottingham grade 6–7), and high- (H, Nottingham grade 8–9) grade breast tumors. Regions selected for use by the multivariate analysis strategy are indicated by shaded areas.

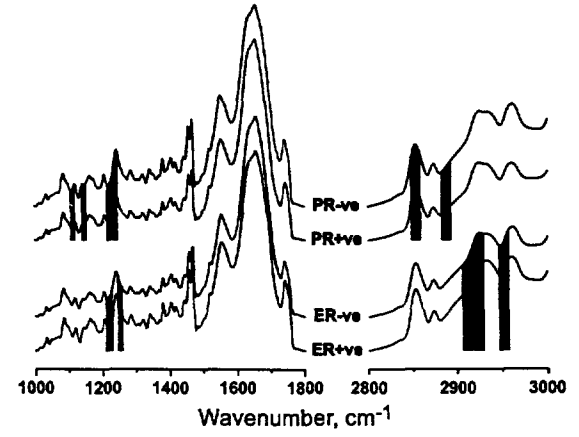

FIGURE 3. Class average spectra of estrogen receptor positive (ER+ve) and negative (ER-ve) and progesterone receptor positive (PR+ve) and negative (PR-ve) breast tumors. Regions selected for use by the multivariate analysis strategy are indicated by shaded areas.

spectrum. In contrast, the prediction of estrogen and progesterone receptor status required subregions in both high- and low-frequency regions of the spectrum (see Figure 3). Although it is difficult to determine exactly the biochemical significance of the spectral regions selected, three interesting points emerge. 1 Classification of tumors by grade, which is strongly influenced by assessment of nuclear size and morphology, was optimal using only spectral regions in which absorptions from nucleic acids are typically found (although as stressed above, collagen and adipose tissue also absorb strongly in these spectral regions). 2 Classification of tumors by receptor status required more spectral regions (i.e., more information) than prediction of tumor grade. 3 Different spectral subregions were selected for classification of tumors by grade, estrogen receptor status, and progesterone receptor status, indicating that, as expected, different biochemical events were detected in each case.

In summary we have shown that infrared spectroscopy, combined with appropriate multivariate classification methods and strategies, can be used to reliably determine the grade of human breast tumors and to classify tumors according to hormone receptor status with an accuracy of about 90%. Tumor grade and receptor status can be obtained from the same spectrum. A number of steps may be taken to improve accuracy. Most obviously, increasing the size of our database should improve accuracy of prediction. An alternative approach to the characterization of sections of breast tumors is the analysis of materials extracted from tumors. This approach has met with some success in the prediction of the biological potential of breast tumors based upon FTIR spectra of extracted DNA.[28,29] However, the extraction of DNA is time-consuming, and the structure (and thus spectroscopic properties) of the DNA may be modified during extraction. In contrast, the method described here requires no extraction and is rapid, requiring only 2–3 min to perform.

The major advantage of this novel approach to the classification of breast tumors will be standardization. The method can readily be trained on data that represented a consensus diagnosis based upon the classifications of a board of pathologists. An instrumental method using such trained data would then in essence provide practitioners with a reliable diagnosis based upon this consensus, and different laboratories analyzing the same tissue sample using such an instrument would achieve the same diagnosis. Thus, variability is removed, and consistent and reliable classification/prediction may be achieved. The clinical utility of such a technique warrants further investigation.

REFERENCES

1. McGuire WL. Prognostic factors for recurrence and survival in human breast cancer. Breast Cancer Res Treat 1987; 10: 5–9.

2. McGuire WL, Clark GM. Prognostic factors and treatment decisions in axillary-node-negative breast cancer. N Engl J Med 1992; 326:1756–1761.
3. Simpson JF, Page DL. Prognostic value of histopathology in the breast. Semin Oncol 1992; 19:254–262.
4. Elston CW, Ellis IO. Pathological prognostic factors in breast cancer. I. The value of histological grade in breast cancer: Experience from a large study with long-term follow-up. Histopathol 1991; 19:403–410.
5. Robbins P, Pinder S, de Klerk N, et al. Histological grading of breast carcinomas. A study of interobserver agreement. Hum Pathol 1995; 26:873–879.
6. Choo LP, Wetzel DL, Halliday WC, et al. In situ characterisation of β-amyloid in Alzheimer's diseased tissue by synchrotron Fourier transform infrared spectroscopy. Biophys J 1996; 71:1672–1679.
7. Schultz CP, Liu KZ, Johnston JB, et al. Study of chronic lymphocytic leukemia by FT-IR spectroscopy and cluster analysis. Leuk Res 1996; 20:649–655.
8. Choo LP, Jackson M, Halliday WC, et al. Infrared spectroscopic characterisation of multiple sclerosis plaques in the human central nervous system. Biochim Biophys Acta 1993; 1182:333–337.
9. Liu KZ, Jackson M, Sowa MG, et al. Modification of the extracellular matrix following myocardial infarction monitored by FTIR spectroscopy. Biochim Biophys Acta 1996; 1315:73–77.
10. Stenkvist B, Westman-Naeser S, Vegelius J, et al. Analysis of reproducibility of subjective grading systems for breast carcinoma. J Clin Pathol 1979; 32:979–985.
11. Somorjai RL, Dolenko B. Split and merge: A new composite strategy for classifying spectra. In: European Society for Magnetic Resonance in Medicine and Biology, 13th Annual Meeting, Prague. New York: Chapman & Hall; 1996; 323–324.
12. Somorjai RL, Nikulin AE, Pizzi N, et al. Computerized consensus diagnosis: A classification strategy for the robust analysis of MR spectra. I. Application to ^{1}H spectra of thyroid neoplasms. Magn Reson Med 1995; 33:257–263.
13. Wolpert DH. Stacked generalization. Neural Networks 1992; 5:241–259.
14. Efron B, Tibshirani RJ. An introduction to the bootstrap. In: Monographs on statistics and applied probability. Vol. 57. New York: Chapman & Hall; 1993.
15. Jackson M, Mantsch HH. Biomembrane structure from FT-IR spectroscopy. Spectrochimica Acta Rev 1993; 15:53–69.
16. Jackson M, Mantsch HH. FTIR spectroscopy in the clinical sciences. In: Clarke RJH, Hester RE, eds. Biomedical applications of spectroscopy. London: John Wiley & Sons; 1996: 185–215.
17. Jackson M, Mantsch HH. Biomedical infrared spectroscopy. In: Mantsch HH, Chapman D, eds. Infrared spectroscopy of biomolecules. New York: Wiley-Liss; 1996:311–340.
18. Jackson M, Mantsch HH. The use and misuse of FTIR spectroscopy in the determination of protein secondary structure. CRC Crit Rev Biochem Mol Biol 1995; 30:95–120.
19. Rigas B, Morgello S, Goldman IS, et al. Human colorectal cancers display abnormal Fourier transform infrared spectra. Proc Natl Acad Sci U S A 1990; 87:8140–8144.
20. Lin AY, Liang RC, Hsu HS, et al. Evidence of possible carcinogenesis during conformational changes in bladder mucosa induced by bladder outlet obstruction. Cancer Lett 1995; 79:221–226.
21. Wong PTT, Goldstein SM, Grekin RC, et al. Distinct infrared spectroscopic patterns of human basal cell carcinoma. Cancer Res 1993; 53:762–765.
22. Wallon J, Yan SH, Tong J, et al. Identification of breast carcinomatous tissue by near infrared reflectance spectroscopy. Appl Spectrosc 1994; 48:190–193.
23. Meurens M, Wallon J, Tong J, et al. Breast cancer detection by Fourier transform infrared spectrometry. Vibrational Spectrosc 1996; 10:341–346.
24. Choo LP, Mansfield JR, Pizzi N, et al. Infrared spectra of human central nervous system tissue: Diagnosis of Alzheimer's disease by multivariate analyses. Biospectroscopy 1995; 1:141–148.
25. Pizzi N, Choo LP, Mansfield JR, et al. Neural network classification of infrared spectra of control and Alzheimer's diseased tissue. Art Int Med 1995; 7:67–69.
26. Shaw RA, Kotowich S, Eysel HH, et al. Classification of arthritic disorders based upon near infrared spectra. Rheumatol Int 1995; 15:159–166.
27. Eysel HH, Jackson M, Nikhulin A, et al. A novel, nonsubjective diagnostic test for arthritis utilising FTIR spectroscopy and multivariate classification. Biospectroscopy 1997; 3:161–167.
28. Malins DC, Polissar NL, Nishikida K, et al. The etiology and prediction of breast cancer. Cancer 1995; 75:503–517.
29. Malins DC, Polissar NL, Gunselman SJ. Tumour progression to the metastatic state involves structural modifications in DNA markedly different from those associated with primary tumour formation. Proc Natl Acad Sci U S A 1996; 93: 14047–14052.
30. McLachlan GJ. Discriminant analysis and statistical pattern recognition. New York: John Wiley; 1992.

APPENDIX 1

For most classification studies the standard linear discriminant analysis (LDA) method[30] with the leave-one-out cross validation works well (with the proviso that the data were appropriately preprocessed). LDA is the classifier of choice due to its simplicity and speed. It explicitly determines the boundaries (defined by the equations for the linear combinations of attributes) that best separate the classes. Class assignment of any given spectrum involves computing its distance from all class centroids (i.e., the representative class average spectra) and allocating it to the class whose centroid is nearest. The "resubstitution" error (rE) is calculated by using all data to determine the optimum

LDA classifier. rE tends to be optimistically low, especially when the number of sample per class is small. The remedy is to make the classifier more realistic and robust with respect to classification error by cross-validation. One common cross-validation technique is called "leave-one-out" (LOO). It works by sequentially omitting one of the n samples, training a classifier using the remaining $n - 1$, assigning the sample that was left out of the training, and carrying out this process for all n samples. The average error committed by these n classifiers is never less than rE, and is a more realistic estimate of the true error rate. However, especially when n is relatively small and the number of spectra per class is widely different, LOO can be unreliable and still too optimistic. The more realistic approach of partitioning the n spectra into a "training" and a "test" set, optimizing the classifier on the training set and validating its classification power on the test set, can exacerbate the reliability problem, since we now use only $\sim n/2$ of the already few n samples. Furthermore, classification of a new sample, not in the original n, would involve assigning it to all $\sim n/2$-trained classifiers. This implies that these classifiers would have to be always available, creating awkward storage problems. The cross-validation approach we have implemented is designed to remedy these problems. It is a type of "bootstrapping" methodology. It consists of repeatedly partitioning, with replacement, the data into approximately equal-sized random training and test subsets. For each of the random training subsets, an optimal classifier is produced, and its accuracy validated on the random test subset. The process is repeated a number of times (25 times at the less critical preprocessing stages, 250 times for the final classifiers). The ultimate classifier is the average of these individual component classifiers. This approach eliminates storage problems, while effectively using all n samples. Its expected classification accuracy can be validated by how well it does on the entire n samples. Although any classifier could be used, LDA, because of its speed and robustness, was the choice for all classifiers, at all stages.

Preprocessing was found to be essential for developing reliable classifiers. The preprocessing method selects relevant features from the spectra by an optimal region selection (ORS) algorithm developed in-house.[11] ORS starts at one end of an N-point spectrum by selecting a window consisting of $M << N$ adjacent data points. Typically, $M = 10$–12. LDA with bootstrapping (25 random samples) is carried out with these M points as local attributes, and the average classification accuracy on the test subsets is recorded. The window is advanced by $M/2$ data points along the spectrum and the process repeated. When the spectra are fully traversed, the nonoverlapping subregions are sorted in decreasing order of accuracy. If the best subregion found satisfies a prescribed accuracy (typically $\geq 90\%$), the subregion selection process is terminated. This happens rarely, and thus the next stage is initiated. The best 6–8 subregions (comprising $6 \times M - 8 \times M$ data points) are tested in all possible combinations (i.e., all pairs, triplets, etc.). The most parsimonious combination (least number L of subregions, $L \leq 8$) that satisfies the accuracy criterion provides the feature set for our final classifier. Typically, $L = 3$–6 combined subregions ($3 \times M - 6 \times M$ data points) are found optimal. The final step is the verification of the accuracy and robustness of the ultimate classifier, using the derived attributes. This is done by carrying out 250 bootstrap steps and creating the averaged classifier. If even this process does not yield a satisfactory classifier, we invoke our classifier aggregation stage,[12] computerized consensus diagnosis (CCD). The idea behind CCD is to combine differently the L optimal subregions (i.e., $L \times M$ data points, $L = 3$–6) found earlier. Our implementation of classifier aggregation is called stacked generalization (SG).[13] SG works by presenting sequentially to classifier j the corresponding M attributes of a given spectrum and recording the C class assignment probabilities p_i^j, $i = 1,2,...,C$, $j = 1,2,...,L$, $\Sigma_i p_i^j = 1$ (C is the number of classes, L the number of classifiers). These $C \times L$ probabilities serve as the new input attributes to a higher level classifier. At this ultimate stage, 250 bootstrap samples are taken again to produce the final robust classifier. Note that SG generally reduces the total number of attributes, since $C < M$. In addition, the class assignment probabilities tend to be much less ambiguous, i.e., fewer spectra are classified ambiguously (unreliably).

British Journal of Cancer (1999) 79(5/6), 978–983

Article no. bjoc.1998.0156

Oestrogen receptor-α variant mRNA expression in primary human breast tumours and matched lymph node metastases

E Leygue[1], RE Hall[2], H Dotzlaw[1], PH Watson[3] and LC Murphy[1]

[1]Department of Biochemistry and Molecular Biology, University of Manitoba, Winnipeg, MB, Canada; [2]Department of Surgery, Flinders University of South Australia, Bedford Park, SA, Australia; [3]Department of Pathology, University of Manitoba, Winnipeg, MB, Canada

Summary We have shown previously that the relative expression of a truncated oestrogen receptor-α variant mRNA (ER clone 4) is significantly increased in axillary node-positive primary breast tumours compared with node-negative tumours. In this study, we have examined the relative expression of clone 4-truncated, exon 5-deleted and exon 7-deleted oestrogen receptor-α variant mRNAs in 15 primary breast tumour samples and in synchronous axillary lymph node metastases. Overall, there were no significant differences between the primary tumours and the matched metastases in the relative expression of these three specific variant mRNAs. Furthermore, the pattern of all deleted oestrogen receptor-α variant mRNAs appeared conserved between any primary and its matched secondary tumour.

Keywords: oestrogen receptor-α variants; breast cancer; metastasis

Multiple oestrogen receptor-α (ER) mRNA species have been identified in human breast cancer samples (Dowsett et al, 1997; Murphy et al, 1997*a*, *b*). The significance of these variant transcripts remains unclear. Although the ability to detect variant ER proteins encoded by such variant transcripts remains controversial (Park et al, 1996; Desai et al, 1997; Huang et al, 1997), alteration of expression of some variant ER mRNAs has been found to occur during both breast tumorigenesis (Leygue et al, 1996*a*, *b*) and breast cancer progression. With regard to the latter, we showed previously that the expression of the truncated, clone 4 variant (C4) ER mRNA (Dotzlaw et al, 1992) was significantly increased relative to wild-type (WT) ER mRNA in a group of primary breast tumours with multiple poor prognostic features compared with a group of primary breast tumours with good prognostic features (Murphy et al, 1995). The 'poor' prognostic features were defined as the presence of lymph node metastases at the time of surgery, large tumour size, lack of progesterone receptor (PR) expression and high S-phase fraction, while 'good' prognostic features were lack of nodal involvement, small tumour size, PR positivity and low S-phase fraction. In the same study, the relative expression of clone 4 ER variant mRNA was significantly higher in primary breast tumours that were PR– than in those that were PR+ (Murphy et al, 1995). This suggested that altered ER variant expression may be a marker of a more aggressive phenotype and lack of endocrine sensitivity in human breast cancer. As a prerequisite to addressing such a possibility, we have investigated the pattern of ER variant expression in a cohort of primary tumours and their matched, concurrent lymph node metastases.

Received 20 April 1998
Revised 3 July 1998
Accepted 14 July 1998

Correspondence to: LC Murphy

MATERIALS AND METHODS

Tumour selection and RNA isolation

Sections from 15 frozen primary human breast tumour samples and their matched frozen lymph node metastases were provided by the Manitoba Breast Tumour Bank (Winnipeg, MB, Canada). For the primary tumour samples, the ER levels, determined by ligand-binding assays, ranged from 0.8 fmol mg^{-1} protein to 89 fmol mg^{-1} protein with a median value of 17.5 fmol mg^{-1} protein. Thirteen tumours were ER+ and two were ER– (ER+ was defined as >3 fmol mg^{-1} protein). PR levels determined by ligand-binding assays ranged from 2.9 fmol mg^{-1} protein to 112 fmol mg^{-1} protein with a median value of 12.6 fmol mg^{-1} protein. Nine tumours were PR+ and 6 were PR– (PR+ was defined as > 10 fmol mg^{-1} protein). ER and PR values were available for only four of the lymph node metastases and the ER and PR status as defined by ligand binding did not differ from their matched primary tumour. RNA was extracted from the sections using Trizol reagent (Gibco/BRL, Ontario, Canada) according to the manufacturer's instructions.

For validation of triple-primer polymerase chain reactions (TP-PCR) by comparison with RNAase protection assays, a second cohort of human breast tumour specimens (25 cases) was also obtained from the Manitoba Breast Tumour Bank. Twenty of these tumours were ER+, as determined by ligand-binding assay, with values ranging from 4.5 to 311 fmol mg^{-1} protein (median 93 fmol mg^{-1}). The five remaining cases were ER–, with values ranging from 0 to 1.8 fmol mg^{-1} protein (median 0.9 fmol mg^{-1}). Total RNA was extracted from frozen tissues using guanidinium

thiocyanate as previously described (Murphy and Dotzlaw, 1989). The integrity of the RNA was confirmed by denaturing gel electrophoresis as previously described (Murphy and Dotzlaw, 1989).

RNAase protection assay

Antisense riboprobes spanning the point at which the C4 ER mRNA sequence diverges from the WT ER mRNA sequence (Dotzlaw et al, 1992) were synthesized as previously described (Dotzlaw et al, 1990). The level of C4 ER mRNA and WT ER mRNA in 10 μg of total RNA was determined using an RNAase Protection Assay kit (RPA II, Ambion, Austin, TX, USA) following the manufacturer's instructions. Briefly, RNA was denatured at 80°C for 5 min in the presence of 5×10^5 d.p.m. ^{32}P-labelled riboprobe, then hybridized at 42°C for 16 h. Following RNAase digestion, samples were electrophoresed on 6% acrylamide gels containing 7 M urea, dried and autoradiographed.

To quantify C4 and WT ER mRNAs within breast tumour samples, a standard curve was established in each assay. C4 and WT ER mRNAs (30, 125, 500 pg C4 RNA and 125, 500, 2000 pg WT ER RNA) synthesized using T7 RNA polymerase were purified on a Sephadex G-50 column and quantitated spectrophotometrically. WT ER RNA was transcribed from linearized pHEO, which contains the entire WT ER coding sequence but is missing the 3′-untranslated portion of the ER mRNA [(kindly provided by P Chambon, Strasbourg, France (Green et al, 1986)]. Full-length C4 RNA was transcribed from linearized pSK-C4 (Dotzlaw et al, 1992). Standard RNAs were analysed together in the same assay as the breast tumour mRNAs. Bands corresponding to the C4 ER mRNA and WT ER mRNA protected fragments were excised from the gel and counted after addition of 5 ml scintillant (ICN Pharmaceuticals, Inc., Irvine, CA, USA) in a scintillation counter (Beckman Instruments, Inc., Fullerton, CA, USA). For each sample, absolute amounts of C4 and WT ER mRNA were determined from the standard curve.

Reverse transcription, PCR and triple-primer (TP) PCR

For each sample, 1 μg of total RNA was reverse transcribed in a final volume of 15 μl as described previously (Leygue et al, 1996*a*). One microlitre of the reaction mixture was taken for subsequent amplification.

The primers and PCR conditions for the long-range PCR were as previously described (Leygue et al, 1996*c*). The primers and PCR conditions for measuring the relative expression of exon 5-deleted and exon 7-deleted ER transcripts relative to WT ER transcripts were as previously described (Leygue et al, 1996*a*).

The TP-PCR conditions were similar to those previously described (Leygue et al, 1996*b*) with minor modifications. ERU (5′-TGTGCAATGACTATGCTTCA-3′, sense, located in WT ER exon 2; 792–811, as numbered in Green et al, 1986) and ERL (5′-GCTCTTCCTCCTGTTTTTAT-3′, antisense, located in WT ER exon 3; 940–921) primers allowed amplification of a 149-bp fragment corresponding to WT ER mRNA. The C4-specific primer (C4L, 5′-TTTCAGTCTTCAGATACCCCAG-3′, antisense; 1336–1315, as numbered in Dotzlaw et al, 1992) spans the only region of the C4 unique sequence that does not have any homology with repetitive LINE-1 sequences (Dotzlaw et al, 1992). ERU and C4L allowed amplification of a 536-bp fragment corresponding specifically to C4 ER variant mRNA.

PCR amplifications were performed in a final volume of 10 μl in the presence of 20 mM Tris-HCl (pH 8.4), 50 mM potassium chloride, 2 mM magnesium chloride, 0.2 mM dATP, 0.2 mM dTTP, 0.2 mM dGTP, 0.2 mM dCTP, 4 ng μl^{-1} of each primer (ERU, ERL and C4L), 0.2 units of *Taq* DNA polymerase (Gibco-BRL) and 1 μCi of [α-^{32}P] dCTP (3000 Ci mmol^{-1}, ICN Pharmaceuticals, Irvine, CA, USA). Each PCR consisted of 30 cycles (1 min at 94°C, 30 s at 60°C and

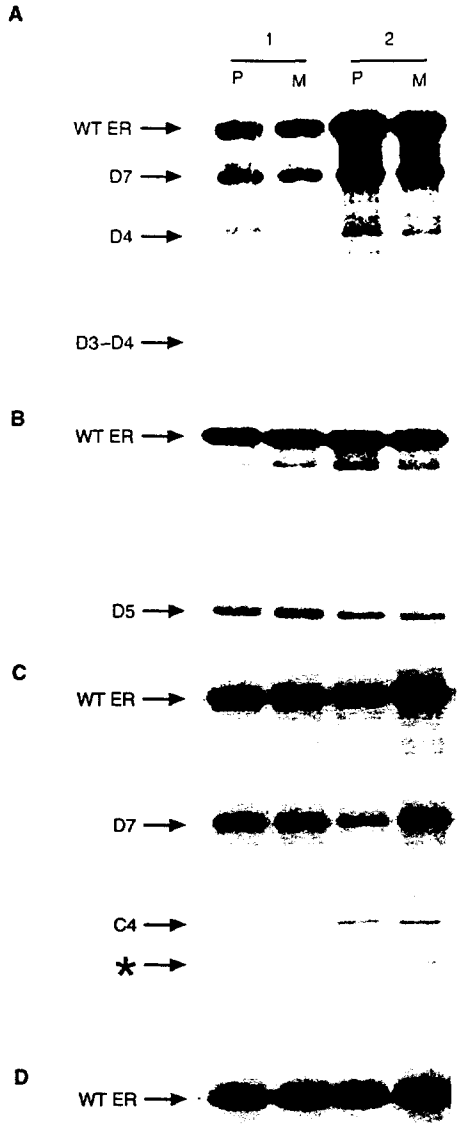

Figure 1 (**A**) Autoradiogram of long-range RT-PCR (Leygue et al, 1996*c*) results from two samples of primary breast tumours (P) and their matched concurrent lymph node metastase (M). WT ER is the expected product corresponding to the WT ER mRNA; D7 is the expected product corresponding to the exon 7-deleted ER variant mRNA; D4 is the expected product for the exon 4-deleted ER mRNA; D3-4 is the expected product for the exon 3+4-deleted ER mRNA; D4/7 is the expected product for the exon 4+7-deleted ER mRNA. (**B**) Autoradiogram of RT-PCR results from two samples of primary breast tumours (P) and their matched concurrent lymph node metastase (M). D5 is the expected product corresponding to the exon 5-deleted ER variant mRNA. WT ER is the expected product corresponding to the WT ER mRNA. (**C**) Autoradiogram of RT-PCR results from two samples of primary breast tumours (P) and their matched concurrent lymph node metastase (M). D7 is the expected product corresponding to the exon 7-deleted ER variant mRNA. WT ER is the expected product corresponding to the WT ER mRNA. (**D**) Autoradiogram of TP-PCR results from two samples of primary breast tumours (P) and their matched concurrent lymph node metastase (M). C4 is the expected product corresponding to the clone 4 ER variant mRNA. WT ER is the expected product corresponding to the WT ER mRNA. *Band coamplified with C4 and WT ER and shown to correspond to an exon 2-duplicated ER variant mRNA

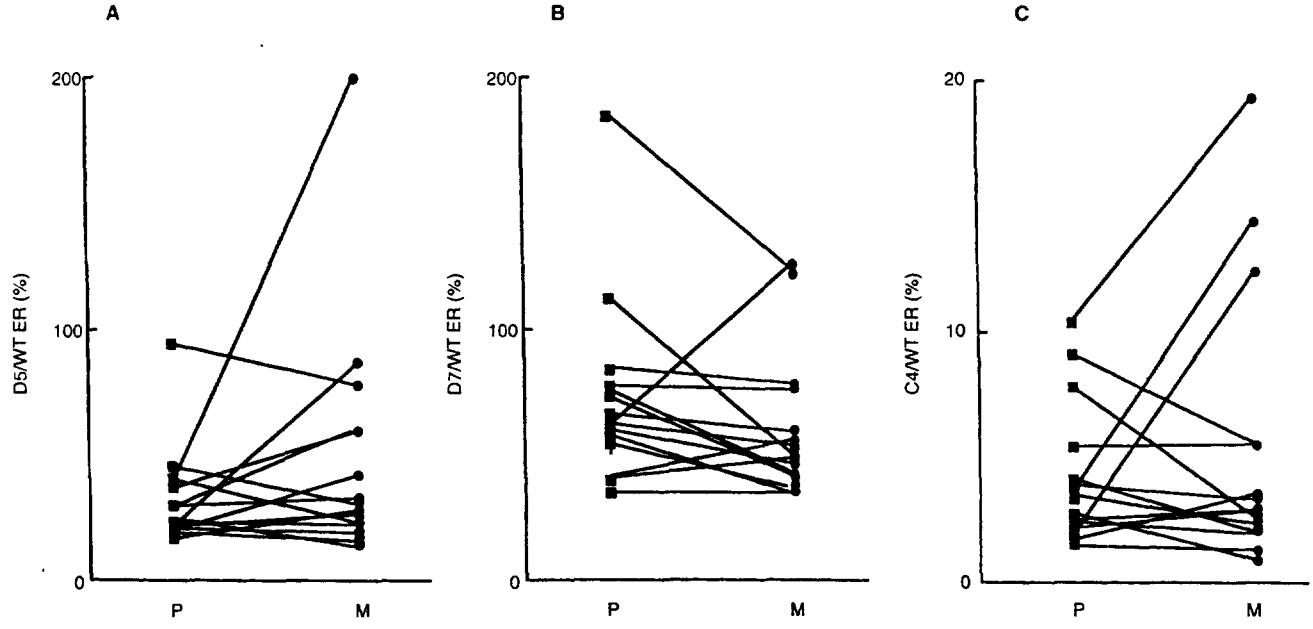

Figure 2 (**A**) Quantitative comparison of the relative expression of exon 5-deleted variant ER mRNA in primary (P) human breast tumours and their concurrent matched lymph node metastases (M). For each sample, the mean of three independent measures of exon 5-deleted ER relative expression expressed as a percentage of the corresponding WT ER signal was determined as described in the Materials and methods section. (**B**) Quantitative comparison of the relative expression of exon 7-deleted variant ER mRNA in primary (P) human breast tumours and their concurrent matched lymph node metastases (M). For each sample, the mean of three independent measures of exon 7-deleted ER relative expression expressed as a percentage of the corresponding WT ER signal was determined as described in the Materials and Methods section. (**C**) Quantitative comparison of the relative expression of clone 4 variant ER mRNA in primary (P) human breast tumours and their concurrent matched lymph node metastases (M). For each sample, the mean of three independent measures of clone 4 relative expression expressed as a percentage of the corresponding WT ER signal was determined as described in the Materials and Methods section

1 min at 72°C) using a thermocycler (Perkin Elmer). Four microlitres of the reaction mix was then denatured by addition of 6 µl of 80% formamide buffer and boiling before electrophoresis on 6% polyacrylamide gels containing 7 M urea (PAGE). Following electrophoresis, the gels were dried and exposed to Kodak XAR Film at –70°C with two intensifying screens for 2 h.

Quantification of RT-PCR and TP-PCR

Bands corresponding to the variant ER mRNA and WT ER mRNA were excised from the gel and counted after addition of 5 ml of scintillant in a scintillation counter. The variant signal was expressed as a percentage of the WT ER signal. It should be noted that the percentage obtained reflects the relative ratio of the variant to WT ER RT-PCR product and does not provide absolute initial mRNA levels. Validation of this approach was described previously (Daffada et al, 1994, 1995; Leygue et al, 1996*a*, *b*). At least two independent PCR assays were performed for each sample in the comparison of RNAase protection assay with TP-PCR assays. For assessment of matched primary and secondary breast tumour samples, at least two and in most cases three independent PCR reactions were performed and the mean determined.

The statistical significance of differences in the relative levels of expression of any single ER mRNA variant between primary tumour and lymph node metastasis was determined using the Wilcoxon signed-rank test.

RESULTS

Determination of the pattern of exon-deleted ER variant mRNA expression

Multiple ER variant mRNAs have been shown to be expressed in any one breast tissue sample (Leygue et al, 1996*a*; Murphy et al, 1997*a*, *b*). To investigate the pattern of multiple exon-deleted ER variant expression between primary breast tumours and their matched lymph node metastases, a long-range RT-PCR approach was used. This approach, based on the competitive amplification of wild-type and exon-deleted ER variant cDNAs, using primers annealing within exons 1 and 8, allows the evaluation of the relative pattern of expression of all exon-deleted ER variant transcripts present in any individual sample (Leygue et al, 1996*c*; Fasco, 1997). Typical results are shown in Figure 1A. The pattern of deleted ER mRNA expression between any one primary tumour and its matched lymph node metastasis was conserved.

Determination of the relative expression of exon 5-deleted and exon 7-deleted ER variant mRNA expression

Using a previously validated semiquantitative PCR approach (Leygue et al, 1996*a*), the measurement of the relative expression of specific individual exon-deleted ER variant mRNAs was also undertaken. Specifically, the relative expressions of exon 5-deleted

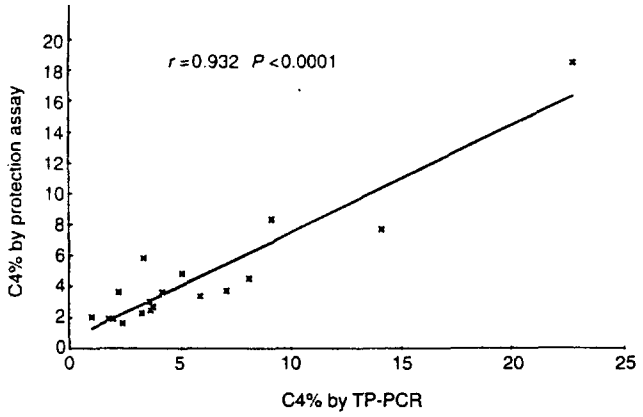

Figure 3 Linear regression analysis of clone 4 expression (expressed as a percentage of the corresponding WT ER expression) as determined by TP-PCR vs standardized RNAase protection assay in 18 human breast tumours

ER cDNA (Figure 1B) using primers in exons 4 and 6, and exon 7-deleted ER cDNA (Figure 1C), using primers in exons 5 and 8, were measured. The median value for the relative expression of the exon 5-deleted ER for the primary tumours was 23.1% (range 17.3–94.3%) and the median value for the matched lymph node metastases was 31.3% (range 14.9–200%). The scatter plot for these results is shown in Figure 2A. The median relative expression of the exon 7-deleted ER for primary tumours was 65% (range 39.3–184.9%) and the median value for the matched lymph node metastases was 52.5% (range 35.5–126%). The scatterplot of these results is shown in Figure 2B. There were no statistically significant differences in the relative expression of either exon-deleted ER mRNA between primary and concurrent metastatic tumours.

Comparison of RNAase protection assay and triple-primer PCR assay for determination of the relative expression of clone 4 truncated ER variant mRNA expression

Another frequently expressed ER variant, which would not be detected in the above assays, is the C4 ER mRNA. This variant was previously found to be significantly elevated in a group of primary breast tumours with poor prognostic features that included concurrent lymph node metastases, compared with a group of primary tumours with good prognostic variables that included lack of concurrent nodal metastases (Murphy et al, 1995). Therefore, it was relevant to determine the level of C4 ER variant expression in primary breast tumours and their matched, concurrent lymph node metastases.

In this previous study, we used RNAase protection assays to measure WT and variant ER mRNA expression (Murphy et al, 1995). However, in order to conduct this study using smaller tissue samples (in particular from nodal metastases) and to ensure a close correlation with the histological composition of the tissue, we used a previously described TP-PCR assay (Leygue et al, 1996*b*) to measure the relative expression of C4 ER mRNA. To facilitate comparison of the current data with our earlier study (Murphy et al, 1995), it was necessary to compare the RNAase protection assay with the TP-PCR assay, before proceeding to analyse the primary and secondary breast tumour samples for C4 mRNA expression by TP-PCR.

RNA from 25 human breast tumours, selected to represent a wide range of ER status by ligand-binding assay (Table 1), was

Table 1 C4 and WT ER mRNA expression in 25 human breast tumours, as determined by RNAase protection assay and TP-PCR

Sample no.	Ligand binding	RNAase protection			TPPCR
	ER (fmol mg^{-1})	C4 (pg 10 μg^{-1})	WT ER (pg 10 μg^{-1})	C4 (%)	C4 (%)
5	0.0	ND	ND	–	1.7
3	0.4	ND	ND	–	2.6
1	0.9	ND	ND	–	3.1
24	1.2	6.2	105.1	5.9	3.3
4	1.8	ND	ND	–	3.7
23	4.5	10.0	54.3	18.4	22.7
8	5.8	ND	26.8	–	2.8
7	6.3	ND	224.6	–	3.4
2	8.7	ND	9.0	–	2.2
19	10.0	22.6	902.9	2.5	3.6
10	17.8	5.3	146.4	3.6	4.1
13	25.0	2.3	112.0	2.0	1.0
15	44.0	5.0	148.5	3.4	5.9
22	57.0	11.8	153.6	7.7	14.1
11	90.0	2.5	129.1	1.9	1.7
21	96.0	9.6	263.4	3.6	2.2
14	105.0	4.6	94.4	4.9	5.0
17	111.0	26.7	320.3	8.3	9.1
9	121.0	4.6	277.7	1.7	2.4
6	146.0	2.0	105.0	1.9	1.9
18	198.0	15.8	422.0	3.7	7.0
20	236.0	8.8	288.4	3.0	3.5
12	289.0	3.6	80.5	4.5	8.0
16	304.0	38.8	1440.8	2.7	3.7
25	311.0	83.9	3651.0	2.3	3.2

ND, not detected.

analysed in a standardized RNAase protection assay in order to determine the absolute amount of C4 and WT ER mRNAs within each sample. The signals corresponding to C4 and WT ER mRNAs were quantified as described in Materials and Methods. In each assay, known amounts of synthetic WT ER and C4 mRNAs were analysed in parallel in order to establish a standard curve allowing the determination of absolute levels of C4 and WT ER mRNAs, expressed as pg 10 μg^{-1} RNA (Table 1). Because of the very low C4 protected fragment signal (≤ 15 d.p.m.) in seven tumours, it was not possible to determine confidently the absolute amount of C4 mRNA in these samples (not detected, ND). All C4-negative tumours by RNAase protection assay were from tumours with ER values lower than 10 fmol mg^{-1} protein, as determined by ligand-binding assay. The absolute amounts of C4 and WT ER mRNAs in the remaining 18 tumours, as determined by RNAase protection assay, varied from 2 to 83.9 pg 10 μg^{-1} RNA and from 9 to 3651 pg 10 μg^{-1} RNA respectively. For each sample, the C4 mRNA signal was expressed as a percentage of WT ER mRNA signal (Table 1).

C4 ER mRNA relative expression was determined by TP-PCR within the same 25 RNA samples as described in Materials and Methods. Both C4 and WT ER cDNAs signals were detected in all 25 tumours studied, independent of their ER status as determined by ligand-binding assay. C4 and WT ER signals were quantified as described in Materials and Methods. The signal corresponding to C4 was expressed as a percentage of the WT ER signal. Table 1 presents the average of a least two independent TP-PCR experiments. Linear regression analysis (Figure 3) shows a highly significant correlation between C4 mRNA relative expression as

determined by RNAase protection assay (in the 18 tumours in which a C4 signal was detectable) and C4 mRNA relative expression determined by TP-PCR ($r = 0.932$, $P < 0.0001$). Interestingly, an additional band was also observed in most of the samples using the TP-PCR assay (see asterisk, Figure 1D). This band was identified after subcloning and sequencing to be a product of an exon 2-duplicated ER variant mRNA. The intensity of the signal obtained from this exon 2-duplicated ER band paralleled that of the WT ER band, and the co-amplification of the exon 2-duplicated ER variant mRNA using TP-PCR did not interfere with the relationship between TP-PCR and RNAase protection assay.

Determination of the relative expression of clone 4 truncated ER variant mRNA expression

The above TP-PCR assay was used to compare the relative expression of C4 and WT ER expression in the matched breast cancer samples (Figure 1D). The median relative expression of the C4 ER for the primary tumours was 3.5% (range 1.6–10.5%) and the median value for the matched lymph node metastases was 3.1% (range 1.0–19.4%). A scatterplot of the results is shown in Figure 2C. There is no statistically significant difference in the relative expression of C4 ER variant expression between primary breast tumours and their concurrent lymph node metastases by Wilcoxon rank-sum analysis. Interestingly, although not statistically significant, we found that the median level of C4 expression in ER+ PR– primary tumours, 3.7% (range 2.5–7.9%, $n = 5$), was approximately 50% higher than the median level of C4 expression in ER+ PR+ primary tumours, which was 2.4% (range 1.6–10.5%, $n = 8$). Such a trend would be consistent with our previous results in which C4 expression was higher in PR– primary breast tumours than in PR+ primary tumours.

DISCUSSION

The data presented in this study provide evidence that both the overall pattern of ER variant expression and the relative level of expression of three individual ER variants are conserved in primary breast tumours and their matched, concurrent lymph node metastases.

The observations presented in this manuscript, showing a conserved pattern and similar relative expression of ER variants between primary tumours and their concurrent lymph node metastases, would be consistent with previous observations that little change of ER status can be found between primary human breast tumours and their concurrent lymph node metastases or their distant metastases (Hahnel and Twaddle, 1985; Robertson, 1996). These findings are not inconsistent with our previously published data, which showed that the relative expression of one ER variant was significantly increased in primary tumours with poor prognostic characteristics, which included having concurrent lymph node metastases, as compared with primary tumours without concurrent lymph node metastases (Murphy et al, 1995). It should be stressed that all the primary tumours in the current study had concurrent lymph node metastases, a major feature of poor prognosis in breast cancer, and most likely resembled our previously described poor prognostic group (Murphy et al, 1995). Therefore in primary tumours that have concurrent lymph node metastases and have detectable levels of C4 ER variant as well as other variant ER mRNAs, mRNA levels do not significantly change between primary tumours and their concurrent lymph node metastases. These data do not, however, shed any light on whether tumours with good prognostic features, as previously described (Murphy et al, 1995), that have a relatively low level of C4 ER variant mRNA subsequently develop higher levels when recurrent disease develops. Although this issue remains to be investigated, our earlier observation of higher relative C4 ER mRNA expression in PR– primary tumours compared with PR+ primary tumours appeared to be conserved in the present cohort, although the numbers were low and the difference did not reach statistical significance. As quantitative differences in the expression of several ER variants have been shown to occur in primary breast tumours compared with normal human breast tissues (Leygue et al, 1996*a*, *b*), as well as between good vs poor prognosis primary breast tumours, the current data suggest that alterations in ER variant expression and any role this may have in altered oestrogen signal transduction probably occurs early in tumorigenesis and well before the acquisition of the ability to metastasize. This is consistent with previous data supporting the concept of an early involvement of perturbations of oestrogen signal transduction and the development of hormone independence in breast tumorigenesis (Khan et al, 1994; Schmitt, 1995). It remains therefore to be determined if altered ER variant expression can predict tumour recurrence and progression in node-negative breast cancers.

To our knowledge, this study is the first to compare an already established quantitative approach, such as the RNAase protection assay, with an RT-PCR based approach in the study of ER variant mRNA expression. Earlier studies have utilized either the RNAase protection assay or RT-PCR only. Considering the potential clinical relevance of the measurement of the relative level of ER variants with respect to WT ER within human breast tissue samples and the sensitivity of an RT-PCR based approach, such a comparative study was deemed necessary. Furthermore, our data provide validation for comparing previous data obtained using a non-amplification-dependent RNAase protection assay with the current data obtained using an amplification-dependent TP-PCR assay.

The lack of sensitivity of the RNAase protection assay for a subset of tumours with very low (<10 fmol mg^{-1}) ER values by ligand-binding assay is an important limiting factor. It effectively means that, in a screening study, ER-negative tumours (< 3 fmol mg^{-1} protein), as well as ER-positive tumours with ER values lower than 10 fmol mg^{-1}, as measured by ligand-binding assay, cannot be reliably assessed for C4 ER variant mRNA expression by RNAase protection assay. This, together with the relatively large amount of RNA needed to perform an RNAase protection analysis, severely limits the usefulness of a standardized RNAase protection assay in such screening studies. The low amount of starting material needed, together with the higher sensitivity observed (samples C4 ER variant negative by RNAase protection assay had detectable levels of C4 ER variant and WT ER mRNA by TP-PCR) make TP-PCR an attractive alternative to the RNAase protection assay in studies in which such factors are limiting.

In conclusion, the current investigation extends our previous studies on the relationship of ER variant expression and progression in human breast cancer. The data presented show that both the pattern and level of expression of ER variants are conserved between matched primary breast tumours and their concurrent lymph node metastases. Therefore, any alteration in ER variant expression that could be a marker of altered ER signal transduction and breast cancer progression probably occurs before breast cancer cells acquire the ability to metastasize.

ACKNOWLEDGEMENTS

This work was supported by the US Army Medical Research and Materiel Command (USAMRMC), grant number DAMD17-95-1-5015. The Manitoba Breast Tumour Bank is supported by funding from the National Cancer Institute of Canada (NCIC). LCM is a Medical Research Council of Canada (MRC) Scientist, PHW is a MRC Clinician-Scientist, EL is a recipient of a USAMRMC Postdoctoral Fellowship (DAMD17-96-1-6174), RH was supported by a University of Manitoba Visiting Scientist Award.

REFERENCES

Daffada AA, Johnston SR, Nicholls J and Dowsett M (1994) Detection of wild type and exon 5-deleted splice variant oestrogen receptor (ER) mRNA in ER-positive and -negative breast cancer cell lines by reverse transcription/polymerase chain reaction. *J Mol Endocrinol* **13**: 265–273

Daffada AA, Johnston SR, Smith IE, Detre S, King N and Dowsett M (1995) Exon 5 deletion variant estrogen receptor messenger RNA expression in relation to tamoxifen resistance and progesterone receptor/pS2 status in human breast cancer. *Cancer Res* **55**: 288–293

Desai A, Luqmani Y, Coope R, Dagg B, Gomm J, Pace P, Rees C, Thirunavukkarasu V, Shousha S, Groome N, Coombes R and Ali S (1997) Presence of exon 5 deleted oestrogen receptor in human breast cancer: functional analysis and clinical significance. *Br J Cancer* **75**: 1173–1184

Dotzlaw H, Miller T, Karvelas J and Murphy LC (1990) Epidermal growth factor gene expression in human breast cancer biopsy samples: relationship to estrogen and progesterone receptor gene expression. *Cancer Res* **50**: 4204–4208

Dotzlaw H, Alkhalaf M and Murphy LC (1992) Characterization of estrogen receptor variant mRNAs from human breast cancers. *Mol Endocrinol* **6**: 773–785

Dowsett M, Daffada A, Chan C and Johnston S (1997) Oestrogen receptor mutants and variants in breast cancer. *Eur J Cancer* **33**: 1177–1183

Fasco M (1997) Quantitation of estrogen receptor mRNA and its alternatively spliced mRNAs in breast tumor cells and tissues. *Anal Biochem* **245**: 167–178

Green S, Walter P, Kumar V, Krust A, Bornert J, Argos P and Chambon P (1986) Human estrogen receptor cDNA: sequence, expression, and homology to v-erb-A. *Nature* **320**: 134–139

Hahnel R and Twaddle E (1985) The relationship between estrogen receptors in primary and secondary breast carcinomas and in sequential primary breast carcinomas. *Breast Cancer Res Treat* **5**: 155–163

Huang A, Leygue E, Snell L, Murphy LC and Watson P (1997) Expression of estrogen receptor variants mRNAs and determination of estrogen status in human breast cancer. *Am J Pathol* **150**: 1827–1833

Khan SA, Rogers MA, Obando JA and Tamsen A (1994) Estrogen receptor expression of benign breast epithelium and its association with breast cancer. *Cancer Res* **54**: 993–997

Leygue ER, Watson PH and Murphy LC (1996*a*) Estrogen receptor variants in normal human mammary tissue. *J Natl Cancer Inst* **88**: 284–290

Leygue E, Murphy LC, Kuttenn F and Watson P (1996*b*) Triple primer polymerase chain reaction. A new way to quantify truncated mRNA expression. *Am J Pathol* **148**: 1097–1103

Leygue E, Huang A, Murphy LC and Watson P (1996*c*) Prevalence of estrogen receptor variant messenger RNAs in human breast cancer. *Cancer Res* **56**: 4324–4327

Murphy LC and Dotzlaw H (1989) Variant estrogen receptor mRNA species detected in human breast cancer biopsy samples. *Mol Endocrinol* **3**: 687–693

Murphy LC, Hilsenbeck SG, Dotzlaw H and Fuqua SAW (1995) Relationship of clone 4 estrogen receptor variant messenger RNA expression to some known prognostic variables in human breast cancer. *Clin Cancer Res* **1**: 155–159

Murphy LC, Dotzlaw H, Leygue E, Douglas D, Coutts A and Watson P (1997*a*). Estrogen receptor variants and mutations: a review. *J Steroid Biochem Mol Biol* **62**: 363–372

Murphy LC, Leygue E, Dotzlaw H, Douglas D, Coutts A and Watson P (1997*b*) Oestrogen receptor variants and mutations in human breast cancer. *Ann Med* **29**: 221–234

Park W, Choi J, Hwang E and Lee J (1996) Identification of a variant estrogen receptor lacking exon 4 and its coexpression with wild type estrogen receptor in ovarian carcinomas. *Clin Cancer Res* **2**: 2029–2035

Robertson J (1996) Oestrogen receptor: a stable phenotype in breast cancer. *Br J Cancer* **73**: 5–12

Schmitt F (1995) Multistep progression from an oestrogen dependent growth towards an autonomous growth in breast carcinogenesis. *Eur J Cancer* **12**: 2049–2052

[CANCER RESEARCH 59, 529–532, February 1, 1999]

Advances in Brief

Estrogen Receptor-β Messenger RNA Expression in Human Breast Tumor Biopsies: Relationship to Steroid Receptor Status and Regulation by Progestins[1]

Helmut Dotzlaw, Etienne Leygue, Peter H. Watson, and Leigh C. Murphy[2]

Departments of Biochemistry and Molecular Biology [H. D., E. L., L. C. M.] and Pathology [P. H. W.], Faculty of Medicine, University of Manitoba, Winnipeg, Manitoba, R3E 0W3 Canada

Abstract

When the level of estrogen receptor (ER)-β mRNA in tumors, determined by reverse transcription-PCR, was assessed according to either ER status or PR status alone, determined by ligand binding assays, the level of ER-β mRNA was significantly lower in PR+ tumors compared with PR− tumors ($P = 0.036$), and no association with ER status was found. Subgroup analysis showed that ER-β mRNA expression in ER+/PR+ breast tumors was significantly less than in ER+/PR− ($P = 0.009$), ER−/PR+ ($P = 0.029$), and ER−/PR− ($P = 0.023$) groups. Interestingly, the ER-β mRNA expression was specifically decreased by progestin in T-47D breast cancer cells. The data suggest the possibility that expression of ER-β in human breast tumors is a marker of endocrine therapy responsiveness.

Introduction

Both estrogen and antiestrogen can mediate transcriptional activity via the recently identified ER[3]-β (1–3). Recently, we have shown the presence of ER-β mRNA in both normal and neoplastic human breast tissues (4, 5). Furthermore, the relative expression of ER-α and ER-β mRNA changes between normal human breast tissues and their concurrent matched ER+ breast tumors (6), suggesting that altered expression of ER-α and ER-β occurs and may be functionally involved in breast tumorigenesis. Interestingly, it also seemed that the level of ER-β mRNA varied among breast tumors but was not correlated with the expression of ER-α (4), although the two receptor mRNAs were often coexpressed in the same tumor. These observations raised the question of whether the expression of ER-β in breast tumors was correlated with known prognostic and endocrine treatment response markers. In this study, the relationship of ER-β mRNA expression to ER and PR status, as determined by ligand binding analysis, was investigated.

Materials and Methods

Materials. All cell culture reagents were obtained from Life Technologies, Burlington, Ontario). MPA and dexamethasone were purchased from Sigma Chemical Co. (St. Louis, MO). R5020 and Org 2058 were purchased from Amersham Corp. (Oakville, Canada). RU 486 was a gift from Roussel Uclaf (Romainville, France). [α-^{32}P]dCTP was purchased from ICN (Montreal, Quebec).

Human Breast Tumors. Forty invasive ductal carcinomas were selected from the National Cancer Institute of Canada-Manitoba Breast Tumor Bank (Winnipeg, Manitoba, Canada). The cases were selected for ER and PR status as determined by ligand binding assays. Ten tumors were classified as ER+/PR+ (ER range, 50–127 fmol/mg protein; PR range, 105–285 fmol/mg protein); 10 tumors were classified as ER+/PR− (ER range, 59–156 fmol/mg protein; PR range, 5–10 fmol/mg protein); 10 tumors were ER−/PR− (ER range, 0–2 fmol/mg protein; PR range, 0–10 fmol/mg protein); and 10 tumors were classified as ER−/PR+ (ER range, 5–9 fmol/mg protein; PR range, 51–271 fmol/mg protein). These tumors spanned a wide range of grade (grade 4–9), determined using the Nottingham grading system.

Cell Culture. T-47D human breast cancer cells were obtained from Dr. D. Edwards (University of Colorado, Denver, CO). The cells were grown in DMEM supplemented with 5% fetal bovine serum, 100 nM glutamine, 0.3% (v/v) glucose, and penicillin/streptomycin, as previously described (7). Cells were plated at 1 times 10^6 in 100-mm dishes and 2 days later were treated as indicated in the text. The steroids and other compounds were added directly from 1000 times stock solutions in ethanol to achieve the concentrations indicated. The cells were harvested at the times indicated by scraping with a rubber policeman. After centrifugation, the cell pellet was frozen and stored at −70°C until RNA was isolated.

RNA Extraction and RT-PCR Conditions. Total RNA was extracted from 20-μm frozen tissue sections (5 sections/tumor) or frozen cell pellets using Trizol reagent (Life Technologies, Inc., Grand Island, NY), according to the manufacturer's instructions. Total RNA (1 μg) was reverse transcribed in a final volume of 25 μl, as previously described (4).

The primers used consisted of ER-β-U primer (5′-GTCCATCGCCAGTTATCACATC-3′; sense; located in ER-β 130-151) and ER-β-L primer (5′-GCCTTACATCCTTCACACGA-3′; antisense; located in ER-β 371-352). Nucleotide positions given correspond to published sequences of the human ER-β cDNA (2). PCR amplifications were performed, and PCR products were analyzed as previously described, with minor modifications (4). Briefly, 1 μl of reverse transcription mixture was amplified in a final volume of 15 μl, in the presence of 1.5 μCi [α-^{32}P]dCTP (3000 Ci/mmol), 4 ng/μl ER-β-U/ER-β-L, and 0.3 units of Taq DNA polymerase (Life Technologies, Inc.). Each PCR consisted of 30 cycles (30 s at 94°C, 30 s at 60°C, and 30 s at 72°C). PCR products were then separated on 6% polyacrylamide gels containing 7M urea. After electrophoresis, the gels were dried and autoradiographed. Amplification of the ubiquitously expressed *GAPDH* cDNA was performed in parallel, and PCR products were separated on agarose gels stained with ethidium bromide, as previously described (4). PCR products were subcloned and sequenced, as previously described (4).

Quantification and Statistical Analysis. Quantification of signals was carried out by excision of the band corresponding to ER-β cDNA, addition of scintillant, and scintillation counting. Three independent PCRs were performed. To control for variations between experiments, a value of 100% was assigned to the case exhibiting the highest signal measured, and all signals were expressed as a percentage of this signal. In parallel, *GAPDH* cDNA was amplified and, after analysis of PCR products on prestained agarose gels, signals were quantified by scanning using NIH Image 161/ppc software. Each *GAPDH* signal was also expressed as a percentage of the highest signal observed in the experiment. Two independent PCRs were performed. For each sample, the average of the ER-β signal was then expressed as a percentage of the average *GAPDH* signal. The statistical significance of any differences of

Received 10/30/98; accepted 12/17/98.

The costs of publication of this article were defrayed in part by the payment of page charges. This article must therefore be hereby marked *advertisement* in accordance with 18 U.S.C. Section 1734 solely to indicate this fact.

[1] Supported by grants from the Canadian Breast Cancer Research Initiative and the United States Army Medical Research and Materiel Command (USAMRMC). The Manitoba Breast Tumor Bank is supported by funding from the National Cancer Institute of Canada. L. C. M. is a Medical Research Council of Canada (MRC) Scientist. P. H. W. is an MRC Clinician-Scientist. E. L. is a recipient of a USAMRMC Postdoctoral Fellowship.

[2] To whom requests for reprints should be addressed, at The University of Manitoba, Department of Biochemistry and Molecular Biology, 770 Bannatyne Avenue, Winnipeg, Manitoba, R3E OW3 Canada. Phone: 204-789-3233; Fax: 204-789-3900; E-mail: lcmurph@cc.umanitoba.ca.

[3] The abbreviations used are: ER, estrogen receptor; MPA, medroxyprogesterone acetate; GAPDH, glyceraldehyde-3-phosphate dehydrogenase; PR, progesterone receptor; RT-PCR, reverse transcription-PCR.

the mean ER-β mRNA level between groups was determined using the Mann-Whitney test (two-tailed).

Results

Measurement of ER-β mRNA Expression in Primary Human Breast Tumors with Different ER and PR Status. Previous data have suggested that the level of ER-β mRNA varied widely in human breast tumor samples (4), which raised the question of whether the expression of ER-β in breast tumors was correlated with the known prognostic and treatment response variables, ER and PR status. Four groups, containing 10 breast tumor samples each, were identified according to their ER/PR status, as defined by ligand binding analysis (see "Materials and Methods"). ER-β mRNA levels were measured by RT-PCR and normalized to the *GAPDH* mRNA level, as measured in parallel by RT-PCR. The primers used in this analysis are located in exons 1 and 2 (Fig. 1*A*) of the human *ER-β* gene (2, 8) and would, therefore, measure the wild-type human ER-β mRNA and all ER-β mRNA variants so far documented (5, 9, 10). Examples of the results obtained are shown in Fig. 1*B*. The results obtained for all tumors assayed are shown in Fig. 1*C*, arranged in groups according to the ER/PR status of the tumor, as measured by ligand binding analysis.

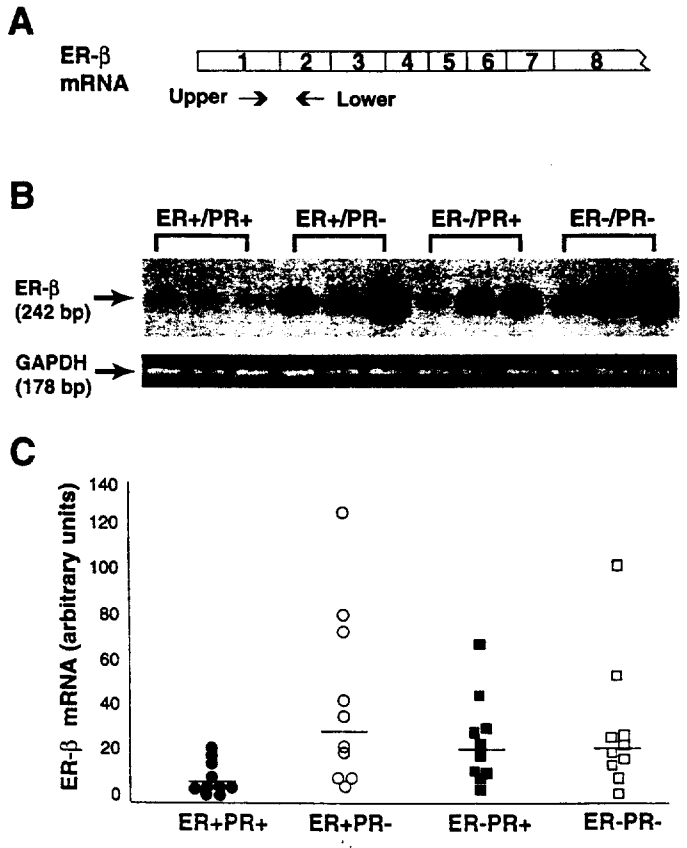

Fig. 1. *A*, schematic diagram of the human ER-β cDNA showing the priming sites of the *upper* and *lower* primers used for the analysis of ER-β mRNA by RT-PCR. *B*, expression of ER-β mRNA in human breast tumor biopsy samples, according to ER and PR status determined by ligand binding assay. *Top*, an autoradiogram of the RT-PCR assays for *ER-β* mRNA obtained from representative samples of tumors that were classified as *ER+/PR+*, *ER+/PR−*, *ER−/PR+*, and *ER−/PR−*, as described in "Materials and Methods." *Bottom*, the ethidium bromide-stained gel of the RT-PCR analysis of *GAPDH* mRNA run in parallel for the same samples. *C*, quantification of ER-β mRNA expression within human breast tumors classified according to ER and PR status, as determined by ligand binding assay. Total RNA, extracted from the tumors, was reverse transcribed, PCR-amplified, and PCR products were separated on acrylamide gel as described in "Materials and Methods." Signals have been quantified and normalized, as indicated in "Materials and Methods." ●, ER+/PR+ tumors; ○, ER+/PR− tumors; ■, ER−/PR+ tumors; □, ER−/PR− tumors. *Horizontal line*, the median value in each group.

Table 1 *Summary of ER-β mRNA levels according to steroid receptor status*

ER/PR status	Number[a]	ER-β mRNA level (mean ± SE)	Statistical significance[b]
A. ER+/PR+	10	11 ± 7.2	
B. ER+/PR−	10	45 ± 12	A *vs.* B, $P = 0.009$
C. ER−/PR−	10	26 ± 6	A *vs.* C, $P = 0.029$
D. ER−/PR−	10	31 ± 9.3	A *vs.* D, $P = 0.023$
E. ER+	20	28 ± 7.2	
F. ER−	20	28 ± 5.4	E *vs.* F, NS
G. PR+	20	19 ± 3.5	
H. PR−	20	38 ± 7.7	G *vs.* H, $P = 0.036$

[a] Number of tumors/group.
[b] Mann-Whitney test (two-tailed).
[c] NS, not significant.

The level of ER-β mRNA in ER+/PR+ breast tumors was significantly less than in all other groups (see Table 1), with no significant differences seen among the ER+/PR−, ER−/PR+, or ER−/PR− groups. When the level of ER-β mRNA in tumors was assessed according to either ER status or PR status alone, as defined by ligand binding analysis, the level of ER-β mRNA was significantly lower in PR+ tumors compared with PR− tumors (Table 1, *G versus H*; $P = 0.036$), with no significant differences associated with ER status alone (Table 1, *E versus F*; $P = 0.323$).

Spearman correlation analysis showed no significant correlations of the level of ER-β mRNA with grade, age, nodal status, or the percentage of normal duct and lobular epithelium, stromal or fat cell content within the tissue section analyzed. However, an inverse relationship was found when the level of ER-β mRNA was correlated with the absolute level of PR, as measured by ligand binding analysis ($r = -0.31$; $P = 0.052$), consistent with the data when analyzed using clinically relevant cut-off values for both ER and PR status as shown above.

Regulation of Steady-state Levels of ER-β mRNA by Progestins in T-47D Human Breast Cancer Cells. The relationship of the level of ER-β mRNA with PR status in human breast tumor biopsies suggested the hypothesis that ER-β expression may be regulated by progestins. This hypothesis was investigated using the PR+ T-47D human breast cancer cell line in culture. The steady-state level of ER-β mRNA was found to decrease after treatment with 10 nM MPA (Fig. 2*A*). A significant decrease was observed at 6 hours after MPA treatment, and the levels remained decreased for up to 48 hours after treatment. The effect of MPA on the steady-state levels of ER-β mRNA in T-47D cells was first seen with 1 nM MPA and was maximal between 10 and 100 nM MPA (Fig. 2*B*). The progestin specificity of this response was assessed by treating T-47D cells for 24 hours with MPA, Org 2058, dexamethasone, and the antiprogestin RU 486 (Fig. 3, *A* and *B*). Both 10 nM MPA and 10 nM of the synthetic progestin Org 2058 significantly decreased the steady-state levels of ER-β mRNA, whereas little, if any, effect was observed with 100 nM of the synthetic glucocorticoid, dexamethasone. Antiprogestin/anti-glucocorticoid RU 486 (500 nM) had little, if any, effect by itself, but inhibited the down-regulation by 10 nM MPA on the level of ER-β mRNA. It was concluded that progestins can down-regulate the steady-state levels of ER-β mRNA and that an antiprogestin can inhibit this effect in T-47D human breast cancer cells.

Discussion

It was previously documented that the level of ER-β mRNA expression in human breast tumors varied widely (4, 8). This raised the question of whether the expression of ER-β in breast tumors was correlated with known prognostic and treatment-response markers. The measurement of both ERs and PRs in human breast biopsies is routinely used to provide both prognostic and treat-

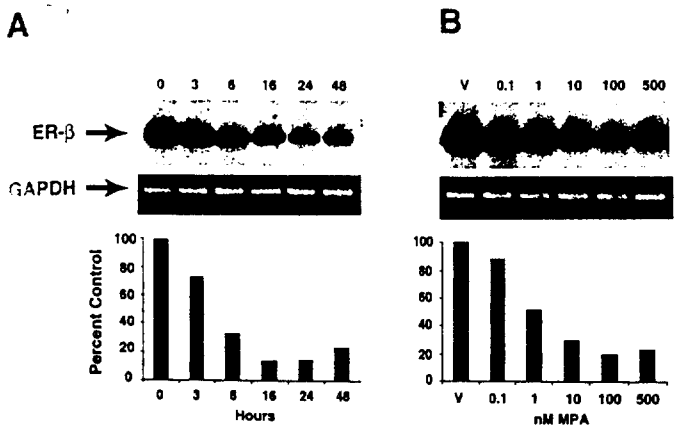

Fig. 2. *A*, time-dependent down-regulation of ER-β mRNA expression in T-47D human breast cancer cells. *Top*, an autoradiogram of *ER-β* mRNA levels determined by RT-PCR after treatment with 10 nM MPA for the indicated time periods. *Middle*, the ethidium bromide-stained gel of the RT-PCR analysis of *GAPDH* mRNA run in parallel for the same samples. *Bottom*, the results presented as a histogram after quantification and normalization of the ER-β signal, as described in "Materials and Methods." This experiment was replicated twice. *B*, dose-dependent down-regulation of ER-β mRNA expression in T-47D human breast cancer cells. *Top*, an autoradiogram of ER-β mRNA levels determined by RT-PCR after treatment with vehicle alone (*V*) and varying concentrations of MPA for 24 h. *Middle*, the ethidium bromide-stained gel of the RT-PCR analysis of *GAPDH* mRNA run in parallel for the same samples. *Bottom*, the results presented as a histogram after quantification and normalization of the ER-β signal, as described in "Materials and Methods."

ment-response information (11). Because ER-β is structurally and functionally related to ER-α (1–3, 12), it was relevant to determine whether the expression of ER-β was related to the ER and PR status of the tumor, as defined by ligand binding assays. Our analysis established that the expression of ER-β mRNA was inversely correlated with PR status generally. Although there was no significant correlation between ER-β mRNA levels and ER status overall, a significant difference in ER-β mRNA levels in those tumors that were ER+/PR+ (lowest expression) and those tumors that were ER−/PR+ (higher expression) was observed. This could be interpreted to mean that both ER status and PR status could influence ER-β mRNA expression. However, the differences observed could also be explained by the significant difference in the absolute level of PR expression between the two groups (PR levels determined by ligand binding assays expressed as mean ± SE, 190 ± 24 fmol/mg protein *versus* 97 ± 21 fmol/mg protein, in ER+/PR+ and ER−/PR+ groups, respectively). This would be consistent with the inverse correlation that was seen with ER-β mRNA and the absolute levels of PR determined by ligand binding analysis, considering all groups together.

These data suggested the possibility that the expression of ER-β may be regulated by progestins. In T-47D cells (which express ER-α, ER-β, and PR), the steady-state level of ER-β mRNA was specifically decreased by progestin treatment in a time- and dose-dependent manner. Our data support the hypothesis that the progestin effect is mediated by PR, however, our data do not address whether this occurs via a transcriptional or post-transcriptional mechanism. Interestingly, progestins are known to also decrease the steady-state levels of ER-α mRNA and protein in T-47D cells (13). Therefore, PR is able to regulate the expression of both ER-α and ER-β in human breast cancer cells in a similar fashion. However, the interaction of PR and the two distinct ERs is likely to be different. It has been well documented that there is a general positive correlation between ER and PR levels, as determined by ligand binding assays in human breast tumors (11). ER status, as determined by ligand binding, correlates well with both immunological detection of the ER-α protein (14) and ER-α mRNA detection (15). Such data together with other studies (6) suggest that the ER level in breast tumors, as determined by ligand binding in most cases, is due to ER-α. Furthermore, ER-β mRNA is the predominant ER mRNA in MDA MB 231 human breast cancer cells (4) and these cells are known to be ER negative by ligand binding assay providing further evidence for the lack of interference of ER-β expression in the determination of ER status by ligand binding assay in the majority of human breast tumors. Interestingly, a significant level of ER-β-like mRNA in human breast cancer cell lines and possibly, therefore, breast tumors may be represented by exon 8 deleted variants (10), which most likely encode nonestrogen binding ER-β variant proteins, which could not contribute to ER ligand binding assays. Therefore, the available data suggest that the previously observed positive correlation of ER and PR in human breast tumors is due to ER-α expression, underscoring the difference in the relationship of ER-α and ER-β with PR in human breast cancer tissue.

Our data are the first to identify a correlation between ER-β mRNA expression and a known prognostic and treatment-response marker in human breast cancer biopsies. The inverse relationship between PR (a good prognostic variable and a marker of response to endocrine therapies) and ER-β suggests that although ER-β is often down-regulated in human breast tumors compared with normal human breast tissue (6), its maintainance and/or increased expression in some breast tumors may correlate with a poorer prognosis and the likelihood of failure of response to endocrine therapies such as antiestrogens. This remains to be tested in samples of breast tumors from patients known to have responded or not to have responded to endocrine therapies, in clinical trials. Furthermore, a functional involvement of ER-β in this phenotype remains to be determined. Interestingly, although no agonist activity of tamoxifen-like antiestrogens can be measured through ER-β in a recombinant expression system using

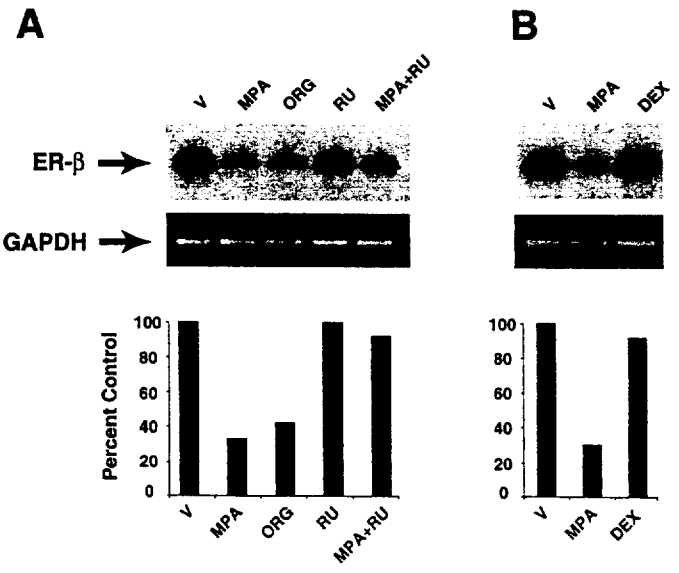

Fig. 3. *A*, steroid specificity of the down-regulation of ER-β mRNA expression in T-47D human breast cancer cells. *Top*, an autoradiogram of *ER-β* mRNA levels determined by RT-PCR after 24 h of treatment with vehicle alone (*V*), 10 nM MPA (MPA), 10 nM Org2058 (*ORG*), 500 nM RU 486 (*RU*), and 10 nM MPA + 500 nM RU 486 (*MPA+RU*). *Middle*, the ethidium bromide-stained gel of the RT-PCR analysis of *GAPDH* mRNA run in parallel for the same samples. *Bottom*, the results presented as a histogram after quantification and normalization of the ER-β signal, as described in "Materials and Methods." This experiment was replicated twice. *B*, steroid specificity of the down-regulation of ER-β mRNA expression in T-47D human breast cancer cells. *Top*, an autoradiogram of ER-β mRNA levels determined by RT-PCR after 24 h of treatment with vehicle alone (*V*), 10 nM MPA (MPA), and 10 nM dexamethasone (*DEX*). *Middle*, the ethidium bromide-stained gel of the RT-PCR analysis of *GAPDH* mRNA run in parallel for the same samples. *Bottom*, the results presented as a histogram after quantification and normalization of the ER-β signal, as described in "Materials and Methods."

transient transfection and a classical ERE-reporter gene (3), all classes of antiestrogens bound to ER-β result in the transcriptional activation of AP-1-driven reporter genes, again in a transient recombinant model system (12). Because AP-1-regulated genes are often associated with growth and proliferation (16–18), it is tempting to speculate that increased expression of ER-β in human breast tumors could play a role in tamoxifen resistance in the small number of tumors that appear to proliferate in response to tamoxifen (19, 20).

Acknowledgments

We thank Caroline Cumins-Leygue and Helen Bergen for laboratory assistance with the cell culture.

References

1. Kuiper, G., Enmark, E., Pelto-Huikko, M., Nilsson, S., and Gustafsson, J-A. Cloning of a novel estrogen receptor expressed in rat prostate and ovary. Proc. Natl. Acad. Sci. USA, *93:* 5925–5930, 1996.
2. Mosselman, S., Polman, J., and Dijkema, R. ER-β: identification and characterization of a novel human estrogen receptor. FEBS Lett., *392:* 49–53, 1996.
3. Tremblay, G., Tremblay, A., Copeland, N., Gilbert, D., Jenkins, N., Labrie, F., and Giguere, V. Cloning, chromosomal localization, and functional analysis of the murine estrogen receptor β. Mol. Endocrinol., *11:* 353–365, 1997.
4. Dotzlaw, H., Leygue, E., Watson, P., and Murphy, L. Expression of estrogen receptor-β in human breast tumors. J. Clin. Endocrinol. Metab., *82:* 2371–2374, 1997.
5. Lu, B., Leygue, E., Dotzlaw, H., Murphy, L. J., Murphy, L. C., and Watson, P. H. Estrogen receptor-β mRNA variants in human and murine tissues. Mol. Cell. Endocrinol., *138:* 199–203, 1998.
6. Leygue, E., Dotzlaw, H., Watson, P., and Murphy, L. Altered estrogen receptor α and β mRNA expression during human breast tumorigenesis. Cancer Res., *58:* 3197–3201, 1998.
7. Alkhalaf, M., and Murphy, L. C. Regulation of c-jun and jun-B by progestins in T-47D human breast cancer cells. Mol. Endocrinol., *6:* 1625–1633, 1992.
8. Enmark, E., Pelto-Huikko, M., Grandien, K., Lagercrantz, S., Lagercrantz, J., Fried, G., Nordenskjold, M., and Gustafsson, J-A. Human estrogen receptor β gene structure, chromosomal localization and expression pattern. J. Clin. Endocrinol. Metab., *82:* 4258–4265, 1997.
9. Vladusic, E., Hornby, A., Guerra-Vladusic, F., and Lupu, R. Expression of estrogen receptor β messenger RNA variant in breast cancer. Cancer Res., *58:* 210–214, 1998.
10. Moore, J., McKee, D., Slentz-Kesler, K., Moore, L., Jones, S., Horne, E., Su, J-L., Kliewer, S., Lehmann, J., and Wilson, T. Cloning and characterization of human estrogen receptor β isoforms. Biochem. Biophys. Res. Commun., *247:* 75–78, 1998.
11. Ravdin, P., Green, S., Dorr, T., McGuire, W., Fabian, C., Pugh, R., Carter, R., Rivkin, S., Borst, J., Belt, R., Metch, B., and Osborne, C. Prognostic significance of progesterone receptor levels in estrogen receptor-positive patients with metastatic breast cancer treated with tamoxifen: results of a prospective Southwest Oncology Group study. J. Clin. Oncol., *10:* 1284–1291, 1992.
12. Paech, K., Webb, P., Kuiper, G., Nilsson, S., Gustafsson, J., angst, Kushner, P. J., and Scanlan, T. S. Differential ligand activation of estrogen receptors ERα and ERβ at AP1 sites. Science (Washington DC) *277:* 1508–1510, 1997.
13. Read, L., Greene, G., and Katzenellenbogen, B. Regulation of estrogen receptor messenger ribonucleic acid and protein levels in human breast cancer cell lines by sex steroid hormones, their antagonists and growth factors. Mol. Endocrinol., *3:* 295–304, 1989.
14. McClelland, R., Berger, U., Miller, L., Powles, T., and Coombes, R. Immunocytochemical assay for estrogen receptor in patients with breast cancer: relationship to biochemical assay and outcome of therapy. J. Clin. Oncol., *4:* 1171–1176, 1986.
15. May, E., Mouriesse, H., May-Leven, F., Contesso, G., and Delarue, J. A new approach allowing an early prognosis in breast cancer: the ratio of estrogen receptor (ER) ligand binding activity to the ER-specific mRNA level. Oncogene, *4:* 1037–1042, 1989.
16. Umayahara, Y., Kawamori, R., Watada, H., Imano, E., Iwama, N., Morishima, T., Yamasaki, Y., Kajimoto, Y., and Kamada, T. Estrogen regulation of the insulin-like growth factor I gene transcription involves an AP-1 enhancer. J. Biol. Chem., *269:* 16433–16442, 1994.
17. Weisz, A., and Bresciani, F. Estrogen regulation of proto-oncogenes coding for nuclear proteins. Crit. Rev. Oncog., *4:* 361–388, 1993.
18. Piechaczyk, M., and Blanchard, J. c-fos protooncogene regulation and function. Crit. Rev. Oncol. Hematol., *17:* 93–131, 1994.
19. Howell, A., Dodwell, D., Anderson, H., and Redford, J. Response after withdrawal of tamoxifen and progestogens in advanced breast cancer. Ann. Oncol., *3:* 611–617, 1992.
20. Howell, A., Defriend, D., Robertson, J., Blamey, R., and Walton, P. Response to a specific antioestrogen (ICI182780) in tamoxifen resistant breast cancer. Lancet, *345:* 29–30, 1995.

[CANCER RESEARCH 59, 1175–1179, March 15, 1999]

Advances in Brief

Expression of Estrogen Receptor β1, β2, and β5 Messenger RNAs in Human Breast Tissue[1]

Etienne Leygue,[2] Helmut Dotzlaw, Peter H. Watson, and Leigh C. Murphy

Departments of Biochemistry and Molecular Biology [E. L., H. D., L. C. M.] and Pathology [P. H. W.], University of Manitoba, Faculty of Medicine, Winnipeg, Manitoba R3E OW3, Canada

Abstract

A triple-primer PCR assay was developed, based on the coamplification of estrogen receptor (ER)-β1, -β2, and -β5 cDNAs, to investigate the relative expressions of the corresponding mRNAs in breast cancer lines and in 53 independent breast tumors. The expression of ER-β2 and ER-β5 mRNAs was higher than that of ER-β1 mRNA in both cancer cell lines and breast tumors. In breast tumors, increases in the ER-β2:ER-β1 and ER-β5:ER-β1 mRNA expression ratios were observed, which positively correlated with the level of tumor inflammation and tumor grade, respectively. A trend toward an increase of these ratios was also found in tumors, as compared to the normal adjacent breast tissue available for 13 cases. Our data suggest that changes in the relative expression of ER-β1, -β2, and -β5 mRNAs occur during breast tumorigenesis and tumor progression.

Introduction

Estrogens regulate the growth and development of normal human mammary tissue and are also involved in breast tumor progression (1). Indeed, estrogens are thought to promote the growth of breast tumors through their mitogenic effects on breast cancer cells. The ability of antiestrogens such as tamoxifen or raloxifene to inhibit estrogenic action provides the basic rationale for the use of endocrine therapies. Estrogen action is believed to be mediated mainly through two ERs[3]: ER-α (2) and ER-β1 (3, 4). These two receptors, which are encoded by two different mRNAs containing eight exons each (5, 6), belong to the steroid/thyroid/retinoic acid receptor superfamily (7). ER-α and ER-β1 share the same structural and functional domain composition (8), defined as region A–F (Fig. 1*A*). The A–B regions contain the NH_2-terminal transactivation function (AF-1) of the receptors, whereas the C region of the molecule contains the DNA binding domain. The ligand binding domain and the second transactivation function (AF-2) are located within the E region of the receptors. The receptors, once bound to the ligand, are subject to conformational changes that result in complexes containing dimers of receptors/hormones that recognize estrogen-responsive elements located upstream of target genes. Interactions between ERs and accessory proteins ultimately lead to the modification of the transcription of these genes (9). The ER-ligand complexes can also interact with c-*fos*/c-*jun* complexes to modify the transcription of target genes through AP1 enhancer elements (10, 11). Differential activation of ER-α and ER-β1 by the antiestrogen 4-hydroxytamoxifen, determined by activation of estrogen response element-regulated reporter genes, and differential activation of AP1-regulated reporter genes by the two ERs have been observed (11, 12). Also, because heterodimerization of ER-α and ER-β1 has also been shown, putative cross-talk between the two signaling pathways is possible (4, 13).

Several variant forms of ER-α and ER-β1 mRNAs have been identified (for reviews see Refs. 14–17). Among them, exon-deleted variant mRNAs, which would encode ER-like proteins missing some of the functional domains of the wild-type receptors, could interfere with ER-α and/or ER-β1 signaling pathways. Indeed, exon 5- and exon 7-deleted ER-α variant proteins have been shown, *in vitro*, to exhibit a constitutive transcriptional (18) and a dominant negative activity (19) on ER-α, respectively. More recently, an ER-β2 variant, deleted of regions encoded by ER-β1 exon 8 sequences, has been shown to heterodimerize with both ER-β1 and ER-α and to inhibit ER-α DNA binding capability (20, 21). The ability of ER-α variants to potentially interfere with the ER-α signaling pathways raised the question of their possible involvement in mechanisms underlying breast tumorigenesis and tumor progression. Although much data have been published documenting the differential expression of ER-α variants at different stages of breast cancer progression (14), no studies have been performed comparing the relative expression of ER-β variant mRNAs in human breast tissue. We have developed a TP-PCR assay to evaluate the relative expression of ER-β1, -β2, -β4, and ER-β5 variant mRNAs. As shown in Fig. 1*A*, ER-β2, -β4, and -β5 variant mRNAs do not contain exon 8 ER-β1 sequences but share similar 3′ end sequences. This assay was used to evaluate the relative expression of ER-β1, -β2, and -β5 mRNA within breast tumors ($n = 53$) and, in some cases ($n = 13$), within adjacent normal breast tissue.

Materials and Methods

Human Breast Tissues and Tumor Cell Lines. Fifty-three cases were selected from the National Cancer Institute of Canada-Manitoba Breast Tumor Bank (Winnipeg, Manitoba, Canada). As reported previously, all cases in the bank have been processed to provide paraffin-embedded tissue blocks and mirror-image frozen tissue blocks (22). Histopathological analysis was performed on H&E-stained sections from the paraffin tissue block to estimate, for each case, the proportions of tumor and normal epithelial cells, fibroblasts, and fat as well as to determine the levels of inflammation and Nottingham grade scores (23). The age of the patients ranged between 39 and 87 years ($n = 53$, median = 67 years). Tumors spanned a wide range of ER (from 0 to 159 fmol/mg protein, $n = 53$, median = 9 fmol/mg protein) and PR (ranging from 0 to 285 fmol/mg protein, $n = 53$, median = 10 fmol/mg protein) levels, as measured by ligand binding assay. These tumors also covered a wide spectrum of grades (Nottingham grading scores from 1 to 9, $n = 47$, median = 7). Inflammation levels were assessed for 51 cases by scoring the extent of lympho-histocystic infiltrates throughout the section using a semiquantitative scale from 0 (low to minimal infiltration) to 5 (marked infiltrate). For 13 cases, matched adjacent normal tissue blocks were also available. The characteristics of this subset of 13 tumors were as follows: ER status ranged from 0 to 159 fmol/mg protein (median = 3.5 fmol/mg protein), PR status ranged from 4.9 to 134 fmol/mg protein (median = 8.5), Nottingham grade scores ranged from 5 to 9 (median = 7), inflammation levels ranged from 1 to 5 (median = 3), and patients were between 39 and 75 years old (median age = 54 years).

MDA-MB-231, MDA-MB-468, ZR-75, BT-20, T-47D, and MCF-7 breast

Received 12/21/98; accepted 1/27/99.

The costs of publication of this article were defrayed in part by the payment of page charges. This article must therefore be hereby marked *advertisement* in accordance with 18 U.S.C. Section 1734 solely to indicate this fact.

[1] This work was supported by grants from the Canadian Breast Cancer Research Initiative and United States Army Medical Research and Materiel Command Grant DAMD17-95-1-5015. The Manitoba Breast Tumor Bank is supported by funding from the National Cancer Institute of Canada. P. H. W. is a Medical Research Council of Canada Clinician-Scientist. L. C. M. is an Medical Research Council Scientist, and E. L. is a recipient of a United States Medical Research and Materiel Command Postdoctoral Fellowship (Grant DAMD17-96-1-6114).

[2] To whom requests for reprints should be addressed, at Department of Biochemistry and Molecular Biology, University of Manitoba, Winnipeg, Manitoba, R3E OW3, Canada. Phone: (204) 789-3812; Fax: (204) 789-3900; E-mail: eleygue@cc.umanitoba.ca.

[3] The abbreviations used are: ER, estrogen receptor; TP-PCR, triple-primer PCR; PR, progesterone receptor.

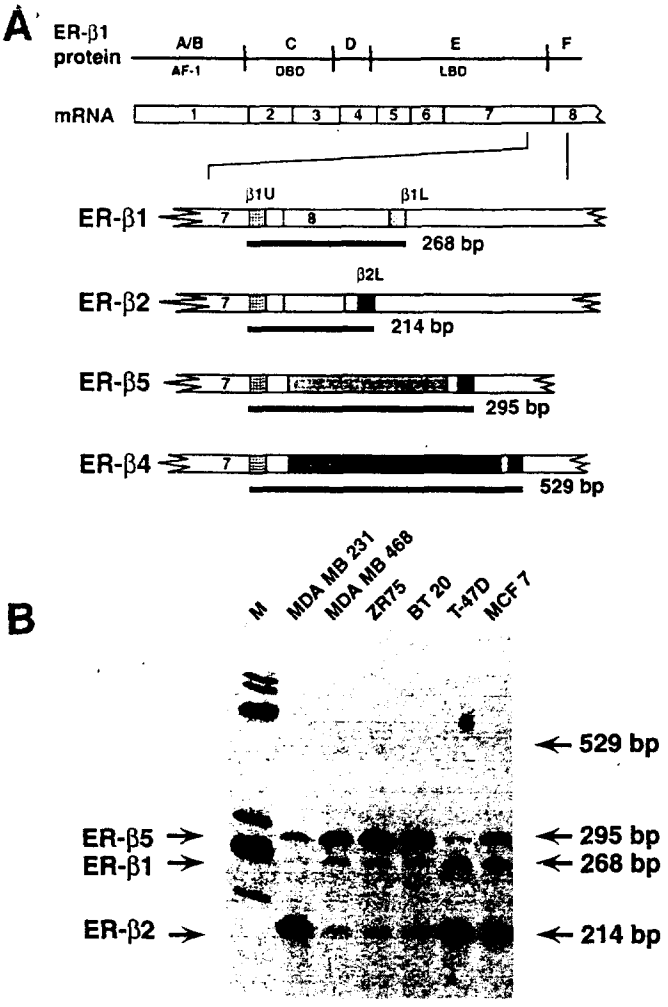

Fig. 1. Presentation of the TP-PCR assay and relative expression of ER-β1, -β2, -β4, and ER-β5 mRNAs in breast cancer cell lines. *A*, structural and functional domains (AF) of the ER-β1 protein (*AF-1*, transactivation function 1; *DBD* and *LBD*, DNA and ligand binding domains, respectively) are shown together with the corresponding exonic structure (*exons 1–8*) of the ER-β1 mRNA. Common sequences (□) and specific sequences (□) are depicted for each cDNA (β1, β2, β4, and β5). ER-β1U (■), ER-β1L (▤), and ER-β2L (■) primer annealing sites are also represented. The sizes of the possible PCR products (*black bars*) obtained after TP-PCR are indicated. *B*, breast cancer cell line (MDA-MB-231, MDA-MB-468, ZR-75, BT-20 T-47D, and MCF-7) poly(A) mRNAs were reverse-transcribed, TP-PCR was performed, and PCR products were separated on an acrylamide gel, as described in "Materials and Methods." PCR products migrating at apparent sizes of 295, 268, and 214 bp have been subcloned, sequenced, and identified as corresponding to ER-β5, -β1, and -β2 mRNAs, respectively. *Lane M*, molecular size markers (φx174 RF DNA/Hae III fragments; Life Technologies, Inc.).

cancer cells were grown and poly(A) mRNA was obtained as described previously (24). Total RNA was extracted from frozen breast tissue sections using Trizol reagent (Life Technologies, Inc., Grand Island, NY) according to the manufacturer's instructions, and quantified spectrophotometrically. One μg of total RNA was reverse-transcribed in a final volume of 25 μl as described previously (25).

Primers and PCR Conditions. The primers used consisted of ER-β1U primer (5′-CGATGCTTTGGTTTGGGTGAT-3′; sense, located in exon 7, positions 1400–1420, GenBank accession no. AB006590), ER-β1L primer (5′-GCCCTCTTTGCTTTTACTGTC-3′; antisense, located in exon 8, positions 1667–1648, GenBank accession no. AB006590), and ER-β2L (5′-CTTTAGGCCACCGAGTTGATT-3′; antisense, located in ER-β2 extrasequences, positions 1933–1913, GenBank accession no. AF051428). PCR amplifications were performed, and PCR products were analyzed as described previously, with minor modifications (25). Briefly, 1 μl of reverse transcription mixture was amplified in a final volume of 15 μl, in the presence of 1 μCi of [α-^{32}P]dCTP (3000 Ci/mmol), 4 ng/μl each primer (ER-β1U, ER-β1L, and ER-β2L), and 0.3 unit of Taq DNA polymerase (Life Technologies, Inc.). Each PCR consisted of 30 cycles (30 s at 60°C, 30 s at 72°C, and 30 s at 94°C). PCR products were then separated on 6% polyacrylamide gels containing 7 M urea. Following electrophoresis, the gels were dried and autoradiographed. Amplification of the ubiquitously expressed *glyceraldehyde-3-phosphate dehydrogenase* cDNA was performed in parallel, and PCR products, separated on agarose gels, were stained with ethidium bromide as described previously (25). Identity of PCR products was confirmed by subcloning and sequencing, as reported previously (25).

TP-PCR Validation. The first series of experiments, performed using cDNAs prepared from breast cancer cell line mRNA, showed that ER-β1, -β2, and -β5 cDNAs can be coamplified, and they led to the production of three PCR products that were subcloned and sequenced as described previously (25). Spiked cDNA preparations containing 1 fg of purified PCR products, corresponding to ER-β1 and -β5 mRNAs, were amplified together with increasing amounts of ER-β2 PCR product (0, 0.2, 0.4, 1, 4, and 8 fg) in a single PCR tube using the three primers (ER-β1U, ER-β1L, and ER-β2L), as described above. Similar experiments were performed using constant amounts of ER-β1 and ER-β2 or of ER-β2 and ER-β5, with increasing amounts of ER-β5 or ER-β1 PCR products, respectively. In parallel, preparations containing 1 fg of each PCR product alone were also amplified. In every case, PCR products were separated on 6% polyacrylamide gels containing 7 M urea. Following electrophoresis, the gels were dried and autoradiographed. Signals were quantified by excision of the appropriate bands and counting in a scintillation counter (Beckman). For each sample, ER-β1, -β2, and -β5 signals were expressed as a percentage of the sum of all signals measured (ER-β1 + ER-β2 + ER-β5 signals). Experiments have been performed in duplicate and the mean of the relative signals calculated. For each ER-β isoform, regression analyses between the relative signal obtained and the relative initial input (*i.e.*, ER-β isoform input expressed as a percentage of ER-β1 + ER-β2 + ER-β5 input) were performed using GraphPad Prism software.

Quantification and Statistical Analyses. To quantitate the relative expression of ER-β1, -β2, and -β5 mRNAs within each breast tissue sample, we used the TP-PCR described above. Quantification of ER-β1, -β2, and -β5 signals was carried out by excision of the bands and scintillation counting. For each sample, ER-β1, -β2, and -β5 signals were expressed as a percentage of the sum of all signals measured (ER-β1 + ER-β2 + ER-β5 signals). Three independent PCRs were performed and the mean of the relative expressions was calculated. Differences between ER-β1, -β2 and -β5 relative expression within the cohort studied were tested using the Wilcoxon signed rank test (two-tailed). Correlations with tumor characteristics were tested by calculation of the Spearman coefficient (*r*).

Results

Validation of TP-PCR as an Approach to Evaluate the Relative Expression of ER-β1, -β2, and -β5 mRNAs. We established previously that TP-PCR provided a reliable method to investigate the expression of a truncated mRNA relative to the wild-type mRNA expression within small breast tissue samples (25). In its initial design, the TP-PCR assay relied on the coamplification of one truncated and a wild-type cDNA molecule using three primers in the PCR. The upper primer recognized both sequences, whereas the two lower primers recognized the variant and the wild-type sequences, respectively. We have shown that the final ratio between the two coamplified products was linearly related to the initial cDNA input (25).

As shown Fig. 1*A*, ER-β1, -β2, -β4, and -β5 mRNAs all have exon 7 sequences but differ from each other in the following sequences. Interestingly, comparison of the sequences revealed that ER-β2, -β4, and -β5 mRNAs have sequence similarities within their 3′ extremities. Therefore, it was possible to use TP-PCR to investigate the relative expression of these variants. Three primers were designed (ER-β1U, ER-β1L, and ER-β2L) that recognized exon 7 sequences common to all transcripts, ER-β1 exon 8-specific sequences, and sequences shared by ER-β2, -β4, and ER-β5 mRNAs, respectively (Fig. 1*A*). As shown in Fig. 1*A*, the expected PCR products resulting from the coamplification of the corresponding cDNAs are different in size and can be easily distinguished on an acrylamide gel.

The assay was used initially to determine the expression of ER-β1, -β2, -β4, and -β5 mRNAs in several different human breast cancer cell lines (Fig. 1*B*). Three bands migrating at apparent sizes of 268, 214, and 295 bp were observed in all samples. Subcloning and

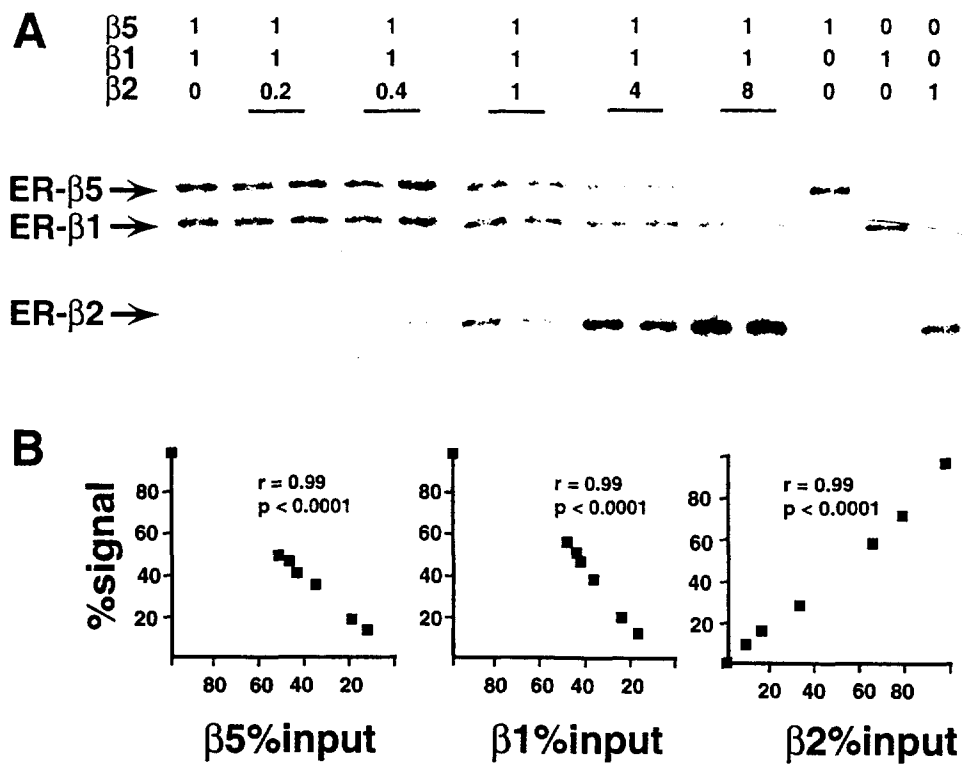

Fig. 2. TP-PCR validation. *A*, spiked cDNA preparations, containing various amounts [indicated above the autoradiogram] of ER-β5, -β1, and -β2 purified PCR products (β5, β1, and β2) were amplified by TP-PCR, and PCR products were separated on an acrylamide gel, as specified in "Materials and Methods." The autoradiogram shows the PCR products obtained. *B*, signals corresponding to ER-β5, -β1, and -β2 PCR products have been quantified in each lane, as described in "Materials and Methods." For each ER-β isoform, the relative signal observed (percentage signal, expressed as a percentage of the sum: β1 + β2 + β5 signals) is presented as a function of the initial relative cDNA input (percentage input, expressed as a percentage of the sum: β1 + β2 + β5 inputs). The regression coefficient (r) and P of the associations are also presented.

sequencing of these bands confirmed their identity as ER-β1, -β2, and -β5 cDNAs, respectively (data not shown). We were unable to detect a product of 529 bp, which would correspond to the ER-β4 PCR product. Interestingly, in all tumor cell lines, the ER-β1 signal was lower than the ER-β2 and/or ER-β5 signals (Fig. 1*B*).

Because TP-PCR performed using these primers produced three PCR products, instead of the two PCR products obtained in the original published validation studies (25), it was necessary to establish the quantitative relationship between the signals obtained and the initial target concentrations. To address this issue, spiked DNA preparations containing equal amounts of ER-β1 and ER-β5 PCR products and increasing amounts of ER-β2 PCR products were amplified (Fig. 2*A*). The relative signals of ER-β1, -β2, and -β5 have been measured and expressed as a percentage of the sum of the signals measured, as described in "Materials and Methods." As expected, in the absence of ER-β2, only two bands, corresponding to ER-β1 and ER-β5 PCR products, are observed. The relative signals of ER-β1 and ER-β5 decreased, whereas the ER-β2 relative signal increased linearly with increasing ER-β2 input. Indeed, for each ER-β isoform, regression analysis showed a linear correlation between the relative signal of the PCR product measured and its relative input (Fig. 2*B*). Similar results were obtained when experiments were performed using constant amounts of ER-β1 and ER-β2 with increasing amounts of ER-β5 PCR products or using constant amounts of ER-β2 and ER-β5 with increasing amounts of ER-β1 (data not shown). It should be noted that the amplification of similar amounts of the three molecules led to the production of three bands of similar intensities (Fig. 2*A*). It should also be stressed that the ER-β5:ER-β1 ratio was not affected by increasing amounts of ER-β2 and that the ER-β2:ER-β5 and ER-β5:ER-β2 ratios varied as a linear function of the initial ER-β2:ER-β5 and ER-β5:ER-β2 input ratios, respectively (data not shown). We concluded that the TP-PCR assay, performed under the described conditions, provided a reliable method with which to compare breast tissue samples for their relative expression of ER-β1, -β2, and -β5 mRNAs.

Comparison of the Relative Expression of ER-β1, -β2, and -β5 mRNAs in Breast Tumor Tissues. To determine whether alterations occur in the balance between ER-β1, -β2, and -β5 mRNAs during breast tumor progression, the relative expression of these transcripts was measured in primary breast tumor tissues from 53 different patients, using the TP-PCR assay described above. These tumors presented a wide spectrum of ER and PR statuses, as determined by ligand binding assay, and also spanned a wide range of grades and inflammation levels (for a more detailed description of the cohort characteristics, see "Materials and Methods"). Total RNA was extracted from frozen tissue sections and reverse-transcribed as described in "Materials and Methods." TP-PCR was then performed. Examples of the results obtained are shown in Fig. 3*A*. Three PCR products migrating at apparent sizes of 268, 214, and 295 bp were obtained. These PCR products were shown by cloning and sequencing to correspond to ER-β1, -β2, and ER-β5 cDNAs, respectively. As in our preliminary study performed in human breast cancer cell lines, no band of 529 bp was detected, which would correspond to ER-β4 PCR product. Amplification of the ubiquitously expressed *glyceraldehyde-3-phosphate dehydrogenase* cDNA, performed to check the integrity of each cDNA studied, revealed similar amounts of cDNA in all samples (data not shown). ER-β1, -β2, and -β5 signals obtained in three independent TP-PCRs were quantified as described in "Materials and Methods." For each sample, the percentage of each band relative to the sum of the signals obtained has been calculated. The medians of ER-β1, -β2, and -β5 relative expression within tumors, sorted according to their grade or to the level of inflammation, are presented in Fig. 3*B*. The ER-β1 relative signal was found to be significantly lower than ER-β2 (Wilcoxon sign rank test, $n = 53$, $P = 0.0002$) and ER-β5 (Wilcoxon sign rank test, $n = 53$, $P = 0.004$) signals. A trend toward a higher expression of ER-β2 as compared to ER-β5 was also observed but did not reach statistical significance (Wilcoxon sign rank test, $n = 53$, $P = 0.09$).

Possible associations between ER-β1, -β2, or -β5 signals and tumor characteristics were then investigated. ER-β1 relative expression was found (Fig. 3*B*) to be inversely related to the grade of the tumor ($n = 47$, Spearman $r = -0.33$, $P = 0.02$) and the level of inflammation ($n = 51$, Spearman $r = -0.28$, $P = 0.04$). No other associations were found between ER-β1 expression and ER status, PR status, or age of the patients. ER-β2 mRNA expression increased

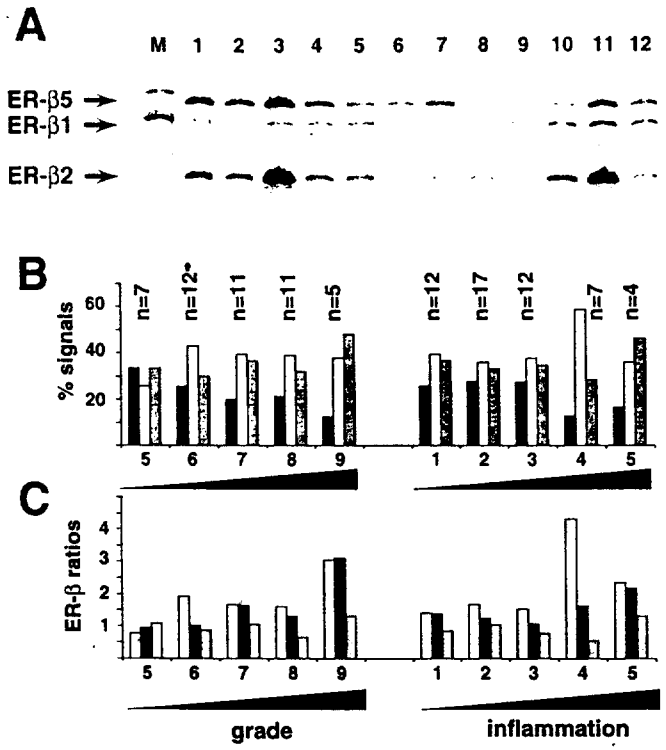

Fig. 3. TP-PCR analysis of the relative expression of ER-β1, -β2, and -β5 mRNAs within a cohort of 53 independent breast tumors. Total RNA was extracted from 53 breast tumors, reverse-transcribed, and analyzed by TP-PCR, as described in "Materials and Methods." PCR products were separated on acrylamide gels. *A*, autoradiogram showing the results obtained for 12 cases (*Lanes 1–12*). *Lane M*, molecular weight marker ϕx174 RF DNA/*Hae*III fragments. *B*, ER-β1, -β2, and -β5 signals have been quantified and expressed relatively to the sum of the signals obtained, as described in "Materials and Methods." Tumors have been sorted according to their Nottingham grade scores (*5–9*) or to their levels of inflammation (*1–5*). For each group, the number of patients (*n*) and the medians of the relative expression of ER-β1 (■), -β2 (□), and -β5 (▩) signals are indicated. *C*, for each group, the number of patients (*n*) and the median of ER-β2:ER-β1 (□), ER-β5:ER-β1 (■) and ER-β5:ER-β2 (▨) signal ratios are indicated.

significantly with the levels of inflammation (n = 52, Spearman r = 0.28, P = 0.04). No other associations were found between ER-β2 and ER-β5 and other characteristics.

Because the ratio between two signals was related to the respective proportion of the two corresponding cDNAs, we also addressed the question of the expression of ER-β2 and ER-β5 relative to ER-β1. The medians of the ER-β2:ER-β1, ER-β5:ER-β1, and ER-β5:ER-β2 ratios within tumors, sorted according to their grade or to the level of inflammation, are presented in Fig. 3*C*. ER-β5 and ER-β2 expression relative to ER-β1 were found positively associated with the tumor grade (n = 47; Spearman r = 0.29, P = 0.04; and Spearman r = 0.28, P = 0.05, respectively). In addition, one should note that ER-β2 expression relative to ER-β1 expression correlated (n = 52, Spearman r = 0.34, P = 0.01) with levels of inflammation. ER-β2 and ER-β5 expression relative to each other did not correlate with grade, degree of inflammation, or any other tumor characteristics. No correlations were found between the content of the tissue sections analyzed, *i.e.*, percentage of normal cells, tumor cells, fibroblasts, or fat, and ER-β1, -β2, and -β5 mRNA relative expression (data not shown).

ER-β1, -β2, and -β5 mRNA Expression within Matched Normal and Tumor Compartments. To determine whether changes in the expression of ER-β1, -β2, and -β5 mRNAs occur during breast tumorigenesis, we compared the relative expression of these transcripts between normal breast tissue and matched adjacent tumors. Normal adjacent breast tissue was available for 13 cases belonging to the cohort described earlier in the text. The characteristics of this tumor subset are detailed in "Materials and Methods." Total RNA was extracted, and following reverse transcription, TP-PCR was performed as described in "Materials and Methods." Typical results are shown in Fig. 4*A*. Quantification of the signals was performed as described above. Fig. 4*B* shows the relative expression within tumor and adjacent normal breast tissues of ER-β1 mRNA. A trend toward a lower ER-β1 signal (9 of 13 cases, Wilcoxon sign rank test, P = 0.06) in the tumor compartment compared to the normal adjacent components was observed. In contrast, trends toward higher expression of ER-β2 (Fig. 4*C*) and ER-β5 (Fig. 4*D*) mRNAs relative to ER-β1 mRNA were observed in tumor compartments (8 of 13 cases, Wilcoxon sign rank test, P = 0.10; and 9 of 13 cases, Wilcoxon sign rank test, P = 0.06, respectively).

Discussion

To evaluate the relative expression of ER-β1, -β2, and -β5 mRNAs within small frozen sections of human breast tissues, we have developed an assay based on the coamplification of the corresponding cDNAs in a single tube, using three primers in the PCR. The quantitative aspect of this assay was validated using preparations containing known amounts of target cDNA. The TP-PCR approach appeared to be a reliable approach to estimate not only the relative expression of each variant within the population of ER-β molecules measured (*i.e.*, ER-β1, -β2, and ER-β5 mRNAs) but also the proportion of each

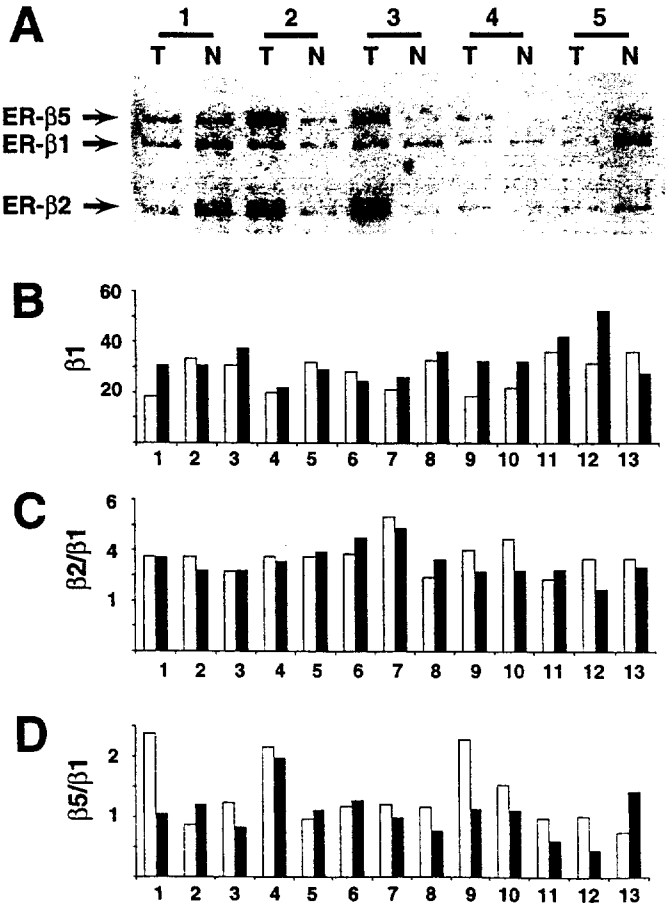

Fig. 4. TP-PCR analysis of the relative expression of ER-β1, -β2, and -β5 mRNAs within matched normal and tumor compartments of human breast tumors. Total RNA was extracted from 13 breast tumors (*Lanes T*) and adjacent normal breast tissues (*Lanes N*), reverse transcribed and analyzed by TP-PCR as described in "Materials and Methods." PCR products were separated on acrylamide gels. *A*, autoradiogram showing the results obtained for five cases (*1–5*). *B*, ER-β1, -β2, and -β5 signals have been quantified and expressed relatively to the sum of the signals obtained, as described in "Materials and Methods." For each case (*1–13*), the relative percentages of ER-β1 in tumor (□) and normal (■) components are shown. *C*, for each case (*1–13*), the ER-β2:ER-β1 ratios in tumor (□) and normal (■) components are shown. *D*, for each case (*1–13*), the ER-β5:ER-β1 ratios in tumor (□) and normal (■) components are shown.

RNA relative to one another. One should note that the set of primers used would detect ER-β4 variant mRNA. However, this variant was not detected in any breast sample or tumor cell line studied. This might result from either a lower efficiency of amplification of this specific variant in our PCR conditions or a lower relative expression of ER-β4 mRNA as compared to ER-β1, -β2, and -β5. A low expression of ER-β4 mRNA would be consistent with data obtained on breast cancer cell lines by Moore *et al.* (20).

Our data show that ER-β1, -β2, and -β5 mRNAs are coexpressed in human breast cancer cells grown in culture. These data confirm the previous observation of Moore *et al.* (20). These authors however, did not address the question of the relative expression of these mRNAs. Striking differences in the pattern of expression of ER-β1, -β2, and -β5 mRNAs were found between breast cancer cell lines. If these differences in expression are conserved at the protein level, one might hypothesize that ER-β signaling pathways, which likely result from the balance between the different forms, vary in these cells. To date, multiple ER-β-like mRNAs that could encode different proteins that would be difficult to distinguish from each other by Western blot analysis have been described. For example, ER-β1 protein (5) and ER-β2 protein (20) have theoretical molecular masses of 54.2 kDa and 55.5 kDa, respectively. Most likely, antibodies specifically recognizing the different ER-β proteins would be the best approach to address the question of the relative expression of ER-β proteins within breast cancer cells. Higher ER-β2 and ER-β5 expression as compared to ER-β1 expression was observed in breast cancer cell lines. This suggests that the respective participation of ER-β2 and ER-β5 variants in ER-β signaling pathways within breast cancer cells might be as significant as or more significant than that of ER-β1.

As observed in breast cancer cell lines, ER-β1, -β2, and -β5 mRNAs were detected in human breast tumors. Consistent with the observations in breast cancer cell lines, ER-β2 and ER-β5 mRNAs were more highly expressed than ER-β1 mRNA in these tissues. However, even though this observation may result directly from the expression of different ER-β isoforms in breast cancer cells, it may also be a consequence of the heterogeneity of the cell populations expressing ER-β molecules and present in different proportions within the tumor sample analyzed. Indeed, because lymphocytes have previously been shown to express ER-β1, -β2, and -β5 mRNAs, one could speculate that infiltrating lymphocytes within the tumor might contribute to the higher level of ER-β2 mRNA expression in tumors with higher inflammation levels. Techniques such as *in situ* hybridization or immunocytochemistry, designed to distinguish between the different ER-β isoforms, are needed to address the question of the cellular origin of ER-β isoform expressions *in vivo*.

We observed an inverse relationship between the relative expression of ER-β1 mRNA and tumor grade. It has been shown that the Nottingham grade provides a useful marker of the length of disease free interval and overall survival (23). We have also observed a decrease of the relative expression of ER-β1 in tumor *versus* normal adjacent components. Taken together, these data suggest that changes in the relative expression of ER-β1, -β2, and -β5 mRNAs occur during breast tumorigenesis and tumor progression. Whether these changes are a cause or a consequence of tumorigenesis remains to be elucidated.

In conclusion, we have developed a TP-PCR assay allowing the investigation of the relative expression of ER-β1, -β2, and -β5 mRNA in human breast tissues. In these tissues, ER-β1 mRNA appeared to have the lowest level of expression when compared to the two other isoforms detected. We found that the relative expression of ER-β1 was inversely related to the grade of the tumor, suggesting that it could be used as a marker of tumor progression. Moreover, a lower relative expression of ER-β1 was observed in tumor *versus* adjacent normal breast tissues, suggesting that changes in the expression of ER-β isoforms occur during breast tumorigenesis. The cellular origin of the expression of ER-β1, -β2, and -β5 in breast tumor tissue *in vivo* remains to be determined, as does the putative role of the different ER-β variant forms in the mechanisms underlying tumorigenesis and tumor progression.

Acknowledgments

We thank Caroline Cumins-Leygue and Helen Bergen for laboratory assistance with the cell culture.

References

1. Vorherr, H. (ed.). Breast Cancer. Baltimore: Urban and Schwarzenberg Press, 1980.
2. Green, S., Walter, P., Kumar, V., Krust, A., Bornert, J. M., Argos, P., and Chambon, P. Human oestrogen receptor cDNA: sequence, expression and homology to v-erb-A. Nature, (Lond.) *320:* 134–139, 1986.
3. Mosselman, S., Polman, J., and Dijkema, R. ER β: identification and characterization of a novel human estrogen receptor. FEBS Lett., *392:* 49–53, 1996.
4. Ogawa, S., Inoue, S., Watanabe, T., Hiroi, H., Orimo, A., Hosoi, T., Ouchi, Y., and Muramatsu, M. The complete primary structure of human estrogen receptor β (hER β) and its heterodimerization with ER α *in vivo* and *in vitro*. Biochem. Biophys. Res. Commun., *243:* 129–132, 1998.
5. Enmark, E., Pelto-Huikko, M., Grandien, K., Lagercrantz, S., Lagercrantz, J., Fried, G., Nordenskjold, M., and Gustafsson, J. A. Human estrogen receptor beta-gene structure, chromosomal localization, and expression pattern. J. Clin. Endocrinol. Metab., *82:* 4258–4265, 1997.
6. Ponglikitmongkol, M., Green, S., and Chambon, P. Genomic organization of the human oestrogen receptor gene. EMBO J., *7:* 3385–3388, 1988.
7. Evans, R. M. The steroid and thyroid receptor super-family. Science (Washington DC), *240:* 889–895, 1988.
8. Kumar, V., Green, S., Stack, G., Berry, M., Jin, J. R., and Chambon, P. Functional domains of the human estrogen receptor. Cell, *51:* 941–951, 1987.
9. Shibata, H., Spencer, T. E., Onate, S. A., Jenster, G., Tsai, S. Y., Tsai, M. J., and O'Malley, B. W. Role of co-activators and co-repressors in the mechanism of steroid/thyroid receptor action. Rec. Prog. Horm. Res., *52:* 141–164, 1997.
10. Umayahara, Y., Kawamori, R., Watada, H., Imano, E., Iwama, N., Morishima, T., Yamasaki, Y., Kajimoto, Y., and Kamada, T. Estrogen regulation of the insulin-like growth factor I gene transcription involves an AP-1 enhancer. J. Biol. Chem., *269:* 16433–16442, 1994.
11. Paech, K., Webb, P., Kuiper, G. G., Nilsson, S., Gustafsson, J., Kushner, P. J., and Scanlan, T. S. Differential ligand activation of estrogen receptors ERα and ERβ at AP1 sites. Science (Washington DC), *277:* 1508–1510, 1997.
12. Watanabe, T., Inoue, S., Ogawa, S., Ishii, Y., Hiroi, H., Ikeda, K., Orimo, A., and Muramatsu, M. Agonistic effect of tamoxifen is dependent on cell type, ERE-promoter context, and estrogen receptor subtype: functional difference between estrogen receptors α and β. Biochem. Biophys. Res. Commun., *236:* 140–145, 1997.
13. Cowley, S. M., Hoare, S., Mosselman, S., and Parker, M. G. Estrogen receptors α and β form heterodimers on DNA. J. Biol. Chem., *272:* 19858–19862, 1997.
14. Murphy, L. C., Leygue, E., Dotzlaw, H., Douglas, D., Coutts, A., and Watson, P. H. Estrogen receptor variants and mutations. Ann. Med., *29:* 221–224, 1997.
15. Vladusic, E. A., Hornby, A. E., Guerra-Vladusic, F. K., and Lupu, R. Expression of estrogen receptor β messenger RNA variant in breast cancer. Cancer Res., *58:* 210–214, 1998.
16. Lu, B., Leygue, E., Dotzlaw, H., Murphy, L. J., Murphy, L. C., and Watson, P. H. Estrogen receptor-β mRNA variants in human and murine tissues. Mol. Cell. Endocrinol., *138:* 199–203, 1998.
17. Shupnik, M. A., Pitt, L. K., Soh, A. Y., Anderson, A., Lopes, M. B., and Laws, E. R., Jr. Selective expression of estrogen receptor α and β isoforms in human pituitary tumors. J. Clin. Endocrinol. Metab., *83:* 3965–3972, 1998.
18. Fuqua, S. A. W., Fitzgerald, S. D., Chamness, G. C., Tandon, A. K., McDonnell, D. P., Nawaz, Z., O'Malley, B. W., and McGuire, W. L. Variant human breast tumor estrogen receptor with constitutive transcriptional activity. Cancer Res., *51:* 105–109, 1991.
19. Wang, Y., and Miksicek, R. J. Identification of a dominant negative form of the human estrogen receptor. Mol. Endocrinol., *5:* 1707–1715, 1991.
20. Moore, J. T., McKee, D. D., Slentz-Kesler, K., Moore, L. B., Jones, S. A., Horne, E. L., Su, J. L., Kliewer, S. A., Lehman, J. M., and Willson, T. M. Cloning and characterization of human estrogen receptor β isoforms. Biochem. Biophys. Res. Commun., *247:* 75–78, 1998.
21. Ogawa, S., Inoue, S., Watanabe, T., Hiroi, H., Orimo, A., Hosoi, T., Ouchi, Y., and Muramatsu, M. Molecular cloning and characterization of human estrogen receptor βcx: a potential inhibitor of estrogen action in human. Nucleic Acids Res., *26:* 3505–3512, 1998.
22. Hiller, T., Snell, L., and Watson, P. H. Microdissection RT-PCR analysis of gene expression in pathologically defined frozen tissue sections. Biotechniques, *21:* 38–44, 1996.
23. Elston, C. W., and Ellis, I. O. Pathological prognostic factors in breast cancer. Histopathology, *19:* 403–410, 1991.
24. Dotzlaw, H., Alkhalaf, M., and Murphy, L. C. Characterization of estrogen receptor variant mRNAs from human breast cancers. Mol. Endocrinol., *6:* 773–785, 1992.
25. Leygue, E., Murphy, L. C., Kuttenn, F., and Watson, P. H. Triple primer PCR: a new way to quantify truncated mRNA expression. Am. J. Pathol., *148:* 1097–1103, 1996.

[CANCER RESEARCH 59, 4190–4193, September 1, 1999]

Advances in Brief

Expression of the Steroid Receptor RNA Activator in Human Breast Tumors[1]

Etienne Leygue,[2] Helmut Dotzlaw, Peter H. Watson, and Leigh C. Murphy

Departments of Biochemistry and Molecular Biology [E. L., H. D., L. C. M.] and Pathology [P. H. W.], University of Manitoba, Faculty of Medicine, Winnipeg, Manitoba, R3E OW3, Canada

Abstract

The expression of the recently described steroid receptor RNA activator (*SRA*) was measured by semiquantitative reverse transcription-PCR within 27 independent breast tumors, spanning a wide spectrum of grade and estrogen receptor (ER) and progesterone receptor (PR) levels. Subgroup analysis showed that *SRA* expression was similar in ER+/PR+ (median = 65.5, $n = 8$) and in ER−/PR− (median = 94.6, $n = 5$) tumors. Interestingly, *SRA* expression in these two subgroups was significantly (Mann-Whitney rank-sum test, $P < 0.05$) lower than that observed in ER+/PR− (median = 156.4, $n = 6$) and ER−/PR+ (median = 144.8, $n = 8$) tumors. A variant form of *SRA*, presenting a deletion of 203 bp within the *SRA* core sequence, was also observed in breast tumor tissues. The relative expression of this new *SRA* isoform correlated with tumor grade (Spearman coefficient $r = 0.53$, $n = 27$, $P = 0.004$). These data suggest that changes in the expression of *SRA*-related molecules occur during breast tumor progression.

Introduction

Estrogens, through their mitogenic action on breast epithelial cells, regulate the growth and the development of normal as well as neoplastic human mammary tissue (1). The ability of antiestrogens such tamoxifen or raloxifene to antagonize this estrogenic action provides the basic rationale for endocrine therapy and prevention (for review see Ref. 2). Estrogen action is mainly mediated through two ERs,[3] ER-α and ER-β (3–5), which belong to the steroid/thyroid/retinoic acid receptors superfamily (6) and act as ligand-dependent transcription factors. The mechanisms by which steroid receptors modulate the transcription of target genes is under extensive investigation (7). Once bound to the ligand, the receptors undergo conformational changes and dimers of receptors recognize specific regulatory DNA sequences upstream of target genes. Activated receptors, through interactions with coactivator proteins, direct the assembly and the stabilization of a preinitiation complex that will ultimately conduct the transcription of these genes (see Ref. 8 and references therein). To an already long list of nuclear receptor coactivators (8), which includes the p160 proteins (such as SRC-1 and AIB1), Lanz *et al.* (9) recently added the *SRA*. *SRA* differs from other coactivators in two main ways. (*a*) *SRA* transcripts do not appear to be translated, and therefore, this coactivator acts as an RNA and not as a protein. Lanz *et al.* (9) showed that *SRA* exists in a ribonucleoprotein complex that contains SRC-1 and is recruited by steroid receptors. (*b*) *SRA* appears to be actually specific for steroid receptors. Indeed, most of the receptor-interacting factors, such as SRC-1 or TIF2/hSRC-2, interact with and coactivate both class I and class II nuclear receptors (9). Because of the importance of ER signaling pathways in the mechanisms underlying breast tumor progression, it was important to establish whether *SRA* could be expressed in breast tumors. If so, it was also of interest to determine whether the expression of *SRA* was related to known markers of endocrine sensitivity and prognostic markers. We have selected a subset of breast cancer cases to look for possible correlations between *SRA* expression and already established predictive and/or prognostic factors, such as grade, ER, and PR status (10).

Materials and Methods

Human Breast Tumors. Twenty-seven cases were selected from the National Cancer Institute of Canada-Manitoba Breast Tumor Bank (Winnipeg, Manitoba, Canada). The cases were selected according to their ER and PR status, as determined by ligand binding assay. Tumors were classified as ER−/PR+ ($n = 8$; ER range, 5–9 fmol/mg protein; PR range, 51–271 fmol/mg protein), ER+/PR− ($n = 6$; ER range, 59–151 fmol/mg protein; PR range, 5–10 fmol/mg protein), ER−/PR− ($n = 5$; ER range, 0–2 fmol/mg protein; PR range, 0–8 fmol/mg protein), and ER+/PR+ ($n = 8$; ER range, 50–127 fmol/mg protein; PR range, 101–285 fmol/mg protein). These tumors covered a wide spectrum of grade (grades 4–9), determined using the Nottingham grading system (11). Patients were 49–87 years old.

RNA Extraction and RT-PCR. Total RNA was extracted from frozen breast tissue sections using Trizol reagent (Life Technologies, Inc., Grand Island, NY) according to the manufacturer's instructions and quantified spectrophotometrically. One μg of total RNA was reverse-transcribed in a final volume of 25 μl, as described previously (12).

Primers and PCR Conditions. The primers used consisted of *SRA*coreU primer (sense, 5′-AGGAACGCGGCTGGAACGA-3′, positions 35–53; GenBank accession no. AF092038) and *SRA* core L primer (antisense, 5′-AGTCTGGGGAACCGAGGAT-3′, positions 696–678; GenBank accession no. AF092038). PCR amplifications were performed and PCR products analyzed as described previously (12), with minor modifications. Briefly, 1 μl of reverse transcription mixture was amplified in a final volume of 15 μl, in the presence of 1.5 μCi of [α-^{32}P]dCTP (3000 Ci/mmol), 4 ng/μl each primer, and 0.3 unit of Taq DNA polymerase (Life Technologies, Inc.). Each PCR consisted of 30 cycles (30 s at 60°C, 30 s at 72°C, and 30 s at 94°C). PCR products were then separated on 6% polyacrylamide gels containing 7 M urea. Following electrophoresis, the gels were dried and exposed for 1 h to a Molecular Imager-FX Imaging screen (Bio-Rad, Hercules, CA). Amplification of the ubiquitously expressed *GAPDH* cDNA was performed in parallel and PCR products separated on agarose gels stained with ethidium bromide as described previously (12). Identity of PCR products was confirmed by subcloning and sequencing, as reported previously (13).

Quantification of *SRA* Expression. Exposed screens were scanned using a Molecular Imager-FX (Bio-Rad), and the intensity of the *SRA* corresponding signal was measured using Quantity One software (Bio-Rad). Three independent PCRs were performed. To control for variations between experiments, a value of 100% was arbitrarily assigned to the *SRA* signal of one particular tumor (tumor 14) measured in each set of PCR experiments, and all signals were expressed as a percentage of this signal. In parallel, *GAPDH* cDNA was amplified and following analysis of PCR products on prestained agarose gels, signals were quantified by scanning using NIH Image 161/ppc software. Three

Received 6/16/99; accepted 7/20/99.

The costs of publication of this article were defrayed in part by the payment of page charges. This article must therefore be hereby marked *advertisement* in accordance with 18 U.S.C. Section 1734 solely to indicate this fact.

[1] This work was supported by grants from the Canadian Breast Cancer Research Initiative and the United States Army Medical Research and Materiel Command. The Manitoba Breast Tumor Bank is supported by funding from the National Cancer Institute of Canada. P. H. W. is a Medical Research Council of Canada Scientist, L. C. M. is a Medical Research Council of Canada Scientist, and E. L. is a recipient of a United States Army Medical Research and Materiel Command Postdoctoral Fellowship.

[2] To whom requests for reprints should be addressed, at Department of Biochemistry and Molecular Biology, University of Manitoba, Winnipeg, Manitoba R3E OW3, Canada. Phone: (204) 789-3812; Fax: (204) 789-3900; E-mail: eleygue@cc.umanitoba.ca.

[3] The abbreviations used are: ER, estrogen receptor; SRA, steroid receptor RNA activator; PR, progesterone receptor; RT-PCR, reverse transcriptase-PCR; GAPDH, glyceraldehyde-3-phosphate dehydrogenase.

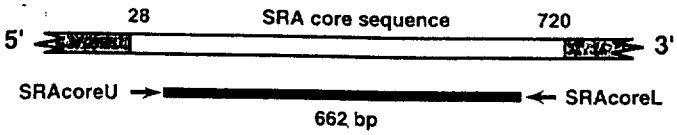

Fig. 1. *SRA* structure and primer presentation. *SRA* isoforms identified to date (9) differ in their 5′ and 3′ terminal regions (■) but present an identical nucleotide sequence (□) in between (*SRA* core sequence, bases 28 to 720). *SRA*coreU and *SRA*coreL primers anneal with *SRA* core sequences and allow the amplification of a 662-bp fragment.

independent PCRs were performed. Each *GAPDH* signal was also expressed as a percentage of the signal observed in the tumor 14. For each sample, the average of *SRA* signal was then expressed as a percentage of the *GAPDH* signal (arbitrary units).

Quantification of *SRA*-Del Relative Expression. It has previously been shown that the coamplification of a wild-type and a deleted variant cDNA resulted in the amplification of two PCR products, the relative signal intensity of which provided a reliable measurement of the relative expression of the deleted variant (13, 14). For each sample, *SRA*-Del corresponding signal was measured using Quantity One software (Bio-Rad) and expressed as a percentage of the corresponding *SRA* signal. For each case, three independent assays were performed, and the mean was determined.

Statistical Analysis. Differences between tumor subgroups were tested using the two-sided Mann-Whitney rank sum test. Correlation between *SRA* expression and tumor characteristics was tested by calculation of the Spearman coefficient *r*.

Results

Detection of *SRA* and a Variant mRNA Deleted Form (*SRA*-Del) in Human Breast Tumor Tissues. The existence of three different *SRA* mRNAs have been reported (9). The sequences of these isoforms differ in their 5′- and 3′-terminal regions but are identical within their central region, called the core (Fig. 1). To investigate the expression of all described *SRA* isoforms in human breast tumor tissues, we designed primers to amplify a 662-bp fragment encompassing almost all of the *SRA* core region. Total RNA was extracted from 27 human breast tumors and reverse-transcribed, and PCR amplification was performed as described in the "Materials and Methods" using SRA core primers. A 662-bp fragment was obtained in all samples. However, the intensity levels varied from one sample to another (Fig. 2*A*). This fragment was sequenced and corresponded to the *SRA* core region. The differences in *SRA* expression were unlikely to result from different cDNA input, as shown by the similar intensities of *GAPDH* signal obtained after amplifying *GAPDH* mRNA in parallel using the same cDNAs (Fig. 2*B*). An additional fragment, migrating at an apparent size of 459 bp was also observed in most samples. Sequencing analysis revealed that this band corresponded to a variant form of *SRA* (referred to as *SRA*-Del) deleted in 203 bp between positions 155 and 357 (corresponding to GenBank accession no. AF092038).

The Expression of *SRA* Correlates with ER and PR Levels in Subgroups of Human Breast Tumors. For each case, the *SRA*-corresponding signal was quantified and expressed in arbitrary units, as described in "Materials and Methods." Results obtained from the 27 cases, grouped according to their ER and PR levels, as determined by ligand binding analysis, are presented Fig. 3*A*. When the cohort of cases was considered as a whole ($n = 27$), no correlation was observed between *SRA* expression and ER or PR levels. Indeed, similar levels of *SRA* were found in ER+/PR+ (median = 65.5, $n = 8$) and ER−/PR− (median = 94.6, $n = 5$) tumors (Fig. 3*A*). However, when only ER− tumors were considered ($n = 13$), a trend toward a positive correlation between *SRA* expression and PR levels was observed (Spearman coefficient $r = 0.527$, $P = 0.064$). *SRA* expression was higher in ER−/PR+ ($n = 8$, median = 144.8) than it was in ER−/PR− tumors (Fig. 3*A*); this difference was statistically significant (two-sided Mann-Whitney rank sum test, $P = 0.045$). In contrast, within ER+ cases ($n = 14$), *SRA* expression negatively correlated with PR levels (Spearman coefficient $r = -0.810$, $P = 0.0004$). *SRA* expression was higher (two-sided Mann-Whitney rank sum test, $P = 0.001$) in ER+/PR− ($n = 6$, median = 156.4) than it was in ER+/PR+ cases. In a similar way, *SRA* expression correlated positively (Spearman coefficient $r = 0.735$, $P = 0.009$) and negatively (Spearman coefficient $r = -0.532$, $P = 0.033$) with ER levels in PR− ($n = 11$) and PR+ ($n = 16$) cases, respectively. *SRA* levels were higher in ER+/PR− than in ER−/PR− tumors (two-sided Mann-Whitney rank sum test, $P = 0.017$) and in ER−/PR+ than in ER+/PR+ cases (two-sided Mann-Whitney rank sum test, $P = 0.047$). *SRA* levels of expression did not correlate with tumor grade scores (Fig. 3*B*).

The Expression of *SRA*-Del Correlates with Breast Tumor Grade Scores. For each case, *SRA*-Del signal was measured and expressed relative to the corresponding *SRA* signal, as described in the "Materials and Methods." *SRA*-Del relative signal did not correlate with ER or PR levels when the cohort of cases was considered as a whole or when ER−, ER+, and PR− subgroups were analyzed. Interestingly, *SRA*-Del expression positively correlated (Spearman coefficient $r = 0.512$, $P = 0.042$) with PR levels in PR+ subgroup ($n = 16$). However, no statistically significant differences (Fig. 4*A*) were observed between ER−/PR+ ($n = 8$, median = 2.346), ER+/PR− ($n = 6$, median = 2.561), ER−/PR− ($n = 5$, median = 6.571) and ER+/PR+ ($n = 8$, median = 3.528). By contrast, *SRA*-Del levels strongly correlated (Spearman coefficient $r = 0.530$, $P = 0.004$) with Nottingham grade scores within the whole cohort ($n = 27$). The level of expression of *SRA* was significantly higher (two-sided Mann-Whitney rank sum test, $P < 0.05$) in tumors of high grade ($n = 7$, median = 6.572) than it was in tumors of low ($n = 4$, median = 2.192) or intermediate ($n = 9$, median = 2.588) grade (Fig. 4*B*).

Discussion

Using primers annealing with the core region of the three previously described *SRA* isoforms (9), we have investigated *SRA* expression in 27 independent breast tumors by means of semiquantitative RT-PCR. These *SRA* isoforms, although different in their 5′- and 3′-terminal regions, are all able to coactivate steroid receptor. Indeed,

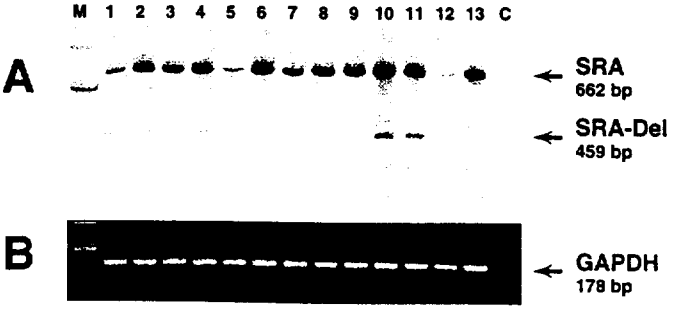

Fig. 2. Detection of *SRA* in human breast tumors by RT-PCR. Total RNA was extracted from 27 breast tumors, reverse-transcribed, and analyzed by PCR as described in "Materials and Methods." PCR products were separated on 6% acrylamide gels. Gels were dried and exposed 1 h to a Molecular Imager-FX Imaging screen. Screens were then scanned using a Molecular Imager-FX. *A*, computerized image showing the results obtained for 13 cases (*Lanes 1–13*). *Lane M*, molecular weight marker (ϕx174 RF DNA/*Hae*III fragments). *Lane C*, control lane, no cDNA added in the PCR. Sequencing analysis of PCR fragments revealed that the 662-bp (*SRA*) and 459-bp (SRA-Del) fragments corresponded to *SRA* and to a variant *SRA* isoform deleted in sequences from position 155 to 357 (GenBank accession no. AF092038), respectively. *B*, ethidium bromide-stained gel of the RT-PCR analysis of *GAPDH* mRNA run in parallel for the same samples.

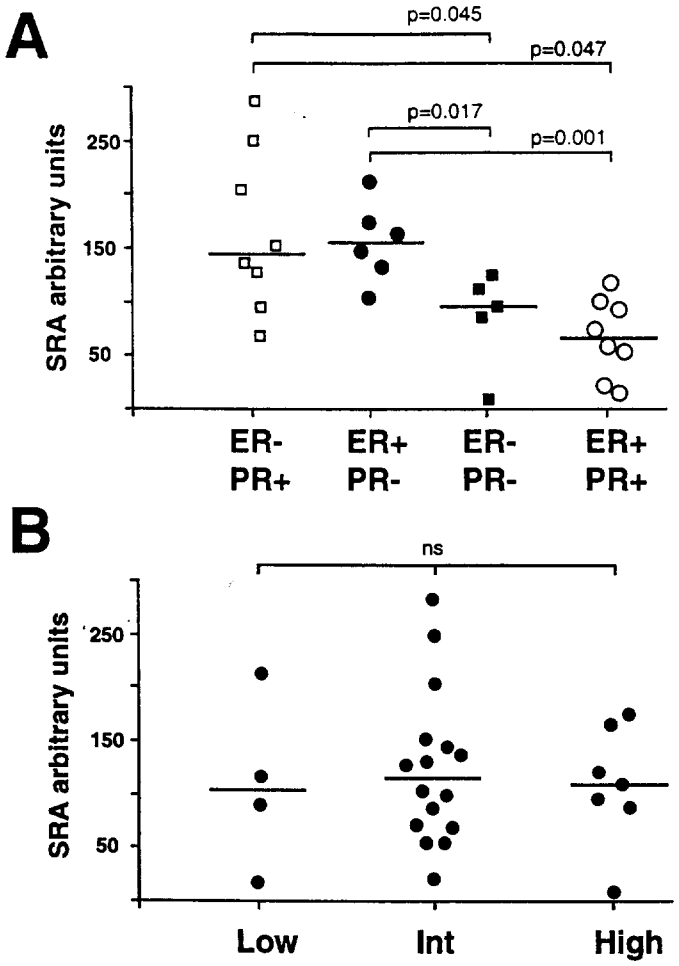

Fig. 3. Subgroup analysis of *SRA* expression within 27 human breast tumors. For each case, *SRA* expression was quantified and expressed in arbitrary units as described in "Materials and Methods." *A*, tumors were grouped according to their ER and PR status, as determined by ligand binding assay. □, ER−/PR+ tumors; ●, ER+/PR− tumors; ■, ER−/PR− tumors; and ○, ER+/PR+ tumors. *B*, tumors were grouped according to their grade: low (Nottingham grading scores 4–5), intermediate (Nottingham grading scores 6–7), and high (Nottingham grading scores 8–9). The *horizontal line* represents the median value in each group. *P*s (two-sided Mann-Whitney rank sum test) are indicated when subgroups were statistically different. *ns*; no statistically significant differences were found between subgroups.

SRA core region was found to be necessary and sufficient for the coactivation properties of *SRA* isoforms (9). Therefore, although PCR performed using primers spanning the *SRA* core region is likely to recognize several different *SRA*-like molecules, the signal obtained corresponds to molecules that should all have essentially the same function, *i.e.*, coactivation of steroid receptors.

The expression of *SRA* did not correlate with ER or PR status when the cohort was considered as a whole. This differs from what has been observed for another coactivator, *AIB1*. Indeed, Anzick *et al.* (15) first showed that a strong expression of *AIB1* that resulted from *AIB1* gene amplification was observed in ER+ but not in ER− breast cancer cell lines. More recently, Bautista *et al.* (16) reported that *AIB1* gene amplification correlated with ER and PR positivity. Our results suggest that the pattern of expression of *SRA* is more complex. Indeed, we found that *SRA* expression could correlate positively or negatively with ER and PR levels, depending on the subgroup considered. The general trend appeared to be that, in tumors expressing a low level of one receptor (ER or PR), a positive correlation was found between *SRA* expression and the second receptor (PR or ER). Inversely, in tumors highly expressing one receptor (ER or PR), *SRA* expression negatively correlated with the level of expression of the second receptor (PR or ER). At this stage of the knowledge of *SRA* biological function, the interpretation of such an observation is difficult. Indeed, *SRA* has been shown to be able to coactivate both ER and PR (9). Moreover, progestins are known to decrease the steady state levels of ER-α mRNA and protein, whereas estrogens increase PR expression (17, 18). Therefore, all combinations and cross-talk appear possible. One could speculate that increased levels of *SRA* in ER−/PR+ cases could partially be responsible, by "boosting" the activity of the weakly expressed ER, of the expression of PR in these tumors. Inversely, in the same ER−/PR+ cases, the strong *SRA* expression could be responsible for an increased down-regulation of ER by PR. Our results suggest that *SRA* expression varies from one particular tumor to another. Changes in *SRA* expression can be associated with known prognostic and predictive factors such as ER and PR in particular tumor subgroups. The question of a direct involvement of *SRA* in the hormonal status changes occurring during breast tumor progression remains unanswered. Also of interest is the fact that *SRA* interacts with the activation function 1 of the steroid receptors (9). Activation function 1 is thought to mediate the agonistic effect of antiestrogens such hydroxytamoxifen (19). This agonistic action of antiestrogens is believed to be involved in part in the mechanisms underlying hormone

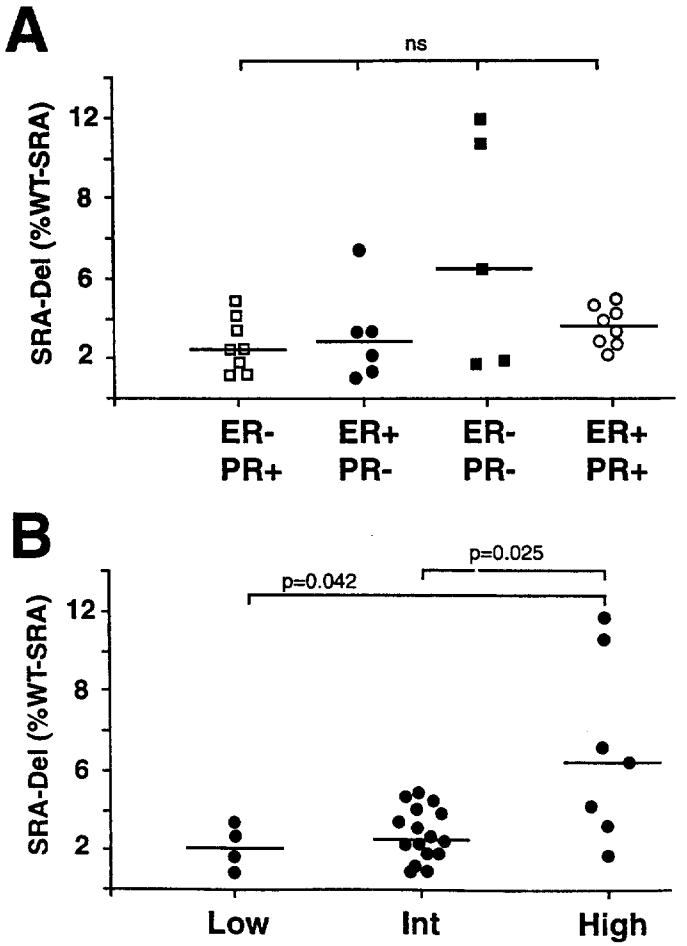

Fig. 4. Subgroup analysis of *SRA*-Del relative expression within 27 human breast tumors. For each case, SRA-D3 expression relative to *SRA* was quantified as described in "Materials and Methods." *A*, tumors were grouped according to their ER and PR status, as determined by ligand binding assay. □, ER−/PR+ tumors; ●, ER+/PR− tumors; ■, ER−/PR− tumors; and ○, ER+/PR+ tumors. *B*, tumors were grouped according to their grade: low (Nottingham grading scores 4–5), intermediate (Nottingham grading scores 6–7), and high (Nottingham grading scores 8–9). The *horizontal line* represents the median value in each group. *P*s (two-sided Mann-Whitney rank sum test) are indicated when subgroups were statistically different. *ns*; no statistically significant differences were found between subgroups.

resistance in breast cancer. One could speculate that the level of *SRA* expression might, therefore, modulate and predict the response of a given tumor to hormone therapy. This hypothesis appears to be refuted by the observation of similar levels of *SRA* in ER+/PR+ and ER−/PR− tumors. But ER+/PR+ tumors, as opposed to ER−/PR− tumors, are likely to respond to endocrine therapy and prevention (see Ref. 2 and references therein). In these cases, the differences in ER levels rather than in *SRA* expression are more likely involved in the mechanisms underlying endocrine sensitivity. On the other hand, the observation of a higher *SRA* expression within ER−/PR+ cases, which are more likely to respond to hormone therapy than ER−/PR− tumors (see Ref. 20 and references therein), would be consistent with the hypothesis of a possible involvement of *SRA* in these mechanisms under some circumstances. One should also note that Berns *et al.* (21) recently reported that, although no correlation was found between the expression of *SRC-1* and ER status, a high expression of this coactivator indicated a favorable response to tamoxifen of patients with recurrent breast cancer. This issue can only be addressed in studies performed on tumors from patients that did and did not respond to endocrine therapy.

We have identified in breast tumor cases a new *SRA* isoform deleted in sequences from nucleotide 155 to 357 (*SRA*-Del). Interestingly, sequence comparison using the BLAST algorithm and the human EST database showed that this deleted *SRA* isoform has already been found in a pooled cDNA library containing cDNAs from melanocyte, fetal heart, and pregnant uterus (GenBank accession no. AA426601). Because uterus is another steroid target tissue, it could be hypothesized that the source of *SRA*-Del in this pooled library was, indeed, uterus. Even though the structure of the *SRA* gene has not yet been published, *SRA*-Del appears to correspond to a perfect exon-3 deleted *SRA* variant. *SRA* gene has recently been located on chromosome 5q31.3-32.[4] Sequence analysis of the corresponding DNA sequence (chromosome 5, BAC clone 319C17; GenBank accession no. AC005214) revealed that the fragment from nucleotide 155 to 357 corresponds to the third *SRA* exon. The putative function of *SRA*-Del remains to be determined. One should, however, note that a recombinantly developed *SRA* mutant, deleted of the region 3′ of a *Bbs*I site (position 341) and, therefore, partially deleted of exon 3 sequences, did not coactivate steroid receptors (9). Moreover, exon 3 deletion introduces a shift in the open reading frames, suggested by Lanz *et al.* (9), and could lead to a premature termination of the putative SRA proteins. One could, therefore, hypothesize that *SRA*-Del might interfere with *SRA* activity. The resulting modifications of the steroid receptor signaling pathways could confer a more aggressive behavior to the tumors expressing higher levels of *SRA*-Del. The positive correlation between *SRA*-Del levels and tumor grade scores would be consistent with this hypothesis.

Interestingly, modifications of the long arm of the chromosome 5 have been reported in breast tumors. Indeed, Hermsen *et al.* (22) found a frequent chromosomal gain in 5q within a subset of 53 lymph node-negative breast carcinoma, whereas Schwendel *et al.* (23) observed a frequent loss of this region in 39 invasive breast carcinomas. Moreover, among *BRCA1* mutation carriers, loss of 5q was observed more frequently than in the control patient (24). One could, therefore, speculate that the loss of *SRA* is selected for during tumor progression in cells lacking *BRCA1* functional gene. Whether changes in *SRA* expression result from chromosomal abnormalities remains to be determined.

In conclusion, we have shown that *SRA* is expressed in breast tumors and that its expression correlates with ER and PR levels in particular tumor subgroups. We speculate that changes in *SRA* expression could be involved in the mechanisms underlying tumor progression and hormone resistance.

References

1. Vorherr, H. (ed.). Breast Cancer. Baltimore: Urban and Schwarzenberg Press, 1980.
2. Jordan, V. C., and Morrow, M. Tamoxifen, Raloxifene, and the prevention of breast cancer. Endocr. Rev., *20:* 253–278, 1999.
3. Green, S., Walter, P., Kumar, V., Krust, A., Bornert, J. M., Argos, P., and Chambon, P. Human oestrogen receptor cDNA: sequence, expression and homology to v- erb-A. Nature (Lond.), *320:* 134–139, 1986.
4. Mosselman, S., Polman, J., and Dijkema, R. ER β: identification and characterization of a novel human estrogen receptor. FEBS Lett., *392:* 49–53, 1996.
5. Ogawa, S., Inoue, S., Watanabe, T., Hiroi, H., Orimo, A., Hosoi, T., Ouchi, Y., and Muramatsu, M. The complete primary structure of human estrogen receptor β (hER β) and its heterodimerization with ER α *in vivo* and *in vitro*. Biochem. Biophys. Res. Commun., *243:* 129–132, 1998.
6. Evans, R. M. The steroid and thyroid receptor super-family. Science (Washington DC), *240:* 889–895, 1988.
7. Shibata, H., Spencer, T. E., Onate, S. A., Jenster, G., Tsai, S. Y., Tsai, M. J., and O'Malley, B. W. Role of co-activators and co-repressors in the mechanism of steroid/thyroid receptor action. Rec. Prog. Horm. Res., *52:* 141–164, 1997.
8. McKenna, N. J., Lanz, R. B., and O'Malley, B. W. Nuclear receptor coregulators: cellular and molecular biology. Endocr. Rev., *20:* 321–344, 1999.
9. Lanz, R. B., McKenna, N. J., Onate, S. A., Albrecht, U., Wong, J., Tsai, S. Y., Tsai, M-J., and O'Malley, B. W. A steroid receptor coactivator, *SRA*, functions as an RNA and is present in an SRC-1 complex. Cell, *97:* 17–27, 1999.
10. Henderson, I. C., and Patek, A. J. The relationship between prognostic and predictive factors in the management of breast cancer. Breast Cancer Res. Treat., *52:* 261–288, 1998.
11. Elston, C. W., and Ellis, I. O. Pathological prognostic factors in breast cancer. Histopathology, *19:* 403–410, 1991.
12. Leygue, E., Murphy, L. C., Kuttenn, F., and Watson, P. H. Triple primer PCR: a new way to quantify truncated mRNA expression. Am. J. Pathol., *148:* 1097–1103, 1996.
13. Leygue, E., Watson, P. H., and Murphy, L. C. Estrogen receptor variants in normal human mammary tissue. J. Natl. Cancer Inst., *88:* 284–290, 1996.
14. Daffada, A. A. I., Johnston, S. R. D., Nicholls, J., and Dowsett, M. Detection of wild type and exon 5-deleted splice variant oestrogen receptor (ER) mRNA in ER-positive and -negative breast cancer cell lines by reverse transcription/polymerase chain reaction. J. Mol. Endocrinol., *13:* 265–273, 1994.
15. Anzick, S. L., Kononen, J., Walker, R. L., Azorsa, D. O., Tanner, M. M., Guan, X. Y., Sauter, G., Kallioniemi, O. P., Trent, J. M., and Meltzer, P. S. AIB1, a steroid receptor coactivator amplified in breast and ovarian cancer. Science (Washington DC), *277:* 965–968, 1997.
16. Bautista, S., Valles, H., Walker, R. L., Anzick, S., Zeillinger, R., Meltzer, P., and Theillet, C. In breast cancer, amplification of the steroid receptor coactivator gene *AIB1* is correlated with estrogen and progesterone receptor positivity. Clin. Cancer Res., *4:* 2925–2929, 1998.
17. Read, L., Greene, G., and Katzenellenbogen, B. Regulation of estrogen receptor messenger ribonucleic acid and protein levels in human breast cancer cell lines by sex steroid hormones, their antagonists and growth factors. Mol. Endocrinol., *3:* 295–304, 1989.
18. Berkenstam, A., Glaumann, H., Martin, M., Gustafsson, J. A., and Norstedt, G. Hormonal regulation of estrogen receptor messenger ribonucleic acid in T47Dco and MCF-7 breast cancer cells. Mol. Endocrinol., *3:* 22–28, 1989.
19. Berry, M., Metzger, D., and Chambon, P. Role of the two activating domains of the oestrogen receptor in the cell-type and promoter-context dependent agonistic activity of the anti-oestrogen 4-hydroxytamoxifen. EMBO J., *9:* 2811–2818, 1990.
20. Osborne, C. K. Steroid hormone receptors in breast cancer management. Breast Cancer Res. Treat., *51:* 227–238, 1998.
21. Berns, E. M., Van Staveren, I. L., Klijn, J. G., and Foekens, J. A. Predictive value of SRC-1 for tamoxifen response of recurrent breast cancer. Breast Cancer Res. Treat., *48:* 87–92, 1998.
22. Hermsen, M. A., Baak, J. P., Meijer, G. A., Weiss, J. M., Walboomers, J. W., Snijders, P. J., and van Diest, P. J. Genetic analysis of 53 lymph node-negative breast carcinomas by CGH and relation to clinical, pathological, morphometric, and DNA cytometric prognostic factors. J. Pathol., *186:* 356–362, 1998.
23. Schwendel, A., Richard, F., Langreck, H., Kaufmann, O., Lage, H., Winzer, K. J., Petersen, I., and Dietel, M. Chromosome alterations in breast carcinomas: frequent involvement of DNA losses including chromosomes 4q and 21q. Br. J. Cancer, *78:* 806–811, 1998.
24. Tirkkonen, M., Johannsson, O., Agnarsson, B. A., Olsson, H., Ingvarsson, S., Karhu, R., Tanner, M., Isola, J., Barkardottir, R. B., Borg, A., and Kallioniemi, O. P. Distinct somatic genetic changes associated with tumor progression in carriers of *BRCA1* and *BRCA2* germ-line mutations. Cancer Res., *57:* 1222–1227, 1997.

[4] http://www.ncbi.nlm.nih.gov/genemap/loc.cgi?ID=12637.

[CANCER RESEARCH 60, 2796–2799, June 1, 2000]

Advances in Brief

Expression of a Repressor of Estrogen Receptor Activity in Human Breast Tumors: Relationship to Some Known Prognostic Markers[1]

Sharon L. R. Simon, Alicia Parkes, Etienne Leygue, Helmut Dotzlaw, Linda Snell, Sandra Troup, Adewale Adeyinka, Peter H. Watson, and Leigh C. Murphy[2]

Departments of Biochemistry and Medical Genetics [S. L. R. S., A. P., E. L., H. D., L. C. M.] and Pathology [L. S., S. T., A. A., P. H. W.], Faculty of Medicine, University of Manitoba, Winnipeg, Manitoba R3E 0W3, Canada

Abstract

The expression of a specific repressor of estrogen receptor activity (REA) was investigated by a semiquantitative reverse transcription-PCR assay in 40 human breast tumor biopsy samples with respect to steroid hormone receptor status and other known prognostic variables. The data showed that REA expression was positively correlated with estrogen receptor (ER) levels as defined by ligand-binding assays (Spearman $r = 0.3231$; $P = 0.042$) and that the median level of REA mRNA was significantly (Mann-Whitney two-tailed test, $P = 0.0424$) higher in ER+ tumors (median = 94.5; $n = 30$) compared with ER− tumors (median = 64.5; $n = 10$), with no significant differences ($P = 0.4988$) associated with progesterone receptor status alone. In addition, REA expression was inversely correlated with tumor grade (Spearman $r = -0.4375$; $P = 0.0054$). When the tumors were divided into two groups based on grade, REA expression was significantly (Mann-Whitney two-tailed test, $P = 0.0024$) higher in low-grade (median = 97; $n = 16$) compared with high-grade (median = 76; $n = 23$) tumors. These results provide preliminary data suggesting that the expression of REA varies among breast tumors and is correlated with known treatment response markers and inversely correlated with a marker of breast cancer progression. REA together with ER status may be an improved marker of endocrine therapy responsiveness in human breast cancer.

Introduction

Estrogens have important roles in both normal and neoplastic mammary tissues; however, marked changes occur in estrogen action during both breast tumorigenesis and breast cancer progression (1). The mechanisms underlying altered estrogen signal transduction in target tissues is the focus of much research at present. Current concepts of estrogen action include cofactors that can either enhance or repress the transcriptional activity of the ER[3] (2). Recently, a highly specific repressor of the transcriptional activity of ligand-occupied ERs (ER-α and ER-β but not other steroid hormone receptors such as PR or type II nuclear receptors) was identified and characterized using a yeast two-hybrid system (3). Furthermore, part of its mechanism of action appeared to involve functional competition with steroid hormone receptor coactivators such as SRC-1 (2). This repressor differed from previously identified corepressors such as nuclear receptor corepressor and silencing mediator for retinoid and thyroid hormone receptor; in that it was not structurally related to either of them, it showed great selectivity for ER as opposed to other steroid hormone or non-steroid-binding members of the nuclear receptor family, and it required ER to be bound to ligand with preferential effects being seen when the ligand was an antiestrogen (3). This repressor was therefore called REA. Because REA is selective for ER, it is highly relevant to investigate the expression of this gene in human breast tissues both normal and neoplastic.

Recently we demonstrated that REA is expressed in both normal and neoplastic human breast tissues,[4] as measured by RT-PCR. Furthermore, the expression of REA was not significantly different between ER+ breast tumors and their matched adjacent normal breast tissues.[4] However, the tumor cohort in the previous study were all ER+ as determined by ligand-binding assays and did not address the question of whether REA expression in breast tumors was correlated with known prognostic and endocrine treatment response markers. In this study, we investigated the relationship of REA expression in breast tumors to ER and PR status and other known prognostic variables.

Materials and Methods

Human Breast Tumors. Forty invasive ductal carcinomas were selected from the National Cancer Institute of Canada-Manitoba Breast Tumor Bank (Winnipeg, Manitoba, Canada). The cases were selected for ER and PR status as determined by ligand-binding assays. The ER levels were 0–151 fmol/mg of protein, and 30 tumors were classified as ER+ (defined as >3 fmol/mg of protein). PR levels were 0–285 fmol/mg of protein, and 20 tumors were classified as PR+ (defined by >10 fmol/mg of protein). These tumors spanned a wide range of grade (grades 4–9), determined using the Nottingham grading system.

Cell Culture. T-47D human breast cancer cells were obtained from Dr. D. Edwards (Denver, CO), and MCF7 cells were obtained from the late Dr. W. McGuire (San Antonio, TX). T-47D cells were grown in DMEM supplemented with 5% fetal bovine serum, 100 nM glutamine, 0.3% (v/v) glucose, and penicillin/streptomycin as described previously (4). Cells were plated at 1×10^6 in 100-mm dishes and 2 days later were treated with 10 nM medroxyprogesterone acetate and harvested at various times (1–48 h). MCF7 human breast cancer cells were depleted of estrogen by passaging stock cells twice in phenol red-free DMEM supplemented with 5% twice charcoal-stripped fetal bovine serum, 100 nM glutamine, 0.3% (v/v) glucose, and penicillin/streptomycin (5% twice charcoal-stripped fetal bovine serum) as described previously (5). Cells were then plated as above in 5% twice charcoal-stripped fetal bovine serum and 2 days later treated with 10 nM estradiol-17β and harvested for analysis at various times (1–48 h). The steroids were added directly from 1000× stock solutions in ethanol to achieve the required concentrations. The cells were harvested by scraping with a rubber policeman. After centrifugation, the cell pellet was frozen and stored at −70°C until RNA was isolated.

Received 1/10/00; accepted 4/11/00.

The costs of publication of this article were defrayed in part by the payment of page charges. This article must therefore be hereby marked *advertisement* in accordance with 18 U.S.C. Section 1734 solely to indicate this fact.

[1] This work was supported by grants from the Canadian Breast Cancer Research Initiative (CBCRI) and the United States Army Medical Research and Materiel Command (USAMRMC). The Manitoba Breast Tumor Bank is supported by funding from the National Cancer Institute of Canada (NCIC). P. H. W. is a Medical Research Council of Canada (MRC) Scientist, and L. C. M. is an MRC Scientist.

[2] To whom requests for reprints should be addressed, at Department of Biochemistry and Molecular Biology, University of Manitoba, Winnipeg, MB R3E OW3, Canada. Phone: (204) 789-3812; Fax: (204) 789-3900; E-mail: lcmurph@cc.umanitoba.ca.

[3] The abbreviations used are: ER, estrogen receptor; PR progesterone receptor; REA, repressor of estrogen receptor activity; RT-PCR, reverse transcription-PCR; GAPDH, glyceraldehyde-3-phosphate dehydrogenase.

[4] L. C. Murphy, S. L. R. Simon, A. Parkes, E. Leygue, H. Dotzlaw, L. Snell, S. Troup, A. Adeyinka, and P. H. Watson. Altered relative expression of estrogen receptor coregulators during human breast tumorigenesis, submitted for publication.

RNA Extraction and RT-PCR Conditions. Total RNA was extracted from 20-μm frozen tissue sections (20 sections per tumor) or cell pellets using Trizol reagent (Life Technologies, Grand Island, NY) according to the manufacturer's instructions and quantified spectrophotometrically. One μg of total RNA was reverse transcribed in a final volume of 25 μl as described previously (6).

Primers and PCR Conditions. The primers used were primer REAU (5'-CGA AAA ATC TCC TCC CCT ACA-3'; sense; positions, GenBank Accession No. AF150962) and primer REAL (5'-CCT GCT TTG CTT TTT CCA-3'; antisense; position, GenBank Accession No. AF150962). PCR amplifications were performed and PCR products analyzed as described previously (7) with minor modifications. Briefly, 1 μl of reverse transcription mixture was amplified in a final volume of 20 μl in the presence of 4 ng/μl of each primer and 0.3 units of *Taq* DNA polymerase (Life Technologies). Each PCR consisted of 27 cycles (30 s at 57°C, 30 s at 72°C, and 30 s at 94°C) for measuring REA. PCR products were then separated on 1.8% agarose gels stained with ethidium bromide as described previously (7). Amplification of the ubiquitously expressed *GAPDH* cDNA was performed in parallel, and PCR products were separated on agarose gels stained with ethidium bromide as described previously (7). The identities of PCR products were confirmed by subcloning and sequencing, as reported previously (6).

Quantification and Statistical Analysis of REA Expression. After analysis of PCR products on prestained agarose gels, signals were quantified by scanning using MultiAnalyst (Bio-Rad, Hercules, CA). At least three independent PCRs were performed. To control for variations between experiments, a value of 100% was arbitrarily assigned to the REA signal of one particular sample and all signals were expressed as a percentage of this signal. In parallel, *GAPDH* cDNA was amplified, and after analysis of PCR products on prestained agarose gels, signals were quantified by scanning using MultiAnalyst. Three independent PCRs were performed. Each *GAPDH* signal was also expressed as a percentage of the signal observed in the same tumor. For each sample, the average of REA signal was then expressed as a percentage of the *GAPDH* signal (arbitrary units).

Correlation between REA expression and tumor characteristics was tested by calculation of the Spearman coefficient, *r*. Differences between tumor subgroups were tested using the Mann-Whitney rank-sum test, two-sided.

Results

Measurement of REA mRNA Expression in Primary Human Breast Tumors with Different ER and PR Status. We previously developed a semiquantitative RT-PCR approach to measure REA mRNA in small amounts of human breast tissues.[4] Cloning and sequencing confirmed the identity of the expected 397-bp PCR product as REA, and this PCR product was used to probe Northern blots of RNA extracted from human breast tumor biopsies as described previously (8). An ~1.5-kb transcript was detected, consistent with the previously described REA mRNA (Fig. 1). Varying levels of REA mRNA were detected in human breast tumor biopsy samples, which raised the question of whether the expression of REA in breast tumors was correlated with the known prognostic and treatment response variables, such as ER and PR status.

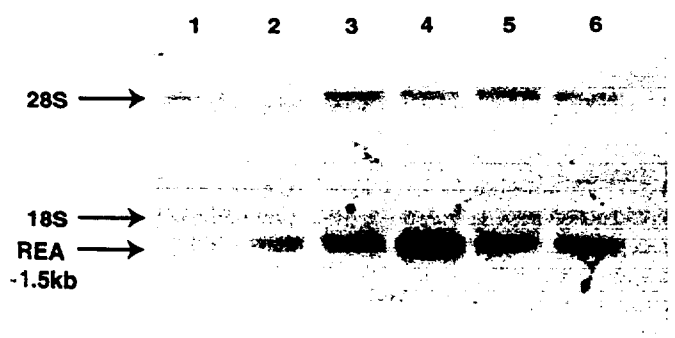

Fig. 1. Northern blot analysis of poly(A)+ enriched RNA (15 μg) isolated from several human breast cancer biopsy samples. The 397-bp REA PCR product was used to probe the Northern blot as described previously (8). Residual 28S and 18S bands are shown, as is the ~ 1.5-kb band corresponding to REA mRNA.

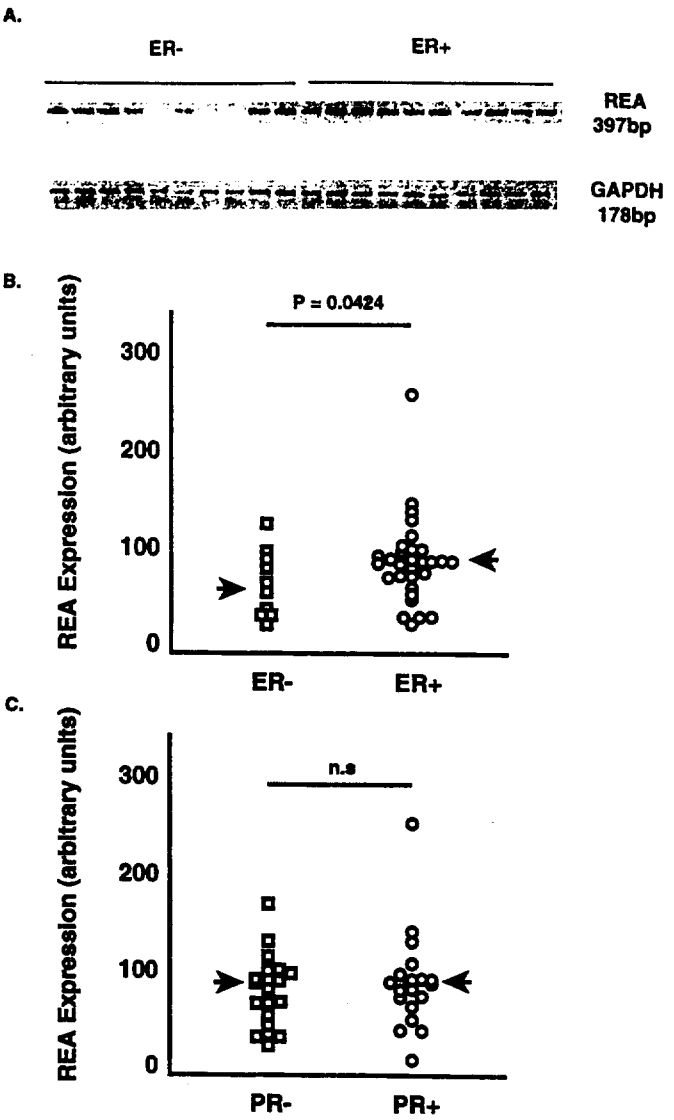

Fig. 2. *A*, RNA was extracted and assayed for REA expression using RT-PCR as described in "Materials and Methods." After analysis of PCR products on prestained agarose gels, signals were quantified by scanning using MultiAnalyst. Ethidium bromide-stained gel of the RT-PCR analysis of some ER− and ER+ breast tumors is shown (*top*). The expected 397-bp REA PCR product (confirmed by sequence analysis) is shown. Ethidium bromide-stained gel of the RT-PCR analysis of *GAPDH* mRNA run in parallel for the same samples is shown *below* the REA analysis. The expected 178-bp *GAPDH* PCR product is shown. *B*, for each tumor ($n = 40$), REA expression was quantified and expressed in arbitrary units corrected for *GAPDH* signal as described in "Materials and Methods." The tumors were divided into ER+ (>3 fmol/mg of protein; ○) and ER− (≤3 fmol/mg of protein; □) as defined by ligand-binding assays. The results are presented as a scatter graph. *Arrows* indicate the median value in each group. REA expression is significantly less in ER− tumors compared with ER+ tumors (Mann-Whitney two-tailed, $P = 0.0424$). *C*, for each tumor ($n = 40$), REA expression was quantified and expressed in arbitrary units corrected for *GAPDH* signal as described in "Materials and Methods." The tumors were divided into PR+ (>10 fmol/mg of protein; ○) and PR− (≤10 fmol/mg of protein; □) as defined by ligand-binding assays. The results are presented as a scatter graph. *Arrows* indicate the median value in each group. REA expression is not significantly (*n.s.*) different between PR− tumors and PR+ tumors.

Tumors were identified according to their ER or PR status as defined by ligand-binding analysis (see "Materials and Methods"). REA mRNA levels were measured by RT-PCR and normalized to the GAPDH mRNA level as measured in parallel by RT-PCR. Examples of the results obtained are shown in Fig. 2*A*. The results obtained for all tumors assayed are shown as scatter graphs in Fig. 2*B* (arranged according to ER) and Fig. 2*C* (arranged according to PR status of the

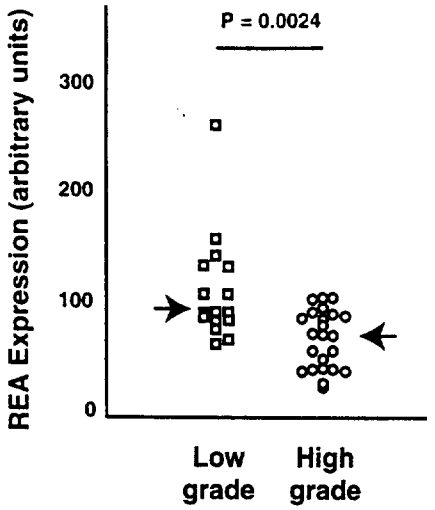

Fig. 3. For each tumor (n = 40), REA expression was quantified and expressed in arbitrary units corrected for *GAPDH* signal as described in "Materials and Methods." The tumors were divided into low-grade (Nottingham grades 3–6; □) and high-grade (Nottingham grades 7–9;○). The results are presented as a scatter graph. *Arrows* indicate the median value in each group. REA expression is significantly higher in low-grade tumors compared with high-grade tumors (Mann-Whitney two-tailed, P = 0.0024).

tumor as measured by ligand-binding analysis). When the level of REA mRNA in tumors was assessed according to either ER status or PR status alone, as defined by ligand-binding analysis, the level of REA mRNA was significantly (Mann-Whitney two-tailed test, P = 0.0424) higher in ER+ tumors (median, 94.5; n = 30) compared with ER− tumors (median, 64.5; n = 10), with no significant differences (P = 0.4988) associated with PR status alone (PR+ median, 91.5; n = 20; PR− median, 87.5; n = 20).

The relationship of the level of REA mRNA levels with ER status in human breast tumor biopsies suggested the hypothesis that REA expression may be regulated by estrogens and/or progestins. However, no effect of estrogen (10 nM estradiol-17β) on the steady-state REA mRNA levels in estrogen-depleted MCF7 cells was observed over a 48-h time span (data not shown). In addition, no effect of progestin (10 nM medroxyprogesterone acetate) treatment on REA mRNA in T-47D cells was observed over a similar time span (data not shown). It was concluded that the expression of REA mRNA was not regulated by estrogens or progestins in human breast cancer cell lines.

Correlation of REA Expression with Tumor Characteristics. Spearman analysis showed a significant correlation of the level of REA mRNA in the tumors with the level of ER as measured by ligand-binding assays (Spearman r = 0.3231; P = 0.042) but no significant correlation with the level of PR as measured by ligand-binding assays (Spearman r = 0.2777; P = 0.0841). These data are consistent with the data analyzed using clinically relevant cutoff values for ER (ER+ >3 fmol/mg of protein) and PR (PR+ >10 fmol/mg of protein) status as shown above. However, statistical significance of the correlation of REA mRNA and ER binding was lost when Spearman analysis was applied only to those tumors that were ER+ (>3 fmol/mg of protein). The level of REA mRNA was also found to be inversely correlated with tumor grade (Spearman r = −0.4375; P = 0.0054). When the tumors were divided into two groups based on grade (low, Nottingham grades 3–6; high, Nottingham grades 7–9), the level of REA mRNA (Fig. 3) was significantly (Mann-Whitney two-tailed test, P = 0.0024) higher in low-grade (median, 97; n = 16) compared with high-grade (median, 76; n = 23) tumors, which is consistent with the Spearman correlation analysis.

No significant correlations were found between the level of REA mRNA and age, nodal status, percentage of normal duct and lobular epithelium, or percentage of stromal or fat cell content within the tumor sections analyzed.

Discussion

Our data show that the level of REA mRNA in human breast tumors is significantly correlated with ER status and inversely correlated with grade. These data are the first to identify a correlation between REA mRNA expression and known prognostic and treatment response markers in human breast cancer biopsies. The positive correlation of REA and ER expression (a good prognostic variable and a marker of response to endocrine therapies) together with inverse correlation of REA expression and grade suggests that REA expression could also be a marker of good prognosis and likelihood of response to endocrine therapies such as antiestrogens. The loss of statistical significance of the correlation between ER levels and REA mRNA when only ER+ breast tumors were analyzed may be due to the reduced numbers of observations in that analysis (n = 30 compared with n = 40 for total tumor cohort) or may indicate the existence of some threshold effect associated with expression of ER and REA. This latter suggestion together with the lack of correlation of absolute ER levels and REA mRNA in ER+ tumors would be consistent with our observation that REA expression, at least at the RNA level, was found not to be regulated by estrogen.

REA has been identified as a protein that interacts in a yeast-two hybrid system with a dominant negative mutant ERα (3). It was shown to be a selective repressor of ER (both ERα and ERβ) transcriptional activity as determined in transient transfection assays using several estrogen-responsive element-containing promoters regulating a chloramphenicol acetyltransferase reporter gene. Cotransfection of a REA expression vector enhanced the potency of antiestrogens such as 4-hydroxytamoxifen and ICI 182780. Furthermore, REA competitively reversed coactivator, *i.e.*, SRC-1, transcriptional enhancement of ER activity. Together these data suggest that REA is a corepressor of ER transcriptional activity.

The current concept of the mechanism by which nuclear hormone receptors regulate gene transcription involves three main components as proposed by Katzenellenbogen *et al.* (9): the receptor, its ligands, and its coregulators. Coregulators appear to consist of at least two classes: those that enhance nuclear hormone receptor activity, referred to as coactivators, and those that repress nuclear hormone receptor activity, referred to as corepressors (2). Furthermore, it has been suggested that differences in the ratios of expression of these two different groups of coregulators may underlie altered responses to steroid hormone agonists and antagonists (10–13). More recently, we have provided the first evidence to suggest that an imbalance between factors that can enhance ER and factors that can repress ER transcriptional activity occurs during human breast tumorigenesis *in vivo*.[4] Our data showed that the levels of expression of the two ER coactivators, steroid receptor RNA activator (14) and amplified in breast cancer-1 (15), were significantly increased in ER+ breast tumors compared with their normal adjacent breast tissues, whereas the level of REA, a repressor of ER activity, was not significantly different between the tumors and normal breast tissues in the same patient cohort. However, this investigation used only ER+ breast tumors and could not address the question of REA expression in relation to steroid receptor status and other prognostic variables in breast tumors. In addition, we and others have shown that the expression of the coactivators, steroid receptor RNA activator (16) and amplified in breast cancer-1 (17), varies among breast tumors and can be correlated with steroid receptor status in some cases.

ER status itself is associated with grade, with most ER+ breast tumors being low grade and having low tumor proliferation rates.

defined by the percentage of S-phase cells (18), and this may contribute to the inverse relationship of REA with grade observed in this study. However, REA expression is more strongly inversely correlated with grade than positively with ER status; therefore, it is possible that a repressor of ER activity that can contribute to the proliferative activity of breast tumor cells could have a significant negative effect on breast cancer progression and thus functionally influence breast cancer progression. It is speculated that the coexpression of ER and REA may therefore provide better prognostic information than either alone.

ER status is also an important treatment response marker in human breast cancer (18) where the presence of ER in breast tumors increases the likelihood of response to endocrine therapies such as antiestrogens. However, a significant portion of ER+ tumors will not respond to tamoxifen initially, and of those tumors that do respond, many eventually will develop resistance to tamoxifen and other endocrine therapies (18). It has been speculated that altered relative ratios of coactivators and corepressors of ER may in part be a mechanism underlying such endocrine resistance. Direct proof of this hypothesis *in vivo* remains to be provided by measuring expression of the relevant genes in human breast tumors that are known to be clinically sensitive or resistant to tamoxifen and/or other endocrine therapies. However, the data presented here provide preliminary information that the expression of a specific repressor of ER activity varies among breast tumors and that expression is correlated with known treatment response markers and inversely correlated with a marker of breast cancer progression.

References

1. Murphy, L. Mechanisms of hormone independence in human breast cancer. In Vivo, *12:* 95–106, 1998.
2. McKenna, N., Lanz, R., and O'Malley, B. Nuclear receptor coregulators: cellular and molecular biology. Endocr. Rev, *20:* 321–344, 1999.
3. Montano, M., Ekena, K., Delage-Mourroux, R., Chang, W., Martini, P., and Katzenellenbogen, B. An estrogen receptor-selective coregulator that potentiates the effectiveness of antiestrogens and represses the activity of estrogens. Proc. Natl. Acad. Sci. USA, *96:* 6947–6952, 1999.
4. Dotzlaw, H., Leygue, E., Watson, P., and Murphy, L. Estrogen receptor-β messenger RNA expression in human breast tumor biopsies: relationship to steroid receptor status and regulation by progestins. Cancer Res., *59:* 529–532, 1999.
5. Coutts, A., Davie, J., Dotzlaw, H., and Murphy, L. Estrogen regulation of nuclear matrix-intermediate filament proteins in human breast cancer cells. J. Cell. Biochem., *63:* 174–184, 1996.
6. Dotzlaw, H., Leygue, E., Watson, P., and Murphy, L. Expression of estrogen receptor-β in human breast tumors. J. Clin. Endocrinol. Metab., *82:* 2371–2374, 1997.
7. Leygue, E. R., Watson, P. H., and Murphy, L. C. Estrogen receptor variants in normal human mammary tissue. J. Natl. Cancer Inst., *88:* 284–290, 1996.
8. Murphy, L. C., and Dotzlaw, H. Variant estrogen receptor mRNA species detected in human breast cancer biopsy samples. Mol. Endocrinol., *3:* 687–693, 1989.
9. Katzenellenbogen, J. A., O'Malley, B. W., and Katzenellenbogen, B. S. Tripartite steroid hormone receptor pharmacology: interaction with multiple effector sites as a basis for the cell- and promoter-specific action of these hormones. Mol. Endocrinol., *10:* 119–131, 1996.
10. Horwitz, K., Jackson, T., Bain, D., Richer, J., Takimoto, G., and Tung, L. Nuclear receptor coactivators and corepressors. Mol. Endocrinol., *10:* 1167–1177, 1996.
11. Smith, C., Nawaz, Z., and O'Malley, B. Coactivator and corepressor regulation of the agonist/antagonist activity of the mixed antiestrogen, 4-hydroxytamoxifen. Mol. Endocrinol., *11:* 657–666, 1997.
12. Szapary, D., Huang, Y., and Simons, S. S., Jr. Opposing effects of corepressor and coactivators in determining the dose-response curve of agonists, and residual agonist activity of antagonists, for glucocorticoid receptor-regulated gene expression. Mol. Endocrinol., *13:* 2108–2121, 1999.
13. Lavinsky, R., Jepsen, K., Heinzel, T., Torchia, J., Mullen, T., Schiff, R., Del-Rio, A., Ricote, M., Ngo, S., Gemsch, J., Hilsenbeck, S., Osborne, C., Glass, C., Rosenfeld, M., and Rose, D. Diverse signaling pathways modulate nuclear receptor recruitment of N-CoR and SMRT complexes. Proc. Natl. Acad. Sci. USA, *95:* 2920–2925, 1998.
14. Lanz, R., McKenna, N., Onate, S., Albrecht, U., Wong, J., Tsai, S., Tsai, M-J., and O'Malley, B. A steroid receptor coactivator, SRA, functions as an RNA and is present in an SRC-1 complex. Cell, *97:* 17–27, 1999.
15. Anzick, S., Kononen, J., Walker, R., Azorsa, D., Tanner, M., Guan, X., Sauter, G., Kallioniemi, O., Trent, J., and Meltzer, P. AIB1, a steroid receptor coactivator amplified in breast and ovarian cancer. Science (Washington DC), *277:* 965–968, 1997.
16. Leygue, E., Dotzlaw, H., Watson, P., and Murphy, L. Expression of the steroid receptor RNA activator (SRA) in human breast tumors. Cancer Res., *59:* 4190–4193, 1999.
17. Bautista, S., Valles, H., Walker, R., Anzick, S., Zeillinger, R., Meltzer, P., and Theillet, C. In breast cancer, amplification of the steroid receptor coactivator gene *AIB1* is correlated with estrogen and progesterone receptor positivity. Clin. Cancer Res., *4:* 2925–2929, 1998.
18. Osborne, C. Steroid hormone receptors in breast cancer management. Breast Cancer Res. Treat., *51:* 227–238, 1998.

American Journal of Pathology, Vol. 155, No. 6, December 1999

Psoriasin (S100A7) Expression and Invasive Breast Cancer

Sahar Al-Haddad,* Zi Zhang,* Etienne Leygue,† Linda Snell,* Aihua Huang,* Yulian Niu,* Tamara Hiller-Hitchcock,* Kate Hole,* Leigh C. Murphy,† and Peter H. Watson*

Departments of Pathology and Biochemistry and Molecular Biology,† University of Manitoba, Faculty of Medicine, Winnipeg, Manitoba, Canada*

Alteration of psoriasin (S100A7) expression has previously been identified in association with the transition from preinvasive to invasive breast cancer. In this study we have examined persistence of psoriasin mRNA and protein expression in relation to prognostic factors in a cohort of 57 invasive breast tumors, comprising 34 invasive ductal carcinomas and 23 other invasive tumor types (lobular, mucinous, medullary, tubular). We first developed an IgY polyclonal chicken antibody and confirmed specificity for psoriasin by Western blot in transfected cells and tumors. The protein was localized by immunohistochemistry predominantly to epithelial cells, with both nuclear and cytoplasmic staining, as well as occasional stromal cells in psoriatic skin and breast tumors; however, *in situ* hybridization showed that psoriasin mRNA expression was restricted to epithelial cells. In breast tumors, higher levels of psoriasin measured by reverse transcriptase-polymerase chain reaction and Western blot (93% concordance) were significantly associated with estrogen and progesterone receptor-negative status ($P < 0.0001$, $P = 0.0003$), and with nodal metastasis in invasive ductal tumors ($P = 0.035$), but not with tumor type or grade. Psoriasin expression also correlated with inflammatory infiltrates (all tumors excluding medullary, $P = 0.0022$). These results suggest that psoriasin may be a marker of aggressive behavior in invasive tumors and are consistent with a function as a chemotactic factor. *(Am J Pathol 1999, 155:2057–2066)*

Earlier diagnosis of breast cancer has increased the need for the identification of molecular alterations that might serve as tissue markers to predict the risk of progression to metastatic disease. Among the most important of these alterations are likely to be those associated with the development of the invasive phenotype and the transition from preinvasive to invasive cancer with the capability for subsequent metastasis.

We have recently identified psoriasin (S100A7) as a gene that is frequently overexpressed in preinvasive ductal carcinoma *in situ* (DCIS) relative to adjacent invasive carcinoma, suggesting a role in breast tumor progression.[1] Other members of the S100 gene family of calcium-binding proteins have been implicated in a range of biological processes, including tumor metastasis.[2] In particular, S100A2 has been shown to be down-regulated in breast tumor cells relative to their normal epithelial cell counterparts,[3] whereas up-regulation of S100A4 has been strongly implicated in breast tumor metastasis.[4–6] In the latter case this may reflect the ability of S100A4 to influence cell motility,[7] the cytoskeleton[6,8,9] or cell adhesion molecules.[10] Psoriasin was initially identified as a highly abundant protein belonging to the S100 gene family,[11] expressed by abnormally proliferating keratinocytes in psoriatic epidermis.[12,13] It has subsequently been shown to be a secreted protein that can exert an effect as a chemotactic factor for inflammatory cells.[14,15] However, the function of psoriasin in breast cancer remains to be determined.[16] In this study we have developed a psoriasin-specific antibody and evaluated the persistence of psoriasin expression in invasive breast tumors with different invasive and metastatic potential as well as host inflammatory response.

Materials and Methods

Human Breast Tissues and Cell Lines

All breast tumor cases used for this study were selected from the NCIC–Manitoba Breast Tumor Bank (Winnipeg, Manitoba, Canada). As has previously been described,[17] tissues accrue to the Bank from cases at multiple centers within Manitoba and are rapidly collected and processed to create matched formalin-fixed embedded and frozen tissue blocks for each case, with mirror-image surfaces

Supported by grants from the Medical Research Council of Canada (MRC) and the U.S. Army Medical Research and Materiel Command (USAMRMC). The Manitoba Breast Tumor Bank is supported by funding from the National Cancer Institute of Canada (NCIC). P. H. W. is an MRC Clinician-Scientist; L. C. M. is an MRC Scientist; E. L. is a recipient of a USAMRMC Postdoctoral Fellowship. T. H.-H. is a recipient of an MRC studentship award.

Accepted for publication August 24, 1999.

Address reprint requests to Dr. Peter Watson, Department of Pathology, D212-770 Bannatyne Ave., University of Manitoba, Winnipeg, MB R3E OW3, Canada. E-mail: pwatson@cc.umanitoba.ca.

oriented by colored inks. The histology of every sample in the Bank is uniformly interpreted in hematoxylin/eosin (H&E)-stained sections from the face of the paraffin tissue block by a pathologist. This information is available in a computerized database along with relevant pathological and clinical information and was used as a guide for the selection of specific paraffin and frozen blocks from cases for this study. For each case interpretations included an estimate of the cellular composition (including the percentage of invasive epithelial tumor cells, collagenous stroma, and fatty stroma), tumor type, and tumor grade for ductal tumors (Nottingham score).[18,19] The inflammatory host response was scored semiquantitatively on a scale of 1 (low) to 5 (high). Steroid receptor status was determined for all cases by ligand binding assay performed on an adjacent portion of tumor tissue. Tumors with estrogen and progesterone receptor levels above 20 fmol/mg and 15 fmol/mg of total protein, respectively, were considered ER- or PR-positive.

Two cohorts of tumors were selected. The first cohort comprised 35 invasive ductal carcinomas selected to include six subgroups differing with respect to estrogen receptor status (ER-positive and ER-negative) and tumor grade (low, intermediate, high). Additional selection criteria also included high tissue quality, presence of invasive tumor within >35% of the cross section of the frozen block for invasive ductal cases, and minimal (<5%) normal or *in situ* epithelial components. The second cohort comprised 23 invasive tumors selected to include four subgroups of different tumor types[18] that vary in differentiation and metastatic potential, including invasive lobular (six), medullary (five), tubular (six), and colloid (six). Similar secondary criteria were also used for this cohort.

For analysis of antibody specificity and for positive controls for tumor assays, MCF7 human breast cancer cells obtained from the American Type Culture Collection (Manassas, VA) were used. MCF7 cells were grown as previously described under normal conditions in the presence of 5% fetal bovine serum, to provide a negative control.[20] Alternatively MCF7 cells were subjected to estrogen-deprived conditions in the presence of charcoal-stripped serum before stimulation by estradiol (10^{-8} mol/L) for 48 hours before harvesting to induce psoriasin expression and provide a positive control. As an additional positive control MDA-MB-231 human breast cancer cells were transfected with a plasmid containing the cytomegalovirus (CMV) promotor adjacent to the psoriasin cDNA (Hiller-Hitchcock T, Leygue E, Cummins-Leygue C, Murphy LC, Watson PH, manuscript in preparation), and stable transfectants (CL7FD3 cell clone) expressing psoriasin mRNA were also used.

Antibody Reagents

A psoriasin-specific chicken IgY polyclonal antibody was generated by immunization of chickens with a 14-amino acid peptide corresponding to the carboxy terminus of psoriasin (KQSHGAAPCSGGSQ; Bionostics, Toronto, and Aves Labs). A >90% pure IgY fraction from chicken egg yolk was obtained in phosphate-buffered saline (PBS) and then further purified by passing it over a psoriasin peptide affinity column made by binding the synthetic peptide to N-hydroxy-succinimide-activated Sepharose 4B (Pharmacia Biotech), according to the manufacturer's instructions. The bound IgY was then eluted with 5.0 mol/L sodium thiocyanate, followed by dialysis against PBS. Additional antibodies used included a commercial anti-S100 antibody (Sigma, St. Louis, MO) as well as a rabbit polyclonal antibody, raised against the recombinant protein (kindly provided by Prof J. Celis, University of Aarhus, Aarhus, Denmark).

Western Blot Analysis

For tumors, multiple sections (10–20 × 20 μm) were cut from the face of frozen tissue blocks immediately adjacent to the face of the matching paraffin block.[17] For cell lines, trypsinized cell pellets were obtained from breast cancer cell lines (grown to ~80% confluence). Total protein lysates were extracted from both the cell line pellets and frozen tissue sections, using Tri-reagent (Sigma), as described by the manufacturer. The recovered protein was dissolved in SDS isolation buffer (50 mmol/L Tris, pH 6.8, 20 mmol/L EDTA, 5% sodium dodecyl sulfate (SDS), 5 mmol/L β-glycerophosphate) and a cocktail of protease inhibitors (Boehringer Mannheim, Laval, PQ). Protein concentrations were determined using the Micro-BCA protein assay kit (Pierce, Rockford, IL). Sixty micrograms of total protein lysates were run on a 16.5% sodium dodecyl sulfate-polyacrylamide gel electrophoresis (SDS-PAGE) mini gel, using Tricine SDS-PAGE to separate the proteins,[21] and then transferred to 0.2-μm Nitrocellulose (Bio-Rad, Mississauga, ON). After blocking in 10% skimmed milk powder in Tris-buffered saline-0.05% Tween (TBST buffer), blots were incubated with chicken IgY anti-psoriasin antibody (~15 μg/ml in TBST), followed by incubation with secondary antibody, rabbit IgG anti-chicken IgY conjugated to horseradish peroxidase (1: 5000 dilution in TBST; Jackson ImmunoResearch Laboratories), and visualization by incubation with Supersignal (Pierce), per the manufacturer's instructions. Exposed x-ray films were photographed, and the band intensities were determined by video image analysis, using MCID M4 software (Imaging Research, ST. Catherine's, ON). All signals were adjusted with reference to the psoriasin-transfected MDA-MB-231 cell control (CL7FD3), run on each blot.

Immunohistochemistry

Immunohistochemistry was performed on 5-μm paraffin-embedded breast tumor tissue sections from tissue blocks fixed in 10% neutral buffered formalin for 18–24 hours. After deparaffinizing, clearing, and hydrating to PBS buffer (pH 7.4) containing 0.05% Tween 20 (Mallinckrodt), the sections were pretreated with hydrogen peroxide (3%) for 10 minutes to remove endogenous peroxidases, and nonspecific binding was blocked with normal rabbit serum (1:50; Sigma). Primary chicken IgY

anti-psoriasin antibody (1:500 dilution in PBS) was applied for 1 hour at 37°C followed by washing and incubation with the secondary antibody, peroxidase-conjugated affinity purified rabbit anti-chicken (1:200 dilution), for 1 hour at room temperature. Detection was performed with 3,3′-diaminobenzidine tetrahydrochloride peroxidase substrate (Sigma) and counterstaining with methyl green (2%), followed by dehydration, clearing, and mounting. A positive tissue control and a negative reagent control (normal rabbit serum only/no primary antibody) were run in parallel in all experiments. Immunostaining was scored semiquantitatively by assessing the average signal intensity (on a scale of 0 to 3) and the proportion of tumor cells showing a positive nuclear signal (0, none; 0.1, less than one-tenth; 0.5, less than one-half; 1.0 greater than one-half). The intensity and proportion scores were then multiplied to give an overall score, and tumors with a score equal to or higher than 1.0 were deemed positive.

In Situ *Hybridization*

In situ hybridization was performed on paraffin sections (5 μm) according to a previously described protocol.[1] Linearized psoriasin plasmid cDNA (1.0 μg/μl) was used to generate UTP^{S35}-labeled sense and antisense RNA probes with the Riboprobe System (Promega, Madison, WI) according to the manufacturer's instructions. Sense and antisense probes were equalized by diluting 1×10^6 cpm/μl in hybridization solution. These were then applied to paraffin sections (approximately 30 μl of probe per section) that had undergone postfixation with 4% paraformaldehyde (pH 7.4) in PBS and further pretreatments with triethanolamine/acetic anhydride and proteinase K before hybridization. Sections were then coverslipped, sealed, and incubated overnight in a humid chamber at 42°C. After coverslip removal, sections underwent incubation in posthybridization solution and buffered RNase A (20 μg/ul), followed by several washes in descending dilutions of standard saline citrate buffer to remove weakly bound nonspecific label. After dehydration in ethanol containing 300 mmol/L ammonium acetate, the sections were coated in NTB-2 Kodak emulsion, subsequently developed after various time intervals from 2 to 5 weeks, and counterstained with Lee's methylene blue and basic fuchsin. Psoriasin expression was assessed by bright-field microscopic examination at low power (10× objective) magnification with reference to the negative sense and positive control tumor sections run with each batch. Levels were scored semiquantitatively as previously described[22] by assessing the average signal intensity (on a scale of 0 to 3) and the proportion of tumor cells showing a positive signal (0, none; 0.1, less than one-tenth; 0.5, less than one-half; 1.0 greater than one-half). The intensity and proportion scores were then multiplied to give an overall score, and tumors with a score equal to or higher than 1.0 were deemed positive.

Reverse Transcriptase-Polymerase Chain Reaction Analysis

Reverse transcriptase-polymerase chain reaction (RT-PCR) was performed based on extracted RNA (600 ng) that was reverse transcribed in a total volume of 20 μl as described previously.[1] Briefly, reverse transcription was completed with the following reaction mixture: for each sample, 200 ng (2 μl of 0.1 μg/μl) of total RNA was added to 16 μl of RT mix (4 μl of 5× RT buffer; 1 μl of each of dATP, dCTP, dGTP, and dTTP, all at 2.5 mmol/L; 2 μl of 0.1% bovine serum albumin; 2 μl of 0.1 mol/L dithiothreitol; 1 μl of 0.25 mol/L random hexamer primer; 2 μl of dimethyl sulfoxide (DMSO), and 1 μl of 200 units/μl of Moloney murine leukemia virus reverse transcriptase) and incubated at 37°C for 1.5 hours. Each PCR was performed in 50-μl volume, using 1 μl of the completed RT reaction (cDNA); 30.8 μl of sterile water; 5 μl of 10× PCR buffer; 5 μl of 25 mmol/L $MgCl_2$; 200 mmol/L each of dATP, dCTP, dGTP, and dTTP; 1 μl of DMSO; 1 unit of Taq DNA polymerase; and 0.5 μl of 50 mmol/L PCR primers. The psoriasin primers were sense (5′-AAG AAA GAT GAG CAA CAC-3′) and antisense (5′-CCA GCA AGG ACA GAA ACT-3′) corresponding to the cDNA sequence,[13] or alternatively, PCR was performed with GAPDH primers, sense (5′-ACC CAC TCC TCC ACC TTT G-3′) and antisense (5′-CTC TTG TGC TCT TGC TGG G-3′).[23] For PCR amplification the reaction comprised an initial step of 5 minutes at 94°C, and then 45 cycles (30 seconds at 94°C, 30 seconds at 56°C, 30 seconds at 72°C) for psoriasin or 35 cycles (45 seconds at 93°C, 45 seconds at 58°C, 30 seconds at 72°C) for GAPDH. PCR products of the two genes amplified from the same RT reaction were loaded into the same wells onto a 1.5% agarose gel before electrophoresis and ethidium bromide staining to visualize psoriasin (246 bp) and GAPDH (198 bp) cDNAs under UV illumination.

Preliminary experiments were performed with cell line and tumor RNA samples to establish the appropriate RNA input and PCR cycle number conditions to achieve amplification with both psoriasin and GAPDH primers in the linear range in a typical sample. Tumors from each cohort were processed as a batch, from frozen sectioning to RNA extraction, reverse transcription in triplicate, and then duplicate PCRs from each RT reaction. For each batch controls included RT-negative and RNA-negative controls and both psoriasin-positive (estradiol-stimulated MCF7) and psoriasin-negative (untransfected, wild-type MDA-MB-231 cells) RNA controls. All primary tumor PCR signals were assessed in gels and autoradiographs by video image capture and with a MCID-M4 image analysis program. Psoriasin expression was standardized to GAPDH expression assessed from the same RT reaction in separate PCR reactions and run in parallel on the same gel, and the mean of each duplicate PCR was then expressed relative to the levels in the MCF7 cell line standard. The invasive tumor component within each section was also assessed in the adjacent mirror image paraffin section, and the percentage area occupied by tumor was

used to correct for differences in epithelial cell content of the tumor sections used for RNA extraction.

Statistical Analysis

For analysis of associations, standardized psoriasin mRNA levels were used either as a continuous variable or transformed into low- or high-expression categories, using a level of one relative density unit. This cutpoint was selected to correspond to the lowest level at which protein could be detected by Western blot. Correlations with estrogen (ER) and progesterone (PR) receptor levels and inflammation were tested using Spearman's test. Associations with categorical variables were tested by either Mann-Whitney or analysis of variance tests for selected dependent variables, or unpaired *t-test for independent variables, or a* χ^2 *test.*

Results

Characterization of Psoriasin-Specific Antibody

Multiple S100 proteins are expressed in individual tissues and cells. To specifically distinguish psoriasin expression within archival formalin-fixed and paraffin-embedded tissues we raised a polyclonal antibody in chicken against a synthetic peptide that corresponded to the COOH terminus of psoriasin. This 14-amino acid region was selected on the basis of very low homology to other S100 proteins. Western blot analysis of an MDA-MB-231 breast cell line transfected with a plasmid incorporating psoriasin cDNA under the control of a CMV promotor (and known to express psoriasin mRNA by Northern blot; unpublished data) and breast tumors showed a single band corresponding to a protein of approx 11.7 kd with the chicken IgY antibody (Figure 1A). This signal could be completely inhibited by preincubation of the primary antibody with psoriasin synthetic peptide (data not shown) and was absent from the wild-type and vector-alone transfected MDA-MB-231 control cells. By comparison, a commercial anti-S100 antibody (Sigma), known to detect several S100 proteins in MDA-MB-231 cells,[24] weakly recognized the same 11.7-kd protein in transfected cells as well as several other S100 proteins in most samples (Figure 1B). Both antibodies reacted with additional higher molecular mass bands in tumor samples. However, specificity of the 11.7-kd psoriasin signal was further confirmed by Western blot using another anti-psoriasin polyclonal rabbit antibody previously raised against a recombinant psoriasin protein (data not shown).

Localization of Cellular Expression of Psoriasin

To assess cellular localization of psoriasin we studied paraffin-embedded tissue blocks from breast, skin, and larynx by immunohistochemistry. The breast tumors studied possessed either high (six cases) or low (seven cases) levels of psoriasin mRNA and total protein expression (determined by Western blot and RT-PCR analysis of

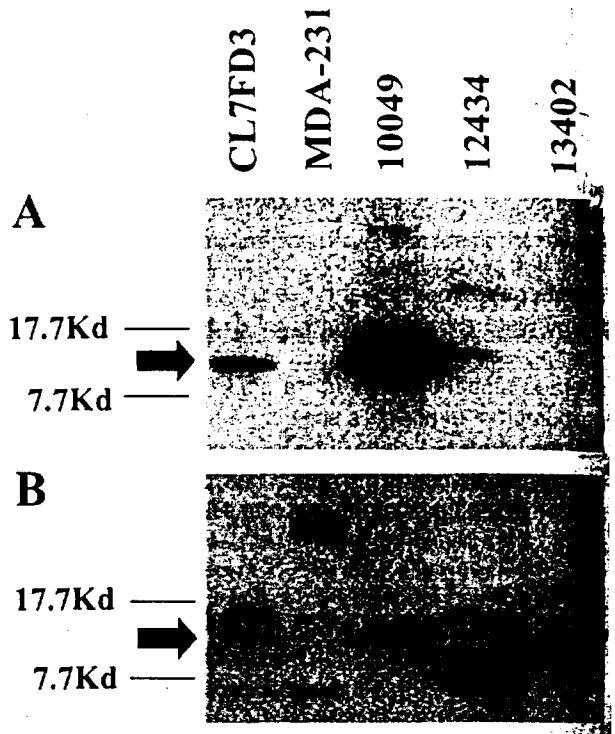

Figure 1. Western blot analysis of cell lines and tumors to demonstrate anti-psoriasin IgY antibody specificity. **A:** A protein band (approx 11.7 kd) detected using a chicken IgY anti-psoriasin antibody in a psoriasin-transfected MDA-MB-231 breast cell line and two tumors (10049, 12434), but absent in tumor 13402 and wild-type MDA-MB-231 cells. **B:** Detection of several S100-like proteins, using a commercial polyclonal S100 antibody applied to the same samples, in addition to weak detection of the same (approx 11.7 kd) protein band seen in A.

protein and RNA extracted from sections cut from the adjacent mirror-image frozen tissue blocks). Skin biopsies from the margins of two psoriatic lesions and a squamous carcinoma of larynx were also studied, as psoriasin was originally identified as a highly expressed protein in psoriatic skin and has also been identified as an expressed sequence tag in a cDNA library from laryngeal squamous carcinoma (http://www.ncbi.nlm.nih.gov/UniGene/Hs.112408). All cases were subjected to both immunohistochemistry and *in situ* hybridization on adjacent paraffin sections, and both signals were assessed independently, using a semiquantitative scoring system as described in Materials and Methods.

In breast tumors psoriasin protein was detected predominantly within epithelial tumor cells and was localized within both tumor cell nuclei as well as cytoplasm. Psoriasin was also present within some stromal cells and in some cases also on the luminal aspects of endothelial cells within small vessels (Figure 2). However, *in situ* hybridization demonstrated that mRNA expression was limited to epithelial tumor cells in all cases (Figure 2). The nuclear immunohistochemical staining was completely abolished by competition with the immunizing peptide and was not present in tumors that were negative for psoriasin but showed additional immunoreactive bands on Western blot (eg, see case 13402, Figure 1, and case 8840, Figure 4). Immunohistochemistry and Western blot were concordant in 12/13 cases. In one case Western blot analysis was negative and weak focal staining was

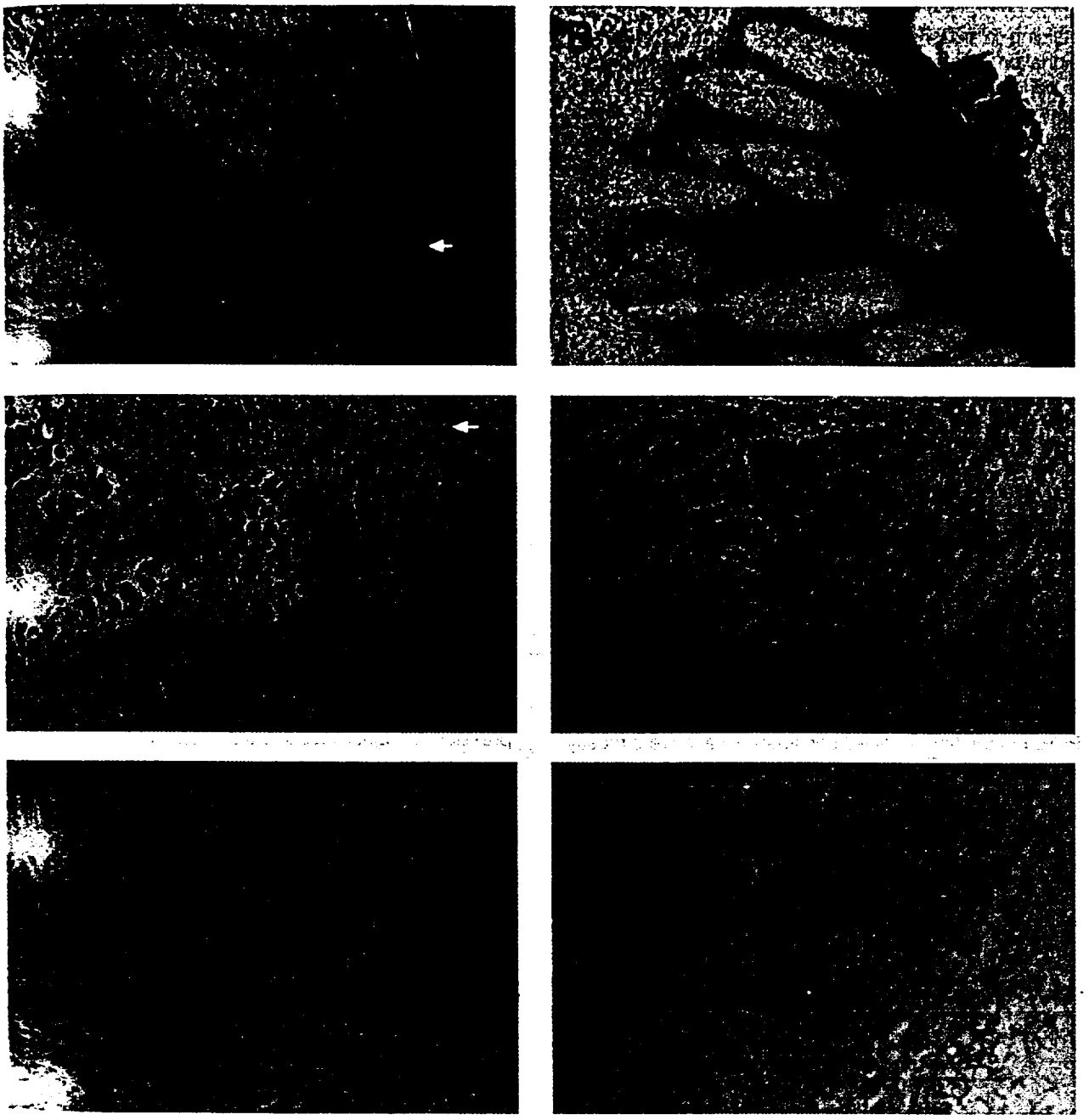

Figure 2. Immunohistochemical and *in situ* hybridization analysis of the cellular distribution and patterns of expression of psoriasin within psoriatic skin and breast carcinoma. Psoriasin protein is localized in hyperplastic epidermis of skin to both nuclei (**A**, **white arrow**) and cytoplasm (**A**, **black arrow**) of keratinocytes. Similar nuclear and cytoplasmic staining is seen in breast epithelial tumor cells (**C**, **black arrow**; case 8965). Psoriasin protein is also detected within occasional stromal inflammatory cells (**C**, **white arrow**). **E:** H&E-stained section from the same region of the tumor shown in **C**. Psoriasin mRNA expression in skin is restricted to epithelial cells in suprabasal layers of epidermis (**B**) and scattered invasive epithelial tumor cells in breast tumors (**D**), detected using antisense probe (**B** and **D**) compared to sense probe (**F**). Original magnification for all panels at the microscope, ×200.

seen by immunohistochemistry. Specificity of the nuclear signal was further confirmed by the fact that the presence of immunohistochemically detected protein expression, assessed on the basis of nuclear staining, was highly concordant (92%) with expression detected by *in situ* hybridization mRNA.

In skin, immunohistochemical staining was localized to keratinocytes within the mid to upper zones of the epidermis of skin showing psoriasiform hyperplasia. These keratinocytes corresponded to the cells that also showed mRNA expression by *in situ* hybridization in adjacent sections (Figure 2). The adjoining normal skin was negative. Occasional positive immunohistochemical staining, but no mRNA signal, was also observed in stromal cells in the dermis underlying the psoriatic lesion. As seen in breast tumor cells, psoriasin protein was localized both to the nucleus and cytoplasm within keratinocytes (Figure 2). The same nuclear and cytoplasmic localization was also detected in a squamous laryngeal carcinoma (data not shown). However, the polyclonal rabbit anti-psoriasin

antibody previously shown to provide immunofluorescent staining in frozen skin sections[13,25] did not detect any signal on paraffin sections from skin or breast. Additional experiments were performed with the chicken IgY anti-psoriasin antibody on skin and breast tumor sections in which immunohistochemical conditions (microwave *versus* protease antigen retrieval) and tissue treatment/fixation conditions (formalin *versus* alcohol *versus* paraformaldehyde *versus* frozen) were varied, and nuclear localization persisted under all conditions (data not shown).

Expression of Psoriasin mRNA in Invasive Breast Tumors

The changes in psoriasin expression previously observed in association with the transition from *in situ* to invasive carcinoma suggested a functional role in the early stages of progression. However, alteration of psoriasin expression in normal skin has also been associated with abnormal keratinocyte differentiation. To examine further the relationship of psoriasin with differentiation and invasiveness, we used RT-PCR and Western blot to examine psoriasin mRNA and protein levels in a cohort of invasive tumors. These tumors included several different tumor types and a range of differentiation, as determined by tumor grade and estrogen receptor status (Table 1).

Psoriasin mRNA was detected in all tumors by RT-PCR, but the levels varied considerably and were mostly low (Figure 3). Within the invasive ductal subgroup there was no significant difference in psoriasin expression with tumor grade. There was also no significant difference between tumor size or type, although there was a trend toward lower levels of expression in both well-differentiated tumor types, tubular and mucinous carcinomas, whereas lobular and medullary carcinomas showed a trend toward higher expression than invasive ductal tumors. However, higher levels of psoriasin mRNA expression showed a significant inverse correlation with both ER and PR levels ($r = -0.66$, $P = 0.0001$; $r = -0.47$, $P = 0.0003$, Spearman) and with ER and PR negative status (ER-ve *vs.* ER+ve; $n = 28$ *vs.* 29, mean (SD) 1.032 (0.7) *vs.* 0.32 (0.36), $P < 0.0001$ Mann-Whitney; PR-ve *vs.* PR+ve, $n = 25$ *vs.* 32, 1.05 (0.72) *vs.* 0.37 (0.40), $P < 0.0001$) in all tumors and within the invasive ductal subgroup. Psoriasin expression was also higher in axillary node-positive cases in all tumors (mean (SD) = 0.86 (0.73) *vs.* 0.59 (0.66), and the difference was statistically significant for the invasive ductal subgroup (mean (SD) = 0.88 (0.79) *vs.* 0.38 (0.28), $P = 0.035$, *t*-test). These relationships with ER, PR, and nodal status (Table 2) were also evident and remained statistically significant after correction of psoriasin levels for the relative tumor cell content, assessed as a percentage within the paraffin sections adjacent to the frozen tissue sections studied.

Psoriasin protein was detected by Western blot analysis in 10 tumors (Table 1 and Figure 4). These tumors (six ductal, two lobular, two medullary) corresponded to those with the highest mRNA levels observed by RT-PCR (above 1.0 arbitrary expression units). Also consistent with RT-PCR analysis, Western blot-positive invasive ductal tumors were also significantly associated with ER-negative ($P < 0.0001$) and PR-negative ($P < 0.0012$) and node-positive ($P = 0.0143$) status (Table 2).

The relationship between psoriasin mRNA and protein expression and host inflammatory response was also examined (Table 2). Psoriasin mRNA showed a significant positive correlation in the entire cohort ($n = 57$, $r = 0.47$, $P = 0.0002$), in the entire cohort excluding the medullary carcinoma subgroup, which includes inflammatory infiltrates as a diagnostic criterion ($n = 52$, $r = 0.42$, $P = 0.0022$), and within the invasive ductal subgroup alone ($n = 34$, $r = 0.39$, $P = 0.023$). Cases with Western blot-detectable psoriasin protein also showed increased inflammatory infiltrates, both in the entire cohort (mean (SD) = 3.6 (1.1) *vs.* 2.3 (1.2), $P = 0.004$) and in the entire cohort excluding the medullary subgroup (mean (SD) = 3.3 (0.89) *vs.* 2.1 (0.98), $P = 0.007$).

Discussion

We have developed a psoriasin-specific antibody and confirmed its specificity as well as its ability to detect the psoriasin protein in formalin-fixed and paraffin-embedded specimens. We have shown that there is a high concordance between psoriasin mRNA and protein levels in invasive tumors, and persistance of psoriasin expression at higher levels is significantly associated with poor prognostic markers, including ER- and PR-negative and lymph node-positive status. Psoriasin expression within breast tumor cells is also associated with inflammatory infiltrates.

Indirect support for a role for S100 genes in breast tumor progression is provided by several observations. Disruption of calcium signaling pathways has been implicated as a central mechanism in tumorigenesis and specifically in the process of invasion and metastasis.[26] Moreover, the chromosomal location of the S100 gene family lies in a region of chromosome 1 that frequently (>50%) shows loss of heterozygosity in invasive tumors.[27] Furthermore, several S100 genes are expressed in breast cell lines and tumors and are known to manifest alteration of their expression in association with tumorigenesis and progression.[11,24] In particular, S100A2 and S100A4 have been identified to be differentially expressed between normal and neoplastic cells[3,28,29] and up-regulated in metastatic as compared to nonmetastatic cells in both mouse and rat mammary tumor cell lines.[5,30] *In vivo* studies of breast tumors have also shown a correlation between high levels of S100A4 expression, nodal metastasis, and ER-negative status.[31] More direct evidence has emerged from modulation of S100A4 expression in transfected cell lines that have shown that overexpression of S100A4 can also induce the metastatic phenotype in mouse, rat, and human cells.[4,6,32] Furthermore, there is evidence that S100A4 may exert its effect on cell cytoskeleton[8,9] and motility,[7] and it has also been demonstrated that up-regulation of S100A4 in mouse tumor cell lines can down-regulate expression of E-

Table 1. Clinicopathological Parameters, Histological Composition of the Tumor Section, and Psoriasin Expression in 57 Invasive Breast Carcinomas Assessed by RT-PCR and Western Blot

	Clinicopathological parameters							Psoriasin		
TB#	Type	ER	PR	GrSc	Size	NS	Inf	RT-PCR	RT-PCR/Inv%	WB
11549	muc	194	133		3	–	2	0.06	0.15	–
10515	muc	341	176		3	–	1	0.08	0.14	–
9948	muc	46	22		6.5	–	1	0.10	0.16	–
10582	muc	109	62		2.3	na	1	0.14	0.34	–
8832	muc	295	177		4	–	2	1.94	2.77	–
8021	muc	331	328		2.3	–	2	0.11	0.15	–
11387	tub	105	35		3.5	na	2	0.09	0.29	–
9483	tub	56	0		1.2	–	2	0.09	0.91	–
11651	tub	67	24		2.2	–	3	0.23	0.77	–
8814	tub	232	103		2	–	2	0.44	1.45	–
[illegible]	tub	29	73		2	–	1	0.52	5.21	–
12072	tub	8.3	5		2.3	+	3	0.67	1.34	–
13041	med	3.4	9		2	–	5	0.40	0.49	–
13153	med	4.9	2.4		3	na	5	0.61	0.76	–
11867	med	1.4	9		1.6	+	5	1.60	2.67	+
13058	med	4.6	12		2.8	–	5	1.63	2.04	–
12434	med	1	1.3		1.2	–	5	1.63	3.27	+
8639	ilc	52	83		na	–	1	0.20	0.67	–
8799	ilc	111	139		6	+	2	0.31	3.15	–
8993	ilc	142	528		8	+	1	0.52	0.86	–
9801	ilc	2.1	9.8		na	–	3	0.56	1.60	–
8921	ilc	2.3	8.9		8	–	2	2.07	3.77	+
8961	ilc	0.7	3.4		2.5	–	3	2.34	5.84	+
9000	idc	392	596	7	2.5	–	1	0.07	0.09	–
13402	idc	49	35	4	2.8	–	2	0.07	0.17	–
11971	idc	97	25	4	1.5	–	2	0.13	0.42	–
8684	idc	74	43	7	5	+	1	0.14	0.35	–
12853	idc	17.3	83	9	4.8	+	4	0.15	0.22	–
8840	idc	74	68	7	1.8	+	3	0.17	0.37	–
8834	idc	10	147	5	2	–	2	0.17	0.34	–
8674	idc	16.7	4.5	9	na	–	2	0.19	0.35	–
12037	idc	225	144	4	3.5	+	2	0.20	0.40	–
12868	idc	93	141	9	3.5	na	1	0.21	0.28	–
8599	idc	58	81	4	3.5	–	1	0.24	0.79	–
10105	idc	0.9	3.8	9	3	+	4	0.24	0.40	–
7928	idc	33	72	5	3	+	2	0.27	0.67	–
13414	idc	15.5	59	5	4.1	–	2	0.28	0.56	–
11343	idc	78	44	4	na	–	3	0.29	0.73	–
10644	idc	130	4.7	9	3.2	+	2	0.32	0.81	–
10137	idc	42	26	7	1.8	–	1	0.44	0.89	–
10064	idc	0.8	4.6	9	2.5	na	2	0.53	0.88	–
11769	idc	1.1	3.5	7	na	–	3	0.56	0.80	–
8932	idc	114	27	4	2	–	1	0.56	1.13	–
10906	idc	46	6.6	9	4.5	na	5	0.58	0.64	–
8789	idc	0.8	0.4	7	na	na	3	0.66	1.64	–
10150	idc	70	42	7	na	–	1	0.67	1.68	–
11459	idc	3.6	98	5	4.6	+	3	0.67	0.96	–
13191	idc	17.2	9.2	9	3.2	–	2	0.69	0.87	–
10124	idc	1.9	12.9	9	3	–	4	1.00	1.42	–
8830	idc	0.7	8	9	6	+	4	1.06	1.32	+
8790	idc	6	50	5	1.5	+	2	1.07	3.58	–
11118	idc	6.6	11.8	5	8.5	+	2	1.10	2.20	–
12715	idc	1.5	16	7	3	na	3	1.24	2.06	+
9631	idc	0.7	4.5	9	na	+	4	1.32	3.10	+
8965	idc	0.4	9.9	7	na	+	4	1.85	2.64	+
10049	idc	0.8	14	9	3.7	+	4	2.01	5.04	+
8704	idc	0.7	3.5	7	3.5	+	2	2.60	6.50	+

TB, tumor bank case number; type, mucinous (muc), tubular (tub), medullary (med), lobular (ilc), ductal (idc); ER, PR, estrogen/progesterone receptor levels (fmol/mg protein); GrSc, Nottingham grade score; Size, tumor size (cms); NS, nodal status, positive (+), negative (–), not available (na); Inf, estimate of inflammatory infiltrate, low (1) to high (5). RT-PCR, psoriasin mRNA level determined by RT-PCR; RT-PCR/Inv%, psoriasin mRNA level determined by RT-PCR and adjusted for the percentage tumor cell content of the tissue section (as described in Materials and Methods); WB, psoriasin protein level determined by Western blot.

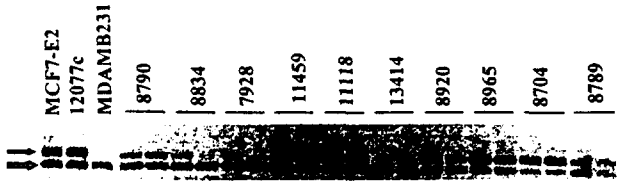

Figure 3. RT-PCR analysis of psoriasin mRNA expression in invasive breast tumors. Psoriasin (**upper black arrow**) and GAPDH (**lower open arrow**) from duplicate PCRs of 10 representative tumors. Control lanes include estradiol-treated MCF7-E2 cells, a tumor control 12077c, and wild-type MDA-MB-231 cells.

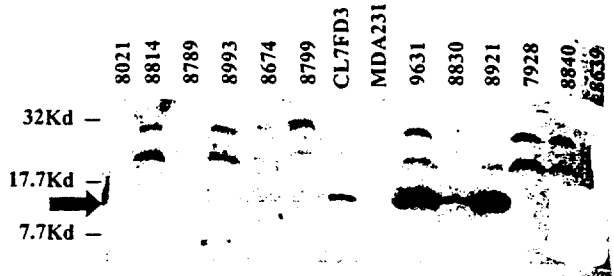

Figure 4. Western blot analysis of psoriasin protein expression in invasive breast tumors. Psoriasin (**black arrow**) is detected in 3/12 representative tumors and within the positive control (CL7FD3).

cadherin and disturb the intracellular distribution of B-catenin.[10]

A possible role for psoriasin (S100A7) in breast cancer first emerged when it was also identified as a cDNA down-regulated in a nodal metastasis relative to a primary breast tumor.[33] Nevertheless, the significance of the initial observation was unclear because of the fact that expression was only detectable in a small proportion of cells within invasive primary tumors studied by *in situ* hybridization and overall could be detected in only 18% of primary tumor specimens assessed by Northern analysis. An explanation for this paradox became apparent when psoriasin was also identified by us as a gene that is particularly highly expressed in the ductal epithelial cells of preinvasive ductal carcinoma *in situ*,[1] which can be present as a significant component with invasive tumor specimens. We have now shown that when higher levels of psoriasin expression persist within invasive tumors, this correlates with indicators of increased metastatic potential. It should be noted that the strong relationship with ER status is compatible with studies of S100A4[31] and the *in vitro* observation[33] (and our unpublished data) that psoriasin is regulated by estradiol in MCF7 cells. Although it is interesting that the nature of this correlation is different between the *in vitro* and *in vivo* situations, similar differences have been found with other genes in breast tumors,[34] suggesting that additional external factors may influence psoriasin regulation *in vivo*.

Although the biological effect of alteration of psoriasin in breast tumors is currently unknown, it is interesting to speculate from this pattern of expression that psoriasin may be important in the invasive phenotype.[16] This role might be mediated through an indirect influence on the effector cells of the host immune response or perhaps through a more direct influence on the epithelial tumor cell. The first hypothesis is supported by the correlation seen here with the degree of host inflammatory cell response within breast tumors and the previous evidence that implicates psoriasin as a chemotactic factor.[14] However, psoriasin protein was only detected in approximately 50% of medullary and ductal tumors with marked inflammatory responses. The second hypothesis is supported by our observation that psoriasin may not only be secreted[13,15] but also can be localized in both nuclear and cytoplasmic compartments in normal skin and breast tumors. Although further studies beyond immunohistochemistry are necessary to confirm this observation, the pattern of expression is consistent between cells in two

Table 2. Relationship between Psoriasin Expression and Prognostic and Tissue Factors

		All				IDC			
		n	Low Ps	High Ps		*n*	Low Ps	High Ps	
ER	–	28	14	4	$P = 0.0001$	19	10	9	$P = 0.0019$
	+	29	28	1		15	15	0	
PR	–	25	13	12	$P = 0.001$	15	8	7	$P = 0.018$
	+	32	29	3		19	17	2	
NS	–	30	24	6	ns ($P = 0.095$)	14	13	1	$P = 0.0002$
	+	19	11	8		15	8	7	
INFL	Low	34	29	5	$P = 0.049$	20	17	3	ns ($P = 0.07$)
	High	18	11	7		14	8	6	
Size	<2	12	9	3		6	5	1	
	2–5	29	22	7	ns	18	14	4	ns
	≥5	7	4	3		3	1	2	
Grade	Low					12	10	2	
	Mod					10	7	3	ns
	High					12	8	4	
Type	idc	34	25	9					
	ilc	6	4	2					
	med	5	2	3	ns				
	muc	6	5	1					
	tub	6	6	0					

ER, PR, estrogen/progesterone receptor status; NS, nodal status; INFL, inflammatory infiltrate; Size, tumor size (cms); Grade, Nottingham grade; Type, mucinous (muc), tubular (tub), medullary (med), lobular (ilc), ductal (idc); Low Ps/High Ps, low/high psoriasin mRNA level determined by RT-PCR (cutpoint values used as described in Materials and Methods). *P* values determined by χ^2 or ANOVA tests. ns, not significant.

closely related epithelia, epidermis and breast ductal epithelium, and the detection of nuclear and cytoplasmic signal was unrelated to tissue fixation or immunohistochemistry protocol, which may effect staining with some antibodies.[35,36] Dual localization and alteration of the subcellular localization with disease has also been observed with another S100 related keratinocyte protein, profilaggrin, expressed in the epidermis.[2,37] Similarly, altered cellular distribution of proteins such as BRCA1 and B-catenin are also recognized to be an important aspect of tumor progression.[38–40] Furthermore, other S100 proteins have previously been associated with both extracellular and intracellular actions,[41] and previous studies have also indicated potential interactions for S100A4 with both cytoskeletal[8,9] and nuclear[42] proteins. It has also recently been shown that other secreted S100 proteins can be localized to cytoplasm and nucleus,[43,44] and specifically S100A2 has been found in breast cell nuclei, whereas S100A6 localizes to the cytoplasm[24]; however, the functional significance of these findings remains unknown.

In conclusion, we have shown that expression of psoriasin (S100A7) mRNA and protein correlates with indicators of poor prognosis in invasive breast tumors, including ER, PR, and nodal status, but is not related to differentiation, as manifested by invasive tumor type or grade. The relationship observed between psoriasin and the inflammatory response is also compatible with a role as a chemotactic factor; however, the possibility of additional intracellular functions is raised by the presence of its nuclear localization in both skin and breast tumors. Further studies will be necessary to confirm the latter observation and pursue the biological functions of psoriasin in relation to breast tumor progression.

Acknowledgments

The authors thank Prof. J. E. Celis (University of Aarhus, Aarhus, Denmark) for kindly providing anti-psoriasin antibody and Helmut Dotzlaw and Caroline Cummins-Leygue for assistance with cell transfections. We also thank Bionostics, North York, for assistance with antibody production. The tissues used in this study were provided by the Manitoba Breast Tumor Bank, which is funded by the National Cancer Institute of Canada.

References

1. Leygue E, Snell L, Hiller T, Dotzlaw H, Hole K, Murphy LC, Watson PH: Differential expression of psoriasin messenger RNA between in situ and invasive human breast carcinoma. Cancer Res 1996, 56:4606–4609
2. Schafer BW, Heizmann CW: The S100 family of EF-hand calcium-binding proteins: functions and pathology. Trends Biochem Sci 1996, 21:134–140
3. Lee SW, Tomasetto C, Swisshelm K, Keyomarsi K, Sager R: Down-regulation of a member of the S100 gene family in mammary carcinoma cells and reexpression by azadeoxycytidine treatment. Proc Natl Acad Sci USA 1992, 89:2504–2508
4. Lloyd BH, Platt-Higgins A, Rudland PS, Barraclough R: Human S100A4 (p9Ka) induces the metastatic phenotype upon benign tumour cells. Oncogene 1998, 17:465–473
5. Sherbet GV, Lakshmi MS: S100A4 (MTS1) calcium binding protein in cancer growth, invasion and metastasis. Anticancer Res 1998, 18: 2415–2421
6. Grigorian M, Ambartsumian N, Lykkesfeldt AE, Bastholm L, Elling F, Georgiev G, Lukanidin E: Effect of mts1 (S100A4) expression on the progression of human breast cancer cells. Int J Cancer 1996, 67:831–841
7. Ford HL, Salim MM, Chakravarty R, Aluiddin V, Zain SB: Expression of Mts1, a metastasis-associated gene, increases motility but not invasion of a nonmetastatic mouse mammary adenocarcinoma cell line. Oncogene 1995, 11:2067–2075
8. Bastholm L, Elling F, Georgiev G, Lukanidin EKM, Tarabykina S, Bronstein I, Maitland N, Lomonosov M, Hansen K, Georgiev G, Lukanidin E: Metastasis-associated Mts1 (S100A4) protein modulates protein kinase C phosphorylation of the heavy chain of nonmuscle myosin. J Biol Chem 1998, 273:9852–9856
9. Ford HL, Zain SB: Interaction of metastasis associated Mts1 protein with nonmuscle myosin. Oncogene 1995, 10:1597–1605
10. Keirsebilck A, Bonne S, Bruyneel E, Vermassen P, Lukanidin E, Mareel M, Van Roy F: E-cadherin and metastasin (mts-1/S100A4) expression levels are inversely regulated in two tumor cell families. Cancer Res 1998, 58:4587–4591
11. Borglum AD, Flint T, Madsen P, Celis JE, Kruse TA: Refined mapping of the psoriasin gene S100A7 to chromosome 1cen-q21. Hum Genet 1995, 96:592–596
12. Hoffmann HJ, Olsen E, Etzerodt M, Madsen P, Thogersen HC, Kruse T, Celis JE: Psoriasin binds calcium and is upregulated by calcium to levels that resemble those observed in normal skin. J Invest Dermatol 1994, 103:370–375
13. Madsen P, Rasmussen HH, Leffers H, Honore B, Dejgaard K, Olsen E, Kiil J, Walbum E, Andersen AH, Basse B, et al.: Molecular cloning, occurrence, and expression of a novel partially secreted protein "psoriasin" that is highly up-regulated in psoriatic skin. J Invest Dermatol 1991, 97:701–712
14. Jinquan T, Vorum H, Larsen CG, Madsen P, Rasmussen HH, Gesser B, Etzerodt M, Honore B, Celis JE, Thestrup-Pedersen K: Psoriasin: a novel chemotactic protein. J Invest Dermatol 1996, 107:5–10.
15. Celis JE, Rasmussen HH, Vorum H, Madsen P, Honore B, Wolf H, Orntoft TF: Bladder squamous cell carcinomas express psoriasin and externalize it to the urine. J Urol 1996, 155:2105–2112
16. Watson PH, Leygue ER, Murphy LC: Psoriasin (S100A7). Int J Biochem Cell Biol 1998, 30:567–571
17. Hiller T, Snell L, Watson PH: Microdissection RT-PCR analysis of gene expression in pathologically defined frozen tissue sections. Biotechniques 1996, 21:38–40
18. Ellis IO, Galea M, Broughton N, Locker A, Blamey RW, Elston CW: Pathological prognostic factors in breast cancer. II. Histological type. Relationship with survival in a large study with long-term follow-up. Histopathology 1992, 20:479–489
19. Elston CW, Ellis IO: Pathological prognostic factors in breast cancer. I. The value of histological grade in breast cancer: experience from a large study with long-term follow-up. Histopathology 1991, 19:403–410
20. Leygue ER, Watson PH, Murphy LC: Estrogen receptor variants in normal human mammary tissue. J Natl Cancer Inst 1996, 88:284–290
21. Schagger H, von Jagow G: Tricine-sodium dodecyl sulfate-polyacrylamide gel electrophoresis for the separation of proteins in the range from 1 to 100 kDa. Anal Biochem 1987, 166:368–379
22. Leygue E, Snell L, Dotzlaw H, Hole K, Hiller-Hitchcock T, Roughley PJ, Watson PH, Murphy LC: Expression of lumican in human breast carcinoma. Cancer Res 1998, 58:1348–1352
23. Ercolani L, Florence B, Denaro M, Alexander M: Isolation and complete sequence of a functional human glyceraldehyde-3-phosphate dehydrogenase gene. J Biol Chem 1988, 263:15335–15341
24. Ilg EC, Schafer BW, Heizmann CW: Expression pattern of S100 calcium-binding proteins in human tumors. Int J Cancer 1996, 68: 325–332
25. Ostergaard M, Rasmussen HH, Nielsen HV, Vorum H, Orntoft TF, Wolf H, Celis JE: Proteome profiling of bladder squamous cell carcinomas: identification of markers that define their degree of differentiation. Cancer Res 1997, 57:4111–4117
26. Kohn EC, Liotta LA: Molecular insights into cancer invasion: strategies for prevention and intervention. Cancer Res 1995, 55:1856–1862
27. Munn KE, Walker RA, Varley JM: Frequent alterations of chromosome

1 in ductal carcinoma in situ of the breast. Oncogene 1995, 10:1653–1657
28. Wicki R, Franz C, Scholl FA, Heizmann CW, Schafer BW: Repression of the candidate tumor suppressor gene S100A2 in breast cancer is mediated by site-specific hypermethylation. Cell Calcium 1997, 22: 243–254
29. Ebralidze A, Tulchinsky E, Grigorian M, Afanasyeva A, Senin V, Revazova E, Lukanidin E: Isolation and characterization of a gene specifically expressed in different metastatic cells and whose deduced gene product has a high degree of homology to a Ca^{2+}-binding protein family. Genes Dev 1989, 3:1086–1093
30. Barraclough R, Rudland PS: The S-100-related calcium-binding protein, p9Ka, and metastasis in rodent and human mammary cells. Eur J Cancer 1994, 30A:1570–1576
31. Albertazzi E, Cajone F, Leone BE, Naguib RN, Lakshmi MS, Sherbet GV: Expression of metastasis-associated genes h-mts1 (S100A4) and nm23 in carcinoma of breast is related to disease progression. DNA Cell Biol 1998, 17:335–342
32. Grigorian MS, Tulchinsky EM, Zain S, Ebralidze AK, Kramerov DA, Kriajevska MV, Georgiev GP, Lukanidin EM: The mts1 gene and control of tumor metastasis. Gene 1993, 135:229–238
33. Moog-Lutz C, Bouillet P, Regnier CH, Tomasetto C, Mattei MG, Chenard MP, Anglard P, Rio MC, Basset P: Comparative expression of the psoriasin (S100A7) and S100C genes in breast carcinoma and co-localization to human chromosome 1q21–q22. Int J Cancer 1995, 63:297–303
34. Yarden RI, Lauber AH, El Ashry D, Chrysogelos SA: Bimodal regulation of epidermal growth factor receptor by estrogen in breast cancer cells. Endocrinology 1996, 137:2739–2747
35. Scully R, Ganesan S, Brown M, De Caprio JA, Cannistra SA, Feunteun J, Schnitt S, Livingston DM: Location of BRCA1 in human breast and ovarian cancer cells (technical comments). Science 1996, 272:123–124.
36. Chen Y, Chen P-L, Riley DJ, Lee W-H, Allred DC, Osborne CK: Location of BRCA1 in human breast and ovarian cancer cells (technical comments). Science 1996, 272:125–126
37. Ishida-Yamamoto A, Takahashi H, Presland RB, Dale BA, Iizuka H: Translocation of profilaggrin N-terminal domain into keratinocyte nuclei with fragmented DNA in normal human skin and loricrin keratoderma. Lab Invest 1998, 78:1245–1253
38. Wilson CA, Ramos L, Villasenor MR, Anders KH, Press MF, Clarke K, Karlan B, Chen JJ, Scully R, Livingston D, Zuch RH, Kanter MH, Cohen S, Calzone FJ, Slamon DJ: Localization of human BRCA1 and its loss in high-grade, non-inherited breast carcinomas. Nature Genet 1999, 21:236–240
39. Chen Y, Chen CF, Riley DJ, Allred DC, Chen PL, Von Hoff D, Osborn CK, Lee WH: Aberrant subcellular localization of BRCA1 in breast cancer. Science 1995, 270:789–791
40. Sheng H, Shao J, Williams CS, Pereira MA, Taketo MM, Oshima M, Reynolds AB, Washington MK, DuBois RN, Beauchamp RD: Nuclear translocation of beta-catenin in hereditary and carcinogen-induced intestinal adenomas. Carcinogenesis 1998, 19:543–549
41. Hessian PA, Edgeworth J, Hogg N: MRP-8 and MRP-14, two abundant Ca(2+)-binding proteins of neutrophils and monocytes. J Leukoc Biol 1993, 53:197–204
42. Albertazzi E, Cajone F, Lakshmi MS, Sherbet GV: Heat shock modulates the expression of the metastasis associated gene MTS1 and proliferation of murine and human cancer cells. DNA Cell Biol 1998, 17:1–7
43. Yang Q, O'Hanlon D, Heizmann CW, Marks A: Demonstration of heterodimer formation between S100B and S100A6 in the yeast two-hybrid system and human melanoma. Exp Cell Res 1999, 246:501–509
44. Mandinova A, Atar D, Schafer BW, Spiess M, Aebi U, Heizmann CW: Distinct subcellular localization of calcium binding S100 proteins in human smooth muscle cells and their relocation in response to rises in intracellular calcium. J Cell Sci 1998, 111:2043–2054

Journal of Pathology
J Pathol 2000; 191: 000–000.

Original Paper

Lumican and decorin are differentially expressed in human breast carcinoma

Etienne Leygue[1], Linda Snell[2], Helmut Dotzlaw[1], Kate Hole[2], Tamara Hiller-Hitchcock[2], Leigh C. Murphy[1], Peter J. Roughley[3] and Peter H. Watson[2]*

[1] Department of Biochemistry and Molecular Biology, University of Manitoba, Faculty of Medicine, Winnipeg, Manitoba, Canada, R3E OW3
[2] Department of Pathology, University of Manitoba, Faculty of Medicine, Winnipeg, Manitoba, Canada, R3E OW3
[3] Genetics Unit, Shriners Hospital for Children, Montreal, Quebec, Canada, H3G 1A6

*Correspondence to:
Dr P. H. Watson, Department of Pathology, D212-770 Bannatyne Ave, University of Manitoba, Winnipeg, Manitoba R3E OW3, Canada.
E-mail: pwatson@cc.umanitoba.ca

Received: 22 June 1999
Revised: 1 February 2000
Accepted: 17 April 2000

Abstract

Previous studies have shown that lumican is expressed and increased in the stroma of breast tumours. Lumican expression has now been examined relative to other members of the small leucine-rich proteoglycan gene family in normal and neoplastic breast tissues, to begin to determine its role in breast tumour progression. Western blot study showed that lumican protein is highly abundant relative to decorin, while biglycan and fibromodulin are only detected occasionally in breast tissues ($n=15$ cases). Further analysis of lumican and decorin expression performed in matched normal and tumour tissues by *in situ* hybridization showed that both mRNAs were expressed by similar fibroblast-like cells adjacent to epithelium. However, lumican mRNA expression was significantly increased in tumours ($n=34$, $p<0.0001$), while decorin mRNA was decreased ($p=0.0002$) in neoplastic relative to adjacent normal stroma. This was accompanied by a significant increase in lumican protein ($n=12$, $p=0.0122$), but not decorin. Further evidence of altered lumican expression in breast cancer was manifested by discordance between lumican mRNA and protein localization in some regions of tumours but not in adjacent morphologically normal tissues. It is concluded that lumican is the most abundant of these proteoglycans in breast tumours and that lumican and decorin are inversely regulated in association with breast tumourigenesis. Copyright © 2000 John Wiley & Sons, Ltd.

Keywords: lumican; decorin; small leucine-rich proteoglycan; breast cancer; tumour progression

Introduction

The development and progression of breast carcinoma are caused by alterations in the expression of multiple genes, most of which are responsible for normal physiological pathways and the necessary cellular interactions to support these functions within the mammary gland. These include alterations in the interactions between the epithelial and stromal cells, which are manifested in tumours by well-recognized morphological changes known as the stromal reaction [1]. Such alterations in stromal–epithelial interactions may influence the risk of transformation of the breast epithelial cell and may contribute very early steps in tumourigenesis, as has recently been proposed in other systems [2]. However, the net effect of these alterations in the stroma on the later stages of tumour progression is unresolved [3].

Resolution of this issue is complicated by the recognition that the stroma is a highly complex tissue that includes a variety of different types of fibroblasts [4] and a range of proteins, glycoproteins, and proteoglycans which may play a role in tumour biology. We have recently extended this list by identifying lumican, a member of the small leucine-rich proteoglycans (SLRPs) as an mRNA that is expressed in the stroma of normal breast tissues and is overexpressed in invasive carcinomas [5]. Members of this family of proteoglycans have been implicated principally in matrix assembly and structure [6], but also more recently in the control of cell growth [7]. While studies of decorin have shown altered expression in neoplastic stroma [3], lumican has previously been studied only in the context of connective tissue and corneal disease [8,9], and the role of SLRPs in human breast cancer is relatively unexplored. To explore further the potential role of lumican and related genes in breast tumour progression, we have now examined the expression of lumican relative to that of other members of the SLRP family, decorin, biglycan and fibromodulin, at both mRNA and protein level, in normal and neoplastic breast tissues.

Materials and methods

Human breast tissues

All breast tumour cases used for this study were selected from the NCIC-Manitoba Breast Tumor Bank (Winnipeg, Manitoba, Canada). As has been previously described [10], tissues are accrued to the bank from cases at multiple centres within Manitoba, rapidly collected, and processed to create matched formalin-fixed, paraffin-embedded, and frozen tissue

blocks with the mirror image surfaces orientated by coloured inks. The histology and cellular composition of every sample in the bank are interpreted in haematoxylin and eosin (H&E)-stained sections from the face of the former tissue block.

For the initial study to compare broadly the expression of different members of the SLRP gene family, a mixed pilot cohort was selected from the Tumor Bank to include nine different invasive carcinomas, three normal tissue samples from patients with cancer, and three normal tissues from normal patients without cancer. The invasive tumours included different tumour types (five ductal, three lobular, and one tubular carcinoma), grades (four high, one moderate, four low Nottingham grades), and oestrogen receptor (ER) levels (three ER < 10 fmol/mg, three ER 10–20, three ER 39–169), and total stromal fractions ranging from 50 to 95% of the cross-sectional area. The mean patient ages were 62, 70, and 28 years for each subgroup, respectively (tumour tissues, normal tissues adjacent to tumours, and normal tissues).

For the subsequent studies to compare lumican and decorin expression, a second more defined and homogeneous cohort of 46 cases was selected to provide matching primary tumour tissues and adjacent normal tissue. This cohort included only invasive ductal carcinomas and was primarily selected to ensure availability of histologically confirmed and distinct regions comprising morphologically normal and tumour tissue elements in different blocks (12 cases, for western blot studies) or the same block (34 cases, for *in situ* hybridization studies). The subset used for western blot studies was also selected to possess equivalent cross-sectional areas [mean section area$^{(SD)}$ in tumour tissues $= 0.86^{(0.44)}$ cm^2, adjacent normal tissues $= 0.85^{(0.35)}$ cm^2] and stromal content [mean stromal area$^{(SD)}$ in tumour tissues $= 68^{(10)}$%, adjacent normal tissues $= 89^{(6)}$%] between the matching blocks and to incorporate cancer cases from both post-menopausal (six cases mean$^{(SD)} = 76^{(7)}$ years) and pre-menopausal patients (six cases mean$^{(SD)} = 44^{(3)}$ years).

Sodium dodecyl sulphate/polyacrylamide gel electrophoresis (SDS/PAGE) and immunoblotting

Total proteins were extracted from frozen tissue sections. These were cut from the face of frozen tissue blocks immediately adjacent to the face of a matching paraffin block [11] from which paraffin sections had been previously cut for pathological assessment and for *in situ* hybridization. For the first cohort of cases, an average of 20 20 μm tissue sections were cut from each typical tissue block (0.5×1.0 cm^2 cross-sectional area) and used for extraction; however, the number of tissue sections was varied for each case according to the measured area of the tissue within individual blocks, to ensure that equivalent volumes of tissue were used for the extraction, which was done as described previously [12]. For the second cohort of matching tissue samples, the same number of frozen sections (20×20 μm) was cut from the measured surface of each tissue block together with a single section from the adjacent paraffin block. This was used as a reference for composition and protein extraction was then performed on the frozen sections with equivalent volumes of extraction buffer. Proteins present in equivalent volumes of extracts were analysed by SDS/PAGE and immunoblotting, using anti-peptide antibodies specific for the carboxyl-terminal regions of the core proteins of lumican, decorin, fibromodulin, and biglycan [12–14]. The specificity of all antibodies was verified by peptide absorption and SLRP cross-reactivity analysis. Protein signals were detected by chemiluminescence and photographed prior to quantitation by video-image analysis and densitometry using an MCID M4 system and software (Imaging Research, St Catherines, Ontario, Canada). All signals were then adjusted with reference to control cartilage samples run with each blot. For the second cohort of matched tissue samples, signals were also adjusted with reference to the measured cross-sectional area and the stromal content of the tissue block to control for equivalent loading. Additional analysis was performed on all signals after further adjustment for relative stromal content of the tissue sections assessed in adjacent H&E sections.

Immunohistochemistry

Immunohistochemistry was performed on paraffin sections using the same antibody to lumican as used for immunoblotting [9,12]. Sections (5 μm thick) were obtained from paraffin-embedded tissue blocks matching the frozen tissue blocks of those cases used for reverse transcription-polymerase chain (RT-PCR) and protein analysis. After deparaffinizing, clearing, and hydrating in TBS buffer (Tris buffered saline, pH 7.6) the sections were pretreated with 3% hydrogen peroxide for 10 min to remove endogenous peroxidases and non-specific binding was blocked with normal swine serum, 1:10 (Vector Laboratories S-4000). TBS was used between steps to rinse and as a diluent. Primary antibody to lumican was applied at a 1:400 dilution overnight at 4°C, followed by biotinylated secondary swine anti-rabbit IgG, 1:200 (DAKO) for 1 h at room temperature. Tissue sections were incubated 45 min at room temperature with an avidin/biotin horseradish peroxidase system (Vectastain ABC Elite, Vector Lab.) followed by detection with DAB (diaminobenzidine), counterstaining with 2% methyl green, and mounting. A positive tissue control (colonic mucosa) and a negative reagent control (no primary antibody) were run in parallel. Immunostaining patterns and intensity were assessed by light microscopic visualization.

In situ hybridization

Paraffin-embedded 5 μm sections of breast tissues were analysed by *in situ* hybridization according to a previously described protocol [5]. For lumican, the

plasmid Lumi-398, which consisted of pGEM-T plasmid (Pharmacia Biotech), containing a 398 bp portion of lumican cDNA between bases 1332 and 1729, was used as a template to generate UTP^{S35} labelled sense and antisense riboprobes using Riboprobe Systems (Promega, Madison, WI, USA) and either the T7 or SP6 promotor at the 5′ or 3′ end of the lumican sequence according to the manufacturer's instructions. For decorin, the plasmid Dec-322 was used as a template. This consisted of pGEM-T plasmid containing a decorin insert with a comparable length (322 bp) to the lumican probe generated by PCR amplification from the decorin cDNA [12] using primers that corresponded to decorin (sense 5′-AAATGCCCAAAACTCTTCAG-3′ and antisense 5′-AAACTCAATCCCAACTTAGCC-3′) [15]. All PCR cDNAs and plasmid inserts were sequenced to confirm their entity. Levels of lumican and decorin expression were assessed in normal and tumour regions by microscopic examination at low magnification and with reference to the negative sense and positive control tumour sections. This was done as previously described [5] by scoring the estimated average signal intensity (on a scale of 0–3) and the proportion of stromal cells showing a positive signal (0, none; 0.1, less than one-tenth; 0.5, less than one-half; 1.0, greater than one-half). The intensity and proportion scores were then multiplied to give an overall score. Regions with a score lower than 1.0 were deemed negative or weakly positive.

Microdissection and protein extraction analysis

To assess protein localization within regions of tumours, two cases were selected that showed marked and well-defined regions within the same tissue section with discrepancies between mRNA and protein expression. This was determined by *in situ* hybridization and immunohistochemistry in adjacent serial sections from paraffin tissue blocks. The mirror image frozen tissue blocks to these paraffin blocks were used for microdissection as previously described [11] and protein was extracted from these histologically defined regions as described above. Briefly, thin 5 μm frozen sections were cut from the faces of the frozen tissue blocks and stained by H&E, and the relevant histological regions of approximately 1–2 mm^2 distinguished and confirmed by reference to the paraffin sections already studied. Multiple thick frozen sections (20 × 20 μm) were then cut, rapidly stained, and microdissected at room temperature from each section in turn, and the microdissected tissue fragments were frozen again prior to protein extraction.

Results

Identification of lumican as the most abundant SLRP in normal and neoplastic breast tissues

To determine the relative importance of altered lumican expression in breast tumourigenesis, the expression of lumican protein was compared with that of three other members of the SLRP family, decorin, fibromodulin and biglycan, by western blot in a heterogeneous panel of nine breast tumours and six normal tissues.

Lumican was highly abundant in all samples and in both neoplastic and normal tissues (Figure 1). A significant increase was seen in the mean level of lumican protein between normal and tumour [$mean^{(SD)}$ tissue adjusted optical density units, normal $= 0.43^{(0.08)}$, tumour $= 0.56^{(0.15)}$, $p = 0.026$, Mann–Whitney test]. Although an apparent difference in the level of lumican between normal samples from normal patients and normal samples adjacent to tumours was seen, this difference did not persist when the different stromal content of these samples was taken into account. Similarly, there was no difference in the levels in tumour tissues on comparing pre- and post-menopausal patients. Nevertheless, an increase in the overall molecular weight and polydiversity was noted between normal tissues and morphologically normal tissue adjacent to tumours, which might be attributable to either different age or association with tumour in the adjacent breast.

In comparison, decorin, although also present in most samples examined by western blot, was much less

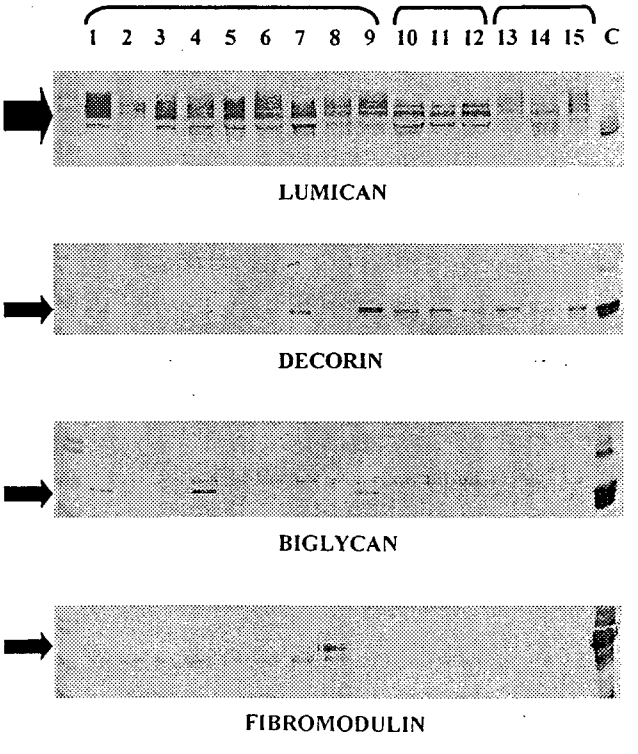

Figure 1. Immunoblotting study of lumican, decorin, biglycan, and fibromodulin protein expression in human breast tumours (lanes 1–9); normal tissues from normal patients (lanes 10–12); and normal tissues adjacent to carcinomas (lanes 13–15). All protein samples were extracted from sets of frozen tissue sections bracketed by sections assessed by H&E stain and light microscopy to confirm content. Chemiluminescent signals for decorin, biglycan, and fibromodulin required three-fold longer exposure times than that for lumican. Molecular markers (left) and cartilage control sample (right) are present in all panels

abundant relative to the cartilage control (Figure 1). It should be noted that the decorin (in common with biglycan and fibromodulin) signals shown in Figure 1 also required a three-fold longer chemiluminescent exposure time (9 s) than that for lumican (3 s). However, in contrast to lumican, there was a marked decrease in decorin between normal and tumour samples [mean$^{(SD)}$ optical density units; normal = $0.21^{(0.06)}$, tumour = $0.13^{(0.14)}$, $p = 0.066$, Mann–Whitney test]. No difference was seen in the signals between normal samples from normal and cancer patients.

Fibromodulin expression was not detected in normal tissues and at only low levels in only 3/9 tumours, where the presence of fibromodulin correlated with those tumours with the highest content of epithelial tumour cells. Biglycan was also only detected at low levels in 2/6 normal tissues and 3/9 tumours, where in contrast to fibromodulin, its presence correlated directly with those tumours with the highest content of collagenous stroma.

Lumican and decorin are differentially expressed between normal and neoplastic tissues

In order to examine further the distinct alterations in the expression of lumican and decorin, the mRNA and protein expression of both genes was examined in 46 cases by *in situ* hybridization (34 cases) and western blot (12 cases) from the second cohort of cases, comprising matched normal and tumour samples.

As previously shown, prominent lumican mRNA expression was detected, using an antisense probe, in stromal fibroblast-like cells within the tumour and immediately adjacent to invasive tumour cells. Assessment of mRNA levels using a semi-quantitative approach, as detailed in the Materials and methods section, also confirmed our previous observations [5] made on a different set of tumours, and lumican mRNA was found to be significantly elevated in the majority of tumours when levels were compared with those present in adjacent normal stroma ($p < 0.0001$, Wilcoxon test, Figures 2 and 3B). Higher levels of lumican (≥ 1) were present in tumour than in normal tissue in 26/34 cases. At the same time, decorin levels also showed a consistent and significant difference, with lower levels seen in stroma associated with tumour, relative to stroma associated with adjacent normal tissue components ($p < 0.0002$, Wilcoxon test, Figures 2 and 3C), with lower levels of decorin (≥ 1) present in tumour than in normal tissue in 22/34 cases. The pattern of expression of decorin was also identical in sections from the same cases studied with a different *in situ* hybridization riboprobe (data not shown). Although we have previously noted a relationship between lumican and poor prognostic factors, these associations were not found in the present larger series.

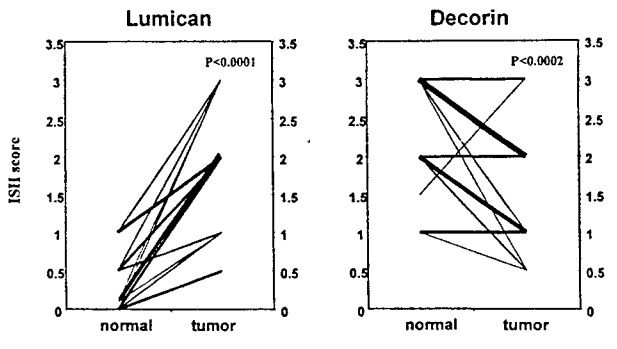

Figure 2. Lumican and decorin mRNA levels in matched normal and tumour tissues, assessed by *in situ* hybridization and semi-quantitative scoring as described in the Materials and methods section. The thickness of each line (on a scale of 1–9) corresponds to the number of cases showing the same differences in scores ($n = 34$ cases)

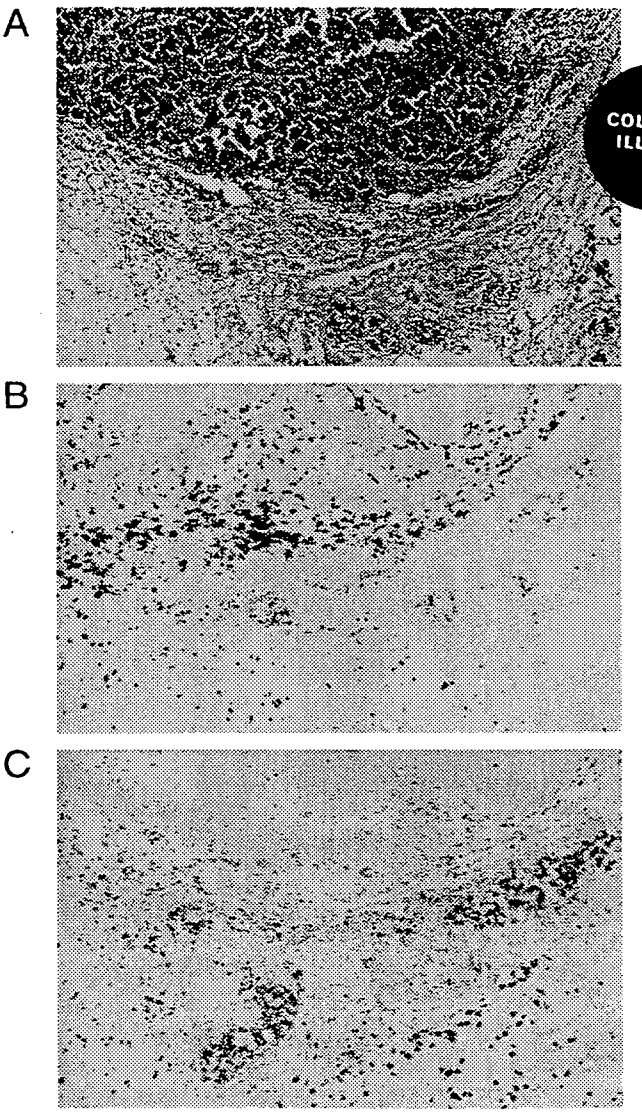

Figure 3. Lumican and decorin mRNA expression detected by *in situ* hybridization within a breast tumour section. Panel A (H&E section) shows the histology including the invasive tumour (upper area), the tumour margin (middle), and adjacent normal tissue including lobular-ductal units (lower area). Lumican expression (B) is high within the tumour and tumour margin and lower in the normal fat and collagenous stroma adjacent to the normal lobules. Decorin (C) shows high expression in the normal stroma adjacent to normal lobules and reduced expression in the tumour. ×340

In keeping with the pattern of mRNA expression, the mean lumican protein signal assessed by western blot was also higher in 9/12 tumours relative to normal tissues [mean$^{(SD)}$ optical density units, normal = $0.22^{(0.15)}$, tumour = $0.43^{(0.19)}$, $p = 0.0122$ Wilcoxon test]. Once again, in contrast to this, decorin protein was lower in 7/12 tumours relative to normal tissues, but in this case the differences were not statistically significant [mean$^{(SD)}$ optical density units, normal = $0.22^{(0.19)}$, tumour = $0.17^{(0.2)}$, p = ns (not significant), Wilcoxon test]. These contrasting patterns of lumican and decorin expression also persisted after standardization of western blot signals for relative stromal content (data not shown).

Lumican mRNA and protein expression can occur in different regions within breast tumours

Immunohistochemical study of the lumican distribution within the same tissues that had already been examined by *in situ* hybridization was performed using the same antibody [9,12] that had been employed for western blot analysis (Figure 4). This showed that lumican was abundant throughout the collagenous stroma of both normal and tumour sections, with prominent deposition around small vessels, breast duct, and lobular structures. There was increased deposition within the collagenous stroma of tumours, in particular at the invasive margins and in areas of dense collagen within central regions of some tumours, compared with adjacent normal tissues. However, in some cases there were distinct regions, up to 2 mm in area within the tumour sections, containing loose stroma in which there was a complete absence of lumican detectable by immunohistochemistry (Figures 4C and 4D); but the same regions showed high expression when examined for lumican mRNA by *in situ* hybridization in adjacent sections (Figures 4A and 4B). Similarly, other areas showed strong staining for lumican protein, but low levels of mRNA.

To explore the possibility that the absence of lumican expression detected by immunohistochemistry might be due to the conformation of the native protein or the binding of lumican to other proteins, resulting in the masking of the carboxy-terminal epitope, specific areas measuring approximately 1 mm^2 each were microdissected from frozen sections of two tumours and lumican protein was assessed under denaturing conditions by SDS/PAGE and western blot. In both cases, those regions with high mRNA expression and negative by immunohistochemistry were also negative by western blot, while areas showing very low mRNA expression but strong staining by immunohistochemistry were positive by western blot (Figure 5).

Discussion

We have shown that lumican is the most abundant proteoglycan in comparison with several other members of the family of small leucine-rich proteoglycans (SLRPs) in breast cancer. We have also extended our previous observations [5], based on the detection of lumican mRNA, in showing that the total lumican protein is also increased in breast tumours relative to adjacent normal tissues. Our results also demonstrate that this pattern of up-regulation of lumican in relation to breast tumourigenesis is distinct from that of the closely related decorin gene, which is inversely regulated and reduced at mRNA and to a lesser extent at protein levels, in tumour relative to adjacent normal tissue. Finally, we have shown that lumican expression in tumours may also be associated with an abnormal distribution within the stroma, manifested by discordance between mRNA and protein deposition within subregions of breast tumours.

The family of SLRPs share several common features, including a central region of leucine-rich repeats bounded by flanking cysteine residues, and localization in the extracellular matrix. The SLRPs can be separated into three subgroups that include decorin and biglycan, lumican and fibromodulin, and epiphycan and osteoglycin, which are distinguishable by amino acid homologies and also by gene structure [16]. Decorin, probably the best studied of these genes, is known to interact with a variety of extracellular matrix molecules and has been shown to be capable of influencing collagen fibril growth and assembly both *in vitro* and *in vivo* [6,7]. Decorin may also influence tumour cell growth through indirect effects on the availability of growth factors from the extracellular matrix, or directly through activation of the EGF receptor and induction of the p21 cell-cycle inhibitor [18]. In contrast, less is known about lumican and other SLRPs. However, *in vitro* and *in vivo* data indicate that lumican is also important in the regulation of collagen fibril assembly [19]. This view is supported by recent observations based on mice with homozygous deletion of the lumican gene, where loss of corneal transparency and increased skin fragility are associated with disorganized and loosely packed collagen fibres related to increased and irregular fibril size, and interfibrillar spacing, as viewed by light and electron microscopy [8].

The observation that lumican is highly abundant compared with other SLRPs in breast tumours cannot be interpreted to mean that it is necessarily the most important. This is underscored by the recent demonstration that although decorin is apparently more abundant than versican in prostate cancer tissue, only an increase in the larger chondroitin sulphate proteoglycan versican correlates with grade, and inversely with progression-free survival, in prostate cancer [20]. Similarly, the increase in lumican as seen here in association with breast tumourigenesis may be less important than the parallel decrease in decorin. It should also be noted that while the present study was focused primarily on examining the relative expression of SLRPs between matched normal and tumour tissues and was not necessarily designed to compare levels between cases, we did not observe any significant

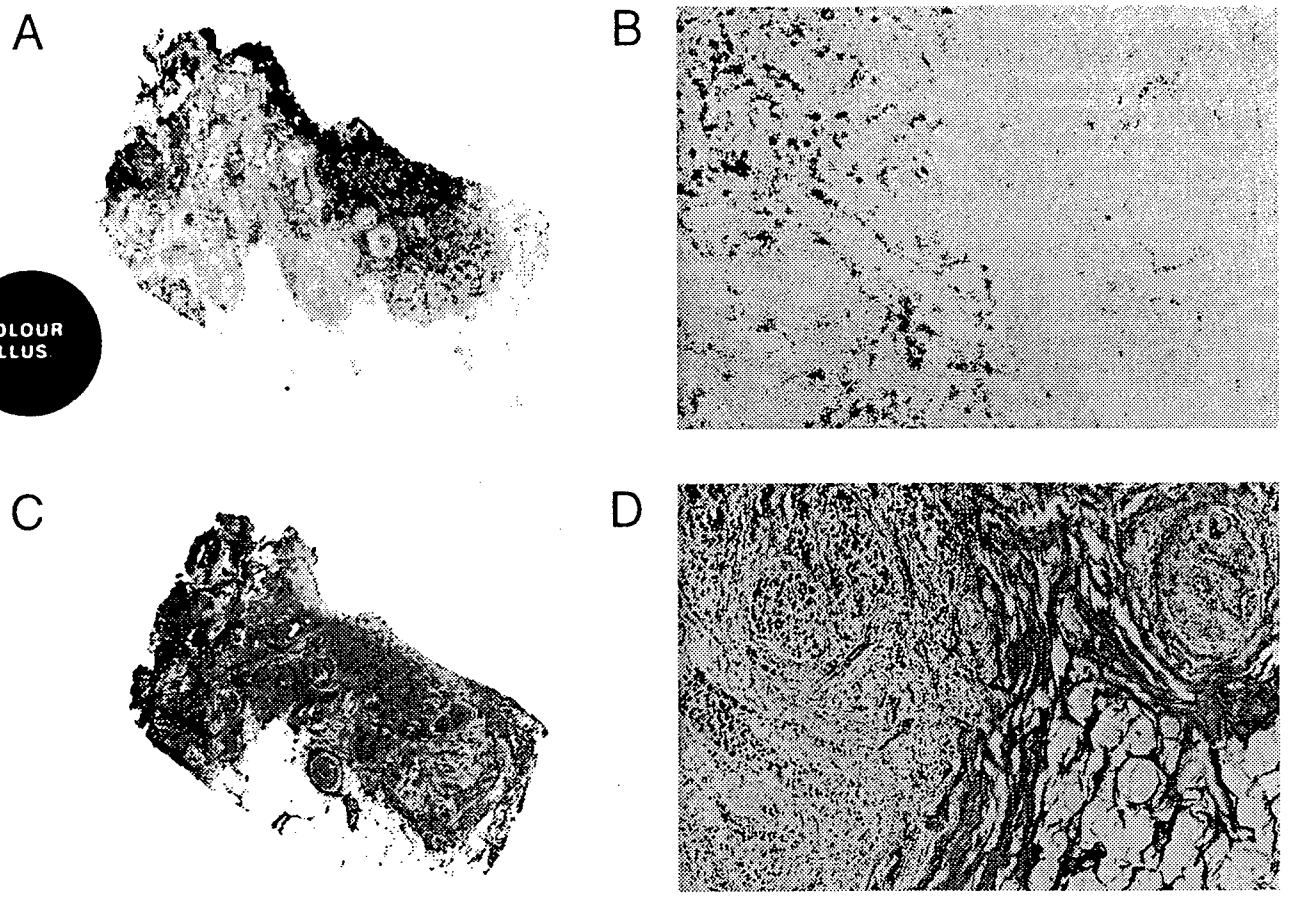

Figure 4. *In situ* hybridization and immunohistochemical study showing regional discordance in lumican mRNA (A, B) and protein expression (C, D) displayed in adjacent sections in breast tumours. Panels A and C show the overall pattern of mRNA (A, black signal) and protein (C, brown staining) within a tissue section (0.4 × 0.8 cm in size) that includes regions of *in situ* and invasive tumour (upper left and upper middle) and adjacent normal tissue (lower left and lower right). Panels B and D show a detailed microscopic view (×400) of the cellular localization of mRNA and protein within a small region at the invasive edge within the same section (tumour component at left, normal component at right)

relationship between lumican or decorin and prognostic factors within this larger tumour cohort, as previously noted [5]. While this leaves open the question of a role for these SLRPs in later tumour progression, the implication of altered expression for the earlier stages of tumourigenesis remains intriguing. It is possible to speculate that both induction of lumican and decrease in decorin in stromal fibroblasts within the invasive tumour may represent a positive host response, to abrogate the disorganization of collagen within the tumour stroma, encourage macrophage localization [21], and inhibit the growth of epithelial cancer cells, through the increased availability of growth factors inhibitory to breast epithelial cell growth [22]. Alternatively, these alterations may represent a negative host response contributing to early tumour development. Increased lumican mRNA expression may reflect a response to locally increased proteolysis or altered deposition of the lumican protein that is the cause of the disorganization of the collagenous stroma, which in turn facilitates tumour cell invasion. Similarly, a decrease in decorin may remove an inhibitory effect on epithelial tumour cell growth through repression of p21 [7]. A role for and the distinction between these opposing potential effects will clearly require further study.

The differences in lumican levels between normal and tumour tissues observed by both immunohistochemistry and western blot are not as marked as those seen at the level of mRNA expression. While differences in the assays may account for some of this discrepancy, it is clear that it may also be attributable to the discordance that can exist between lumican mRNA and protein expression detected by *in situ* and immunohistochemical techniques respectively, within the same regions of breast tumour stroma. A similar discordance between mRNA and protein expression has been previously observed in the course of studies on lumican and other large and small proteoglycans in different tissues. For example, in corneal development in the chicken, the mRNA levels for lumican and decorin do not always reflect the rate of synthesis of the corresponding proteins and the efficiency of translation of lumican varies over time [23]. Similar discordance between aggrecan and versican mRNA and protein has been seen in normal tendon [24], between decorin and biglycan mRNA and protein localization in normal and reactive gastric mucosa [25],

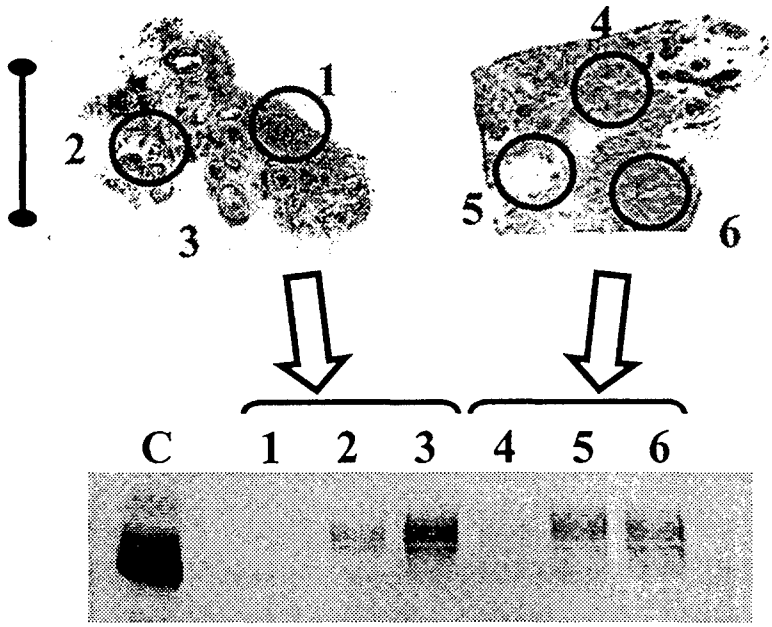

Figure 5. Lumican protein expression detected by immunohistochemistry (upper panel) and western blot (lower panel) demonstrating concordance in the assessment of protein levels in microdissected subregions within two breast tumour sections. The upper panels show IHC sections (tumour A, right; tumour B, left; scale bar =5 mm). The mRNA and protein signals were detected by *in situ* hybridization (ISH) and immunohistochemistry (IHC) in each region in adjacent sections and ISH/IHC levels were assessed semi-quantitatively (negative, weak +, strong + +) as follows: tumour A: region 1 = + +/−, region 2 = −/+ +, region 3 (remainder of section) = +/+ +; tumour B: region 4 = +/−, region 5 = −/+ +, region 6 = + +/+ +. The lower panel shows the western blot (C= cartilage control; lanes 1–6 correspond to regions assessed and microdissected above)

and in regions of cartilage matrix around vascular channels and the growth plates of long bones in normal cartilage [26]. In this latter instance, the discordance was attributed to a high rate of breakdown and removal at these sites. This conclusion is supported by studies on endothelial cells which show that growth factors such as bFGF can increase not only both biglycan transcription and protein synthesis, but also the corresponding rate of proteolysis [27]. The absence of protein could also reflect masking of the epitope by conformational changes in the native protein, by changes in post-translational modification, or by binding to another protein. Alternatively, this could reflect reduced translation, increased breakdown, or failure to bind within the immediate stroma and rap translocation of the protein to adjacent areas of the tissue. Our microdissection experiments, applied to small regions where lumican mRNA is highly expressed, suggest that the corresponding protein is truly absent in these areas and that epitope masking due to conformation or binding proteins is an unlikely explanation for the observation. However, it could also be the case that the necessary binding sites are not available in the immature stroma associated with rapid growth of tumours and that this allows translocation of newly synthesized lumican to binding sites in adjacent tissue.

The reciprocal nature of the changes in the expression of lumican and decorin is intriguing. Although definitive characterization of the stromal cell types awaits primary culture studies, direct comparison of *in situ* hybridization performed on serial sections suggests that expression of both genes apparently occurs in the same fibroblast-like cells in breast tissue stroma. While lumican has not previously been studied in human tumours, the expression of decorin mRNA and proteoglycans incorporating chondroitin sulphate epitopes has been shown to be increased in colon, prostate, and basal cell carcinomas [28–30], but a more recent study of multiple stromal genes in breast tumours found no difference in the levels of decorin mRNA between tumour and normal tissue, although noting increased expression in the stroma immediately adjacent to *in situ* components [31]. However, the normal tissue examined was selected to be well away from the primary tumour and this, together with differences in the method of quantitation, the definition of tumour regions, and the focus on matched samples, limits a full comparison with our observations. For example, morphologically normal tissue immediately adjacent to carcinomas may be influenced by paracrine growth factors derived from the tumour and may also harbour molecular alterations [32] that might influence local gene expression. However, similar immunohistochemical studies of breast tumours using monoclonal antibodies raised against chondroitin sulphate and dermatan sulphate small proteoglycan have shown reduced decorin expression within invasive as compared with surrounding normal stroma, consistent with our findings [33]. Decorin and other SLRPs are known to be independently regulated and mutually exclusive [26] and compensatory changes in the expression between different SLRPs have been observed [34]. However, this appears to be usually

manifested by genes within subgroups of the SLRP family. At the same time, reciprocal changes in the expression between lumican and decorin have not been described in lumican or decorin 'knockout' mice [8,17]. The factors that influence altered expression of these genes in breast tumour stroma remain to be elucidated.

In summary, we have shown that lumican is highly abundant relative to decorin, biglycan, and fibromodulin in normal and neoplastic breast tissues. We have also shown that increased lumican protein expression and altered regional localization occur in breast tumours and that different and reciprocal alterations in expression occur between lumican and decorin. The functional significance and the role of alterations in these stromal proteoglycans in breast tumourigenesis and progression remain to be determined.

Acknowledgements

This work was supported by grants from the Medical Research Council of Canada (MRC) and the US Army Medical Research and Materiel Command (USAMRMC). The Manitoba Breast Tumor Bank is supported by funding from the National Cancer Institute of Canada (NCIC). PHW is an MRC Scientist; LCM is an MRC Scientist; and EL is a recipient of a USAMRMC Postdoctoral Fellowship. TH-H is a recipient of an MRC studentship award.

References

1. Peyrol S, Raccurt M, Gerard F, Gleyzal C, Grimaud JA, Sommer P. Lysyl oxidase gene expression in the stromal reaction to *in situ* and invasive ductal breast carcinoma. *Am J Pathol* 1997; **150**: 497–507.
2. Kinzler KW, Vogelstein B. Landscaping the cancer terrain [comment]. *Science* 1998; **280**: 1036–1037.
3. Iozzo RV. Tumor stroma as a regulator of neoplastic behavior. Agonistic and antagonistic elements embedded in the same connective tissue [editorial]. *Lab Invest* 1995; **73**: 157–160.
4. Spanakis E, Brouty-Boye D. Discrimination of fibroblast subtypes by multivariate analysis of gene expression. *Int J Cancer* 1997; **71**: 402–409.
5. Leygue E, Snell L, Dotzlaw H, *et al.* Expression of lumican in human breast carcinoma. *Cancer Res* 1998; **58**: 1348–1352.
6. Iozzo RV. The family of the small leucine-rich proteoglycans: key regulators of matrix assembly and cellular growth. *Crit Rev Biochem Mol Biol* 1997; **32**: 141–174.
7. Santra M, Mann DM, Mercer EW, Skorski T, Calabretta B, Iozzo RV. Ectopic expression of decorin protein core causes a generalized growth suppression in neoplastic cells of various histogenetic origin and requires endogenous p21, an inhibitor of cyclin-dependent kinases. *J Clin Invest* 1997; **100**: 149–157.
8. Chakravarti S, Magnuson T, Lass JH, Jepsen KJ, LaMantia C, Carroll H. Lumican regulates collagen fibril assembly: skin fragility and corneal opacity in the absence of lumican. *J Cell Biol* 1998; **141**: 1277–1286.
9. Cs-Szabo G, Melching LI, Roughley PJ, Glant TT. Changes in messenger RNA and protein levels of proteoglycans and link protein in human osteoarthritic cartilage samples. *Arthritis Rheum* 1997; **40**: 1037–1045.
10. Watson PH, Snell L, Parisien M. The NCIC-Manitoba Breast Tumor Bank: a resource for applied cancer research. *Cmaj* 1996; **155**: 281–283.
11. Hiller T, Snell L, Watson PH. Microdissection RT-PCR analysis of gene expression in pathologically defined frozen tissue sections. *Biotechniques* 1996; **21**: 38–40.
12. Grover J, Chen XN, Korenberg JR, Roughley PJ. The human lumican gene. Organization, chromosomal location, and expression in articular cartilage. *J Biol Chem* 1995; **270**: 21942–21949.
13. Roughley PJ, White RJ, Cs-Szabo G, Mort JS. Changes with age in the structure of fibromodulin in human articular cartilage. *Osteoarthritis Cart* 1996; **4**: 153–161.
14. Roughley PJ, White RJ, Magny M-C, Liu J, Pearce RH, Mort JS. Non-proteoglycan forms of biglycan increase with age in human articular cartilage. *Biochem J* 1993; **295**: 421–426.
15. Vetter U, Vogel W, Just W, Young MF, Fisher LW. Human decorin gene: intron–exon junctions and chromosomal localization. *Genomics* 1993; **15**: 161–168.
16. Hocking AM, Shinomura T, McQuillan DJ. Leucine-rich repeat glycoproteins of the extracellular matrix. *Matrix Biol* 1998; **17**: 1–19.
17. Danielson KG, Baribault H, Holmes DF, Graham H, Kadler KE, Iozzo RV. Targeted disruption of decorin leads to abnormal collagen fibril morphology and skin fragility. *J Cell Biol* 1997; **136**: 729–743.
18. Moscatello DK, Santra M, Mann DM, McQuillan DJ, Wong AJ, Iozzo RV. Decorin suppresses tumor cell growth by activating the epidermal growth factor receptor. *J Clin Invest* 1998; **101**: 406–412.
19. Ying S, Shiraishi A, Kao CW, *et al.* Characterization and expression of the mouse lumican gene. *J Biol Chem* 1997; **272**: 30306–30313.
20. Ricciardelli C, Mayne K, Sykes PJ, *et al.* Elevated levels of versican but not decorin predict disease progression in early-stage prostate cancer. *Clin Cancer Res* 1998; **4**: 963–971.
21. Funderburgh JL, Mitschler RR, Funderburgh ML, Roth MR, Chapes SK, Conrad GW. Macrophage receptors for lumican. A corneal keratan sulfate proteoglycan. *Invest Ophthalmol Vis Sci* 1997; **38**: 1159–1167.
22. Santra M, Skorski T, Calabretta B, Lattime EC, Iozzo RV. *De novo* decorin gene expression suppresses the malignant phenotype in human colon cancer cells. *Proc Natl Acad Sci U S A* 1995; **92**: 7016–7020.
23. Cornuet PK, Blochberger TC, Hassell JR. Molecular polymorphism of lumican during corneal development. *Invest Ophthalmol Vis Sci* 1994; **35**: 870–877.
24. Waggett AD, Ralphs JR, Kwan AP, Woodnutt D, Benjamin M. Characterization of collagens and proteoglycans at he insertion of the human Achilles tendon. *Matrix Biol* 1998; **16**: 457–470.
25. Schonherr E, Lugering N, Stoll R, Domschke W, Kresse H. Differences in decorin and biglycan expression in patients with gastric ulcer healing. *Scand J Gastroenterol* 1997; **32**: 785–790.
26. Bianco P, Fisher LW, Young MF, Termine JD, Robey PG. Expression and localization of the two small proteoglycans biglycan and decorin in developing human skeletal and non-skeletal tissues. *J Histochem Cytochem* 1990; **38**: 1549–1563.
27. Kinsella MG, Tsoi CK, Jarvelainen HT, Wight TN. Selective expression and processing of biglycan during migration of bovine aortic endothelial cells. The role of endogenous basic fibroblast growth factor. *J Biol Chem* 1997; **272**: 318–325.
28. Adany R, Heimer R, Caterson B, Sorrell JM, Iozzo RV. Altered expression of chondroitin sulfate proteoglycan in the stroma of human colon carcinoma. Hypomethylation of PG-40 gene correlates with increased PG-40 content and mRNA levels. *J Biol Chem* 1990; **265**: 11389–11396.
29. Hunzelmann N, Schonherr E, Bonnekoh B, Hartmann C, Kresse H, Krieg T. Altered immunohistochemical expression of small proteoglycans in the tumor tissue and stroma of basal cell carcinoma. *J Invest Dermatol* 1995; **104**: 509–513.
30. Iozzo RV, Cohen I. Altered proteoglycan gene expression and the tumor stroma. *Experientia* 1993; **49**: 447–455.
31. Brown LF, Guidi AJ, Schnitt SJ, *et al.* Vascular stroma formation in carcinoma *in situ*, invasive carcinoma, and metastatic carcinoma of the breast. *Clin Cancer Res* 1999; **5**: 1041–1056.
32. Deng G, Lu Y, Zlotnikov G, Thor AD, Smith HS. Loss of heterozygosity in normal tissue adjacent to breast carcinomas. *Science* 1996; **274**: 2057–2059.

33. Nara Y, Kato Y, Torii Y, *et al.* Immunohistochemical localization of extracellular matrix components in human breast tumours with special reference to PG-M/versican. *Histochem J* 1997; **29**: 21–30.

34. Nelimarkka L, Kainulainen V, Schonherr E, *et al.* Expression of small extracellular chondroitin/dermatan sulfate proteoglycans is differentially regulated in human endothelial cells. *J Biol Chem* 1997; **272**: 12730–12737.

DEPARTMENT OF THE ARMY
US ARMY MEDICAL RESEARCH AND MATERIEL COMMAND
504 SCOTT STREET
FORT DETRICK, MARYLAND 21702-5012

REPLY TO
ATTENTION OF:

MCMR-RMI-S (70-1y) 28 July 03

MEMORANDUM FOR Administrator, Defense Technical Information Center (DTIC-OCA), 8725 John J. Kingman Road, Fort Belvoir, VA 22060-6218

SUBJECT: Request Change in Distribution Statement

1. The U.S. Army Medical Research and Materiel Command has reexamined the need for the limitation assigned to technical reports written for this Command. Request the limited distribution statement for the enclosed accession numbers be changed to "Approved for public release; distribution unlimited." These reports should be released to the National Technical Information Service.

2. Point of contact for this request is Ms. Kristin Morrow at DSN 343-7327 or by e-mail at Kristin.Morrow@det.amedd.army.mil.

FOR THE COMMANDER:

Encl

PHYLIS M. RINEHART
Deputy Chief of Staff for
Information Management

ADB233865
ADB265530
ADB244706
ADB285843
ADB240902
ADB264038
ADB285885
ADB274458
ADB285735
ADB286597
ADB285707
ADB274521
ADB259955
ADB274793
ADB285914
ADB260288
ADB254419
ADB282347
ADB286860
ADB262052
ADB286348
ADB264839
ADB275123
ADB286590
ADB264002
ADB281670
ADB281622
ADB263720
ADB285876
ADB262660
ADB282191
ADB283518
ADB285797
ADB269339
ADB264584
ADB282777
ADB286185
ADB262261
ADB282896
ADB286247
ADB286127
ADB274629
ADB284370
ADB264652
ADB281790
ADB286578
ADB264750
ADB282776
ADB286264
ADB260563
ADB277918
ADB286365
ADB275327
ADB286736
ADB286137
ADB286146
ADB286100
ADB286266
ADB286308
ADB285832